PROTEOMIC ANALYSIS ON HOST RESPONSES TO CHIKUNGUNYA VIRUS INFECTION

CHRISTINA THIO LI PING

FACULTY OF SCIENCE
UNIVERSITY OF MALAYA
KUALA LUMPUR

2013

PROTEOMIC ANALYSIS ON HOST RESPONSES TO CHIKUNGUNYA VIRUS INFECTION

CHRISTINA THIO LI PING

DISSERTATION SUBMITTED IN FULFILLMENT OF THE REQUIREMENTS FOR THE DEGREE OF MASTER OF SCIENCE

INSTITUTE OF BIOLOGICAL SCIENCES
FACULTY OF SCIENCE
UNIVERSITY OF MALAYA
KUALA LUMPUR

2013

ABSTRACT

Chikungunya virus (CHIKV) is an arthropod-borne virus that has caused multiple unprecedented outbreaks in both tropical and temperate countries over the past five decades. There is no commercial vaccine or antiviral drug to date, due in part to the lack of knowledge and understanding of the biology and pathogenesis of this virus. Thus, there is an increasing need for researchers to focus their research efforts in this area of virology. The current study employed proteomics to investigate alterations of the whole cell proteome and secretome of WRL-68 cells during early CHIKV infection, with the main aim being to identify the key proteins modulated in response to infection. Two-dimensional gel electrophoresis (2-DGE) was used to compare the whole cell proteome and secretome profiles between mock control cells and cells infected at the optimised multiplicity of infection (MOI) of 5.0 at 24 hours post-infection. Protein spots that were found to be differentially expressed were identified by MALDI-TOF/TOF mass spectrometry (MS) analysis, and three selected proteins were validated by Western blot. The functional association between these proteins were determined by STRING network analysis, and the mRNA expression level of selected proteins was investigated via real-time quantitative PCR. Overall, 50 and 25 protein spots from the whole cell proteome and secretome samples, respectively, were found to be differentially expressed (fold-change > 1.3, $p < 0.05$) and were successfully identified. The mRNA expression of 15 whole cell proteins was found to correlate with the corresponding protein expression. On the contrary, only one of the 15 selected proteins from the secretome sample showed positive correlation with its transcript expression level. By combining the proteomics and bioinformatics data from STRING network analysis, it was deduced that CHIKV disrupt the overall host cell metabolic machinery and ubiquitin-proteasome pathway (UPP). Suppression of the host immune response was also observed through the inhibition of immune-related protein secretion, mainly

cathepsin D, cathepsin L1, C3 protein and β-2 microglobulin. Several gene expression-related proteins were also down-regulated, including the mRNA processing factor, hnRNP E1, and translational factors, namely elongation factor-2, eukaryotic initiation factor eIF-2BA and eIF3 subunit H. Meanwhile, up-regulation of hnRNP C1/C2 suggests that this protein may be beneficial to CHIKV. Cell cycle regulation via cyclin-dependent kinase 1 (CDK1) activity may also play an important role during early CHIKV infection. CDK1 was down-regulated, whereas several other proteins (such as SET protein) that indirectly regulate the activity of CDK1, were altered in favour of the inhibition of CDK1 activity. In conclusion, CHIKV infection in the human liver cells induced a widespread alteration of the whole cell proteome and secretome. Nevertheless functional characterisations of these proteins are entailed to provide more insights into the actual mechanisms at play during early infection.

ABSTRAK

Virus chikungunya (CHIKV) adalah virus bawaan-artropoda yang telah mencetuskan beberapa wabak di negara-negara tropika dan iklim sederhana sejak lima dekad yang lalu. Sehingga kini, tiada lagi vaksin atau ubat anti-virus komersial bagi merawat jangkitan ini. Ini adalah disebabkan oleh kekurangan pengetahuan dan pemahaman mengenai biologi dan patogenesis virus tersebut. Oleh yang demikian, wujud keperluan yang semakin meningkat bagi penyelidik untuk menumpukan usaha penyelidikan mereka dalam bidang virologi tersebut. Kajian ini menggunakan kaedah proteomik untuk menyiasat perubahan *proteome* seluruh sel dan *secretome* sel-sel WRL-68 pada peringkat awal jangkitan CHIKV, dengan tujuan utama untuk mengenalpasti protein penting yang dimodulasikan sebagai tindakbalas terhadap jangkitan tersebut. Elektroforesis gel dua-dimensi (2-DGE) telah digunakan untuk membandingkan profil-profil sel seluruh *proteome* dan *secretome* di antara sel-sel normal dan sel-sel yang dijangkiti CHIKV pada keadaan optimum, iaitu *multiplicity of infection* (MOI) sebanyak 5.0, selama 24 jam. Bintik-bintik protein yang berubah ekspresinya telah dikenalpasti dengan mengunakan kaedah MALDI-TOF/TOF spektrometri jisim (MS), dan tiga protein telah dipilih untuk disahkan melalui kaedah *Western blot*. Hubungkait antara protein-protein yang telah dikenalpasti ditentukan melalui analisis rangkaian STRING, dan ekspresi mRNA bagi protein terpilih disiasat melalui *real-time quantitative PCR*. Secara keseluruhannya, 50 dan 25 bintik protein dari *proteome* seluruh sel dan sampel *secretome*, masing-masing, menunjukkan perubahan ekspresi (Gandaan perubahan > 1.3, $p < 0.05$), dan telah berjaya dikenalpasti. Ekspresi mRNA bagi 15 protein seluruh sel didapati berkorelasi dengan ekspresi protein. Sebaliknya, hanya satu daripada 15 protein yang dipilih dari sampel *secretome* menunjukkan hubungan yang positif dengan tahap ekspresi transkrip. Dengan menggabungkan data proteomik and bioinformatik daripada analisis rangkaian

STRING, boleh disimpulkan bahawa CHIKV mengganggu keseluruhan jentera metabolik sel perumah dan laluan *ubiquitin-proteasome* (UPP). Penindasan reaksi imun juga diperhatikan melalui perencatan protein rembesan yang berkaitan imunisasi, terutamanya *cathepsin D, cathepsin L1*, protein *C3* dan *β-2 microglobulin*. Beberapa protein yang memainkan peranan dalam ekspresi gen juga menunjukkan penurunan ekspresi, termasuk faktor pemprosesan mRNA, hnRNP E1, dan faktor translasi, iaitu *elongation factor-2, eukaryotic initiation factor eIF-2BA and eIF3 subunit H*. Sementara itu, peningkatan ekspresi protein hnRNP C1/C2 mencadangkan bahawa protein ini boleh memberi manfaat kepada CHIKV. Regulasi kitaran sel melalui *cyclin-deendent kinase 1*(CDK1) juga memainkan peranan yang penting pada awal jangkitan CHIKV. CDK1 menunjukkan penurunan ekspresi, manakala beberapa protein lain (seperti protein SET) yang mengawal regulasi aktiviti CDK1 secara tidak langsung, menunjukkan perubahan ekspresi yang memihak kepada perencatan aktiviti CDK1. Kesimpulannya, jangkitan CHIKV dalam sel-sel hati manusia menyebabkan perubahan *proteome* seluruh sel dan *secretome*. Namun begitu, ciri-ciri fungsi protein-protein tersebut adalah penting untuk memberi maklumat yang mendalam tentang mekanisme sebenar yang berlaku pada awal jangkitan.

ACKNOWLEDGEMENT

First and above all, I praise God, the almighty for the wisdom, perseverance and strength that He has bestowed upon me during the course of my study. The completion of my project and thesis would also have been impossible without the help and guidance of several people whom I dedicate this page to.

My deepest and sincerest appreciation goes out to both my project supervisors, Dr. Saiful Anuar Karsani and Dr. Puteri Shafinaz Akmar Abdul Rahman for their constant encouragement, guidance and motivation. Their invaluable advices, critical comments and constructive suggestions have contributed to the success of this research and the completion of my thesis. Special thanks also to Prof. Datuk Dr. Rohana Yusof for welcoming me into the Drug Design and Development Research Group (DDDRG), and for providing me the facilities to conduct my research.

I am also indebted to my seniors and colleagues, Tan Eng Chong, Dr. Shatrah Othman, Nadia Yaacob, Shafina Habib, Nurshamimi Nor Rashid, Hani Shahira and Tan Wei Lian for their support, advice and skilful technical help. Thanks for being selfless in sharing your knowledge and wisdom, for the friendship and memories we share, and for making the lab an enjoyable place to work in. Thanks also to those who indirectly contributed to this research, your generosity means a lot to me.

Last but definitely not least, I would like to thank my beloved parents for their unconditional love, understanding and endless moral support throughout my life. Thanks for believing in me and for being there for me through my ups and downs. Once again, my sincerest thanks to you all.

CONTENTS

		Page
ABSTRACT		i
ABSTRAK		iii
ACKNOWLEDGEMENT		v
CONTENTS		vi
LIST OF FIGURES		xii
LIST OF TABLES		xiv
LIST OF ABBREVIATIONS		xv
1.0	**INTRODUCTION**	1
2.0	**LITERATURE REVIEW**	5
2.1	CHIKV	6
2.1.1	CHIKV classification	6
2.1.2	Viral structure and genome organisation	7
2.1.3	Transmission cycle	9
2.1.4	Replication cycle of CHIKV	11
2.2	Epidemiology of CHIKV infection	13
2.3	Clinical manifestation	16
2.4	Prevention and treatment	19
2.5	Current status of CHIKV research	20
2.5.1	CHIKV cellular and tissue tropism	20
2.5.2	CHIKV genetic mutation and evolution	23
2.5.3	CHIKV-host immune interaction	24
2.5.4	Vaccine and antiviral development	26

2.6 Proteomics 27

2.6.1 Tools of proteomics 28

2.6.2 2-DGE 29

2.6.2.1 Sample preparation 29

2.6.2.2 IEF 32

2.6.2.3 SDS-PAGE 33

2.6.3 MS 33

2.6.3.1 Proteomic data analysis 35

2.6.4 Viral proteomics: Evaluation of virus-host interaction 36

3.0 MATERIALS AND METHODS 37

3.1 Cell culture and maintenance 38

3.1.1 Cell lines 38

3.1.2 Virus stock 38

3.1.3 Cell culture media and solutions 38

3.1.4 Cell culture and maintenance procedures 41

3.1.4.1 Cultivation of cell lines 41

3.1.4.2 Cryopreservation and thawing 42

3.2 CHIKV stock production 43

3.3 Cell counting and seeding 44

3.3.1 Chemicals and reagents 44

3.3.2 Procedure 44

3.4 CHIKV titration: Plaque assay 45

3.4.1 Chemicals and reagents 45

3.4.2 Virus dilution 46

3.4.3 Virus infection 46

3.4.4 Plaque staining and counting 46

3.5 Determination of multiplicity of infection (MOI) 47

3.6 Optimisation of infection condition 48

3.6.1 Confirmation of infection by indirect immunofluorescence Assay (IIFA) 48

3.6.1.1 Chemicals and reagents 48

3.6.1.2 Procedure 49

3.6.2 Quantitative analysis of cell infection via flow cytometry 50

3.6.2.1 Chemicals and reagents 50

3.6.2.2 Procedure 51

3.6.3 Quantitative analysis of cell death by Annexin V (AV)/ propidium iodide (PI) co-labelling 52

3.6.3.1 Kits and reagents 52

3.6.3.2 Procedure 52

3.7 Optimisation of the condition for secretome sample preparation 54

3.7.1 Kits and reagents 54

3.7.2 MTS cell proliferation assay 54

3.7.3 Dead-cell protease release assay 55

3.8 WRL-68 cell infection for 2-DGE 56

3.8.1 Infection protocol of WRL-68 cells for whole cell proteome study 56

3.8.2 Infection protocol of WRL-68 cells for secretome study 56

3.9 Protein sample processing 57

3.9.1 Protein extraction 57

3.9.1.1 Chemicals and reagents 57

3.9.1.2 Extraction procedure for whole cell proteins 59

3.9.1.3 Extraction procedure for secretome 59
3.9.2 Protein clean-up and quantification 60
3.9.2.1 Kits and reagents 60
3.9.2.2 Protein clean-up: 2-D Clean-Up kit 60
3.9.2.3 Protein estimation: Bradford assay 61
3.10 First dimensional electrophoresis: IEF 62
3.10.1 Chemicals and reagents 62
3.10.2 Passive rehydration 62
3.10.3 IEF 63
3.11 Second dimensional electrophoresis: SDS-PAGE 64
3.11.1 Chemicals and reagents 64
3.11.2 Polyacrylamide gel casting 66
3.11.3 Drystrip equilibration 67
3.11.4 SDS-PAGE 67
3.11.5 Silver staining 68
3.11.5.1 Silver staining solutions (For 2 gels) 68
3.11.5.2 Procedure 69
3.11.6 Differential image analysis 70
3.12 MS analysis 71
3.12.1 Chemicals and reagents 71
3.12.2 In-gel trypsin digestion/peptide extraction 73
3.12.3 Desalting with ZipTip® 74
3.12.4 MALDI-TOF/TOF analysis 75
3.12.5 Bioinformatics 75
3.13 Western blot 76
3.13.1 Chemicals and reagents 76

3.13.2 Protein extraction and quantification 79

3.13.3 1-D Western blot 79

3.13.3.1 Gel casting 79

3.13.3.2 SDS-PAGE 80

3.13.3.3 Protein transfer 82

3.13.3.4 Antibody staining 82

3.13.3.5 Image analysis 83

3.13.4 2-D Western blot 83

3.13.4.1 2-DGE 83

3.13.4.2 Protein transfer, staining and image analysis 84

3.14 Real-time qPCR 85

3.14.1 Kits and reagents 85

3.14.2 RNA extraction 86

3.14.3 RNA quantitation 87

3.14.4 Determination of RNA integrity 87

3.14.5 Conversion of RNA to cDNA 88

3.14.6 Primer amplification efficiency test 89

3.14.7 Quantitation of mRNA expression 91

4.0 RESULTS 92

4.1 Determination of virus titre by plaque assay 93

4.2 Optimisation of infection condition for early host response study 95

4.2.1 Morphological changes of WRL-68 cells upon CHIKV infection 95

4.2.2 Confirmation of CHIKV infection in WRL-68 cells via IIFA 98

4.2.3 Quantitative analysis of infection via flow cytometry 101

4.2.4 Quantitative analysis of cell death via AV/PI co-labelling 105
4.3 Optimisation of sample harvesting for secretome study 109
4.3.1 Effect of serum deprivation on cell viability 109
4.3.2 Effect of serum deprivation and CHIKV infection on cell membrane integrity 109
4.4 Comparative proteomic study 112
4.4.1 Differential protein expression of CHIKV-infected WRL-68 whole cell proteome and secretome 112
4.4.2 MS identification of differentially expressed proteins 120
4.4.3 Functional classification and sub-cellular location distribution of altered proteins 128
4.4.4 Protein network analysis 131
4.4.5 Protein validation by Western blot analysis 135
4.5 Transcript expression analysis 138
4.5.1 Determination of RNA purity and integrity 138
4.5.2 Primer efficiency test 138
4.5.3 Real-time qPCR of differential mRNA expression 140

5.0 DISCUSSION 143

6.0 CONCLUSION 161

REFERENCES 164

APPENDICES 179

LIST OF FIGURES

Figure		Page
2.1	CHIKV genome and its products	8
2.2	Transmission cycles of CHIKV	10
2.3	Replication cycle of CHIKV in mammalian host cells	12
2.4	Geographic distribution of CHIKV genotypes	14
2.5	Typical symptoms experienced by patients	17
2.6	Dissemination of CHIKV in vertebrates	22
2.7	Schematic diagram of the conventional 2-DGE workflow	30
4.1	Plaque titration of CHIKV in Vero cells at different dilutions	94
4.2	Morphological changes of WRL-68 cells infected with CHIKV	96
4.3	Confirmation of CHIKV infection through anti-CHIK mAb 3E4 immunostaining	99
4.4	Representative flow cytometric dot plots of mock control and CHIKV-infected WRL-68 cells at different MOI at 24 and 48 hours post-infection	102
4.6	Representative AV/PI flow cytometric dot plots of mock and CHIKV-infected WRL-68 cells at different MOI at 24 and 48 hours post-infection	106
4.7	Mean percentage of cell death (%) of WRL-68 cells infected at different MOI at 24 and 48 hours post-infection	108

4.8	Relative cell viability of WRL-68 cells grown in DMEM growth medium (10% FBS) and serum-free medium for 24 hours	110
4.9	Relative percentage of cell lysis between WRL-68 cells incubated in DMEM growth medium, serum-free medium and CHIKV-infected cells incubated in serum-free medium for 24 hours	111
4.10	Representative proteome map of WRL-68 whole cell proteome	114
4.11	Expanded views showing the location of differentially expressed spots on the mock control and CHIKV-infected WRL-68 whole cell proteome gels	115
4.12	Representative proteome map of WRL-68 secretome	117
4.13	Expanded views showing the location of differentially expressed spots on the mock control and CHIKV-infected WRL-68 secretome gels	118
4.14	Functional classification of differentially expressed proteins from the whole cell proteome (A) and secretome (B) samples.	129
4.15	Sub-cellular distribution of differentially expressed proteins from the whole cell proteome (A) and secretome (B) samples.	130
4.16	Whole cell proteome (A) and secretome (B) networks showing functional linkages between identified proteins	132
4.17	Western blot validation of CDK1, PDHA1 and RAN proteins	136
4.18	Representative gel profile of intact total RNA samples extracted from mock control and CHIKV-infected cells for whole cell proteome study	139

LIST OF TABLES

Table		Page
3.1	IEF protocol for whole cell proteome samples	63
3.2	IEF protocol for secretome samples	63
3.3	Recipe for casting two 12.5% polyacrylamide gels	66
3.4	SDS-PAGE running protocol	67
3.5	Recipe for casting the resolving gel solution (12% polyacrylamide gel)	81
3.6	Recipe for casting the stacking gel solution (4% polyacrylamide gel)	81
3.7	IEF protocol for secretome samples	83
3.8	Volume of components required per reaction	88
3.9	Real-time qPCR protocol	90
4.1	List of differentially expressed proteins in the whole cell proteome sample identified by MALDI-TOF/TOF MS	122
4.2	List of differentially expressed proteins in the secretome sample identified by MALDI-TOF/TOF MS	126
4.3	GO enrichment analysis of biological processes involved in the whole cell proteome and secretome networks	134
4.4	Comparison of real-time qPCR and proteomics results for 36 selected proteins from the whole cell proteome sample	141
4.4	Comparison of real-time qPCR and proteomics results for 36 selected proteins from the secretome sample	142

LIST OF ABBREVIATIONS

ACN	Acetonitrile
AMP	Adenosine monophosphate
ANOVA	Analysis of variance
APS	Ammonium persulphate
ATCC	American Type Culture Collection
AV	Annexin V
BCA	Bicinchoninic acid
BSA	Bovine serum albumin
C	Capsid
CBB	Coomassie brilliant blue
CD	Cluster of differentiation
CDKs	Cyclin-dependent kinases
cDNA	Complementary DNA
CHAPS	3-[(3-cholamidopropyl) dimethyl-ammonio]-1-propanesulfonate
CHCA	α-Cyano-4-hydroxycinnamic acid
CHIK	Chikungunya
CHIKV	Chikungunya virus
cm	centimetre
CMV	Cytomegalovirus

CNS	Central nervous system
CO_2	Carbon dioxide
CPE	Cytopathic effect
CTL	Cytotoxic T lymphocytes
Da	Dalton
ddH_2O	De-ionised water
dH_2O	Distilled water
DEN	Dengue
DENV	Dengue virus
DNA	Deoxyribonucleic acid
DMAPP	Dimethylallyl pyrophosphate
DMEM	Dulbecco's Modified Eagle Medium
DMSO	Dimethyl sulfoxide
DTT	Dithiothreitol
E	Envelope
ECM	Extracellular matrix
ECSA	East/Central/South African
EDTA	Ethylenediaminetetraacetic acid
EF	Elongation factor
e.g.	*Exempli gratia* (For example)

ELISA	Enzyme-linked immunosorbent assay
ER	Endoplasmic reticulum
ESI	Electrospray ionisation
EST	Expressed sequence tag
EtBr	Ethidium bromide
FBS	Foetal bovine serum
FDR	false discovery rate
FITC	Fluorescein isothiocyanate
FITC-A	Fluorescein isothiocyanate-Area
FSC	Forward scatter
g	Gram
g	Gravity
GO	Gene ontology
h	Hour
HCl	Hydrochloric acid
HCV	Hepatitis C virus
HEPES	4-(2-hydroxyethyl)-1-piperazineethanesulfonic acid
HLA	Human leukocyte antigen
hnRNP	Heterogeneous nuclear riboprotein
HRP	Horseradish peroxidase

IAA	Iodoacetamide
IEF	Isoelectric focusing
IIFA	Indirect immunofluorescence assay
IFN	Interferon
IgG	Immunoglobulin G
IIFT	Indirect immunofluorescence test
IL	Interleukin
IL1rα	Interleukin-1 receptor antagonist
IL2RA	Interleukin-2 receptor alpha
IMP	Inosine monophosphate
IPG	Immobilised pH gradient
IPP	Isopentenyl pyrophosphate
J	Junction
kb	Kilobase
kDa	KiloDalton
L	Litre
LC	Liquid chromatography
LDL	Low-density lipoprotein
M	Molarity
mA	Milliampere

mAb	Monoclonal antibody
MALDI	Matrix assisted laser desorption/ionisation
mg	Milligram
MHC	Major histocompatibility
MIF	Migration inhibitory factor
min	Minutes
MIP-1β	Macrophage inflammatory protein-1β
ml	Millilitre
mM	Millimolar
MMPs	Matrix metalloproteinases
MOI	Multiplicity of infection
M_r	Molecular mass
mRNA	Messenger RNA
MS	Mass spectrometry
MTS	3-(4,5-dimethylthiazol-2-yl)-5-(3-carboxymethoxyphenyl)-2-(4-sulfophenyl)-2H-tetrazolium)
NaCl	Sodium chloride
NCBI	National Centre for Biotechnology Information
ng	Nanogram
NIAID	National Institute of Allergy and Infectious Diseases

nm	Nanometre
NSAIDS	Non-steroidal anti-inflammatory drugs
NSD	No significant differences
nsP	Non-structural protein
NTC	Non-template control
ORF	Open reading frame
PBS	Phosphate buffered saline
PCR	Polymerase chain reaction
PES	Polyethersulfone
pfu	Plaque forming unit
pH	Power of hydrogen
pI	Isoelectric point
PI	Propidium iodide
PKR	Protein kinase R
PMF	Peptide mass fingerprinting
ppm	Parts per million
PRPP	Phosphoribosylpyrophosphate
PVDF	Polyvinylidene fluoride
Q	Quadrant
qPCR	Quantitative PCR

RANTES	Regulated on activation, normal T cell expressed and secreted
RC	Replication complex
RLU	Relative luminescence unit
RNA	Ribonucleic acid
rRNA	Ribosomal RNA
ROS	Reactive oxygen species
RT	Reverse transcription
RT-PCR	Reverse transcription polymerase chain reaction
SD	Standard deviation
SDS-PAGE	Sodium dodecyl sulphate-polyacrylamide gel electrophoresis
sec	Seconds
SIB	Swiss Institute of Bioinformatics
SSC	Side scatter
STRING	Search Tool for the Retrieval of Interacting Genes/Proteins
TBE	Tris/Borate/EDTA
TBST	Tris-buffered saline with Tween-20
TCA	Tricarboxylic acid
TCA	Trichloroacetic acid
TEMED	Tetramethylethylenediamine
TFA	Trifluoroacetic acid

ThBMEC	Transfected human brain microvascular endothelial cells
TNF	Tumour necrosis factor
TOF	Time-of-flight
TPB	Tryptose phosphate broth
UPP	Ubiquitin-proteasome pathway
V	Voltage
Vhr	Voltage-hour
VSV	Vesicular somatitis virus
1-D	1-dimension
2-D	2-dimension
2-DGE	2-dimensional gel electrophoresis
α	Alpha
β	Beta
γ	Gamma
m/z	Mass-to-charge
µg	Microgram
µM	Micromolar
µm	Micrometer
µl	Microlitre

°C	Degrees Celsius
%	Percentage

CHAPTER 1

INTRODUCTION

Previously a non-fatal and relatively benign disease, chikungunya (CHIK) has emerged as a potential global threat, as evidenced by sudden outbreaks of unprecedented magnitude over the past decade, with greater morbidity seen in each successive outbreak. Since its first appearance in 1953, many countries have reported its re-emergence, including Malaysia, Indonesia, Thailand, India and the Réunion Island, with more than seven million reported cases to date. Recent epidemiological documentation provided further evidence of the spread of CHIK infection to temperate countries such as Italy, Australia and the United States, where sporadic outbreaks have been reported. Deaths attributed to complications of this disease are no longer unheard of, and the fatality rate is now estimated to be 1:1000 cases. Moreover, most surviving patients are often incapacitated by recurring polyarthralgia that persists for years. Combining these factors altogether, it can be said that the epidemiological and socioeconomic burden brought about by this disease is a great cause for concern, and is beginning to garner researchers' attention worldwide.

The causative agent for this viral infection is chikungunya virus (CHIKV), an arbovirus belonging to the genus *Alphavirus* and family *Togaviridae.* The genome of the virus comprise a small, positive sense, single-stranded RNA of approximately 11.8 kb in length, organised as 5' cap-nsP1-nsP2-nsP3-nsP4-(junction region)-C-E3-E2-6K-E1-poly(A) 3'. Transmitted by the same vectors responsible for the dissemination of dengue virus, namely *Aedes aegypti* and *Aedes albopictus*, CHIKV causes an acute illness in humans, with fever, maculopapular rash, arthralgia and myalgia being the hallmark symptoms. More severe, yet unusual clinical manifestations such as neurological complications have also been reported, suggesting the emergence of a new disease. To date, palliative treatment is the only available means to treat patients, as no effective antiviral drug or vaccine has yet to be developed. Given the lack of preventive

or therapeutic measures along with the recurring emergence and rapid spread of infection, it is not surprising that CHIK is now regarded as a potential global health problem.

Despite extensive research over the past several years, much is still unknown about the biology and mechanisms behind CHIKV pathogenesis. To unravel and comprehend key aspects of the infection, it is important to first grasp the mechanisms by which the virus interacts with its human host, and how the human host responds to the foreign pathogen. Different approaches have been pursued in attempts to elucidate virus-host interaction, one of which is through proteomic study. Termed as 'the large-scale study of total proteins', proteomics is the leading tool used to study structure, function, and control of biological processes and pathways via analysis of the cellular proteome. This approach has been successfully employed to study host responses towards numerous pathogenic viruses including hepatitis C and dengue virus.

Given the scarcity of knowledge on the association between CHIKV and its human host in general, and the promising results obtained in other studies using proteomic approaches as the tool of study, it is therefore of great interest to look into changes in global protein profiles of the host cells during CHIKV infection. Previous proteomic studies have looked at the host response during the late stages of CHIKV infection. The present research endeavours to look at the proteins involved during early stages of infection using WRL-68 cell line as the *in vitro* model. To attain a more comprehensive overview of the proteins contributing to the observed pathogenesis, the whole cell proteome and secretome profiles were investigated using 2-dimensional gel electrophoresis (2-DGE) as the study platform, coupled with real-time quantitative polymerase chain reaction (real-time qPCR) analysis of transcriptional profiles of the

altered proteins. In line with the general purpose of this research, several specific objectives were set, as stated below:

i) To optimise the infection conditions (Multiplicity of infection (MOI) and time-point) for protein sample collection for early infection study.

ii) To generate and compare global proteome profiles of whole cell proteome and secretome between CHIKV-infected and mock control WRL-68 cells.

iii) To identify and validate differentially expressed proteins via mass spectrometry (MS) and Western blot, respectively.

iv) To analyse the mRNA expression of selected differentially expressed proteins.

v) To investigate the functional roles of altered proteins and their potential relation to the pathogenesis of CHIKV using pathway analysis software.

CHAPTER 2

LITERATURE REVIEW

2.1 CHIKV

CHIKV belongs to the *Alphavirus* genus of the *Togaviridae* family. It is a part of the Semliki Forest virus group of the Old World Alphavirus, also known as arthritogenic alphavirus, which causes polyarthritis in infected patients (Schwartz & Albert, 2010). The name Chikungunya is derived from the Makonde language, meaning 'to walk bend over', which is attributed to the painful arthralgia that can persist for months (Chevillon *et al.*, 2008). This arbovirus (arthropod-borne virus) has been re-emerging and spreading throughout Asia, Africa and parts of Europe, and is listed as a category C priority pathogen by the National Institute of Allergy and Infectious Diseases (NIAID) (Wang *et al.*, 2008). Category C priority pathogens are the third highest priority pathogens that pose a global health threat as they can be engineered for mass dissemination due to their ease of production and dissemination, availability and the potential in causing high mortality and morbidity rates (NIAID, 2012).

2.1.1 CHIKV classification

Based on phylogenetic analysis of the E1 gene sequence, CHIKV can be clustered into three main genotypes: West African, Asian and East/Central/South African (ECSA) genotype (Tsetsarkin *et al.*, 2007). The West African genotype was determined to be the ancestral cluster, appearing between 150 and 1350 years ago. The ECSA genotype diverged from the ancestral genotype between 100 and 800 years ago, while the Asian genotype evolved from the ECSA variants approximately 50 to 430 years ago (Powers *et al.*, 2000). The ECSA and West African genotypes are the primary clusters causing epidemics/outbreaks in Africa whereas the ECSA and Asian genotypes are the predominantly circulating phylogroups in Asia (Singh & Unni, 2011).

2.1.2 Viral structure and genome organisation

CHIKV is small, about 50-70 nm in diameter, and has an icosahedral-like nucleocapsid surrounded by a lipid bilayer envelope derived from the host plasma membrane (Simizu *et al.*, 1984). The nucleocapsid contains the single-stranded, positive sense RNA genome which is approximately 11.8 kb in size and has two open reading frames (ORFs) (Singh & Unni, 2011). The first ORF in the 5' end encodes for the non-structural proteins (nsP1, 2, 3 and 4) in the form of two polyprotein precursors whereas the second ORF in the 3' end encodes for the structural polyproteins (Capsid (C) and envelope (E) proteins; E1, E2, E3) (Pardigon, 2009), as shown in Figure 2.1. The 5' end is capped with 7-methylguanosine while the 3' is polyadenylated (Khan *et al.*, 2002). The CHIKV genome also has an untranslated junction (J) region in between the two ORFs and a small peptide 6K of unknown functions (Singh & Unni, 2011).

The functions of alphaviral proteins are well characterised. Non-structural protein 1, nsP1, is involved in RNA capping and synthesis of the negative sense viral RNA (Salonen *et al.*, 2005), while nsP2 possesses RNA helicase and protease activities (Pastorino *et al.*, 2008). The macro-domain containing nsP3 is a part of the helicase unit whereas nsP4 is the viral RNA polymerase. The E1 and E2 structural glycoproteins function in mediating virus-host cell membrane fusion and interaction with host cellular receptors, respectively. E3 protein, conversely, is involved in proper folding of precursor E2 and its association with E1 protein (Schwartz & Albert, 2010).

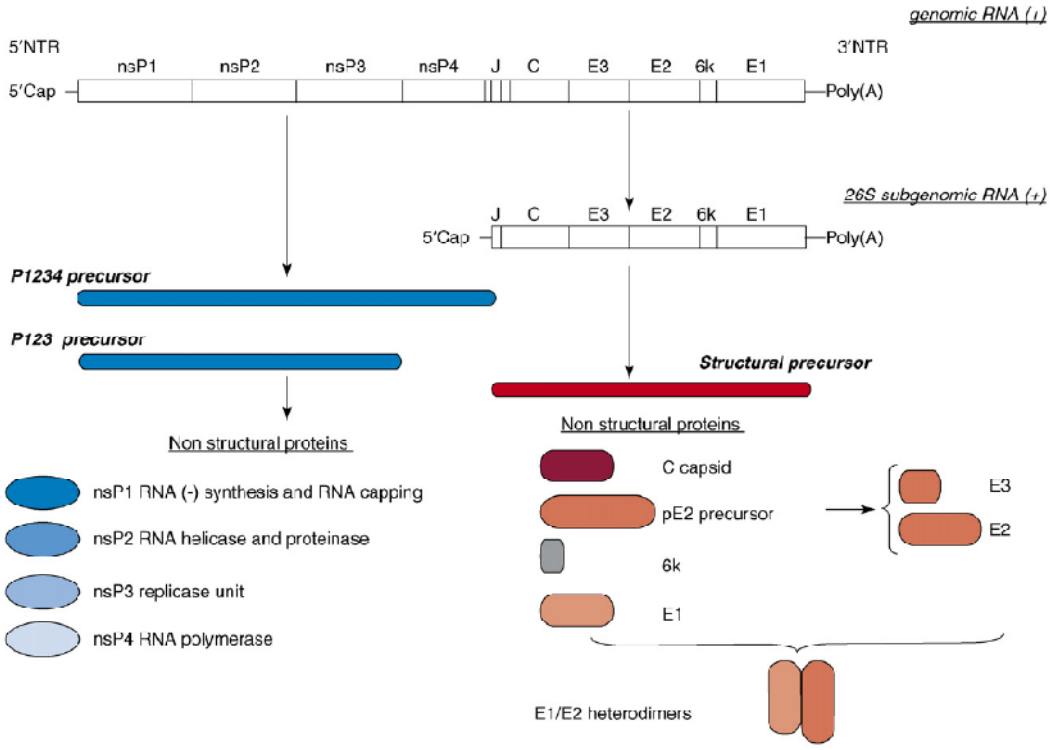

Figure 2.1: CHIKV genome and its products (Adapted from Chevillon *et al.*, 2007)

2.1.3 Transmission cycle

CHIKV is transmitted via two cycles, the sylvatic cycle (animal-mosquito-animal) and urban cycle (man-mosquito-man), as illustrated in Figure 2.2. The virus is transmitted and maintained in the sylvatic cycle in Africa, involving forest dwelling *Aedes* species (e.g. *Ae. furcifer-taylori*, *Ae. africanus* and *Ae. dalzieli*), and wild primates (e.g. baboons and chimpanzees), squirrels, birds and rodents (Thiboutot *et al.*, 2010). In Asia, CHIKV transmission occurs through the urban cycle, with the primary anthropophilic mosquito vectors being *Ae. aegypti* and *Ae. albopictus* (Singh & Unni, 2011). CHIKV maintenance outside epidemic or outbreak periods is primarily associated with the urban cycle and virus persistence is attributed to continuous introduction of CHIKV to new areas with immunologically naive population (Tsetsarkin *et al.*, 2011). Nevertheless, recent isolation of CHIKV from wild monkeys in Malaysia suggests the possible existence of the sylvatic cycle in Asia (Apandi *et al.*, 2009).

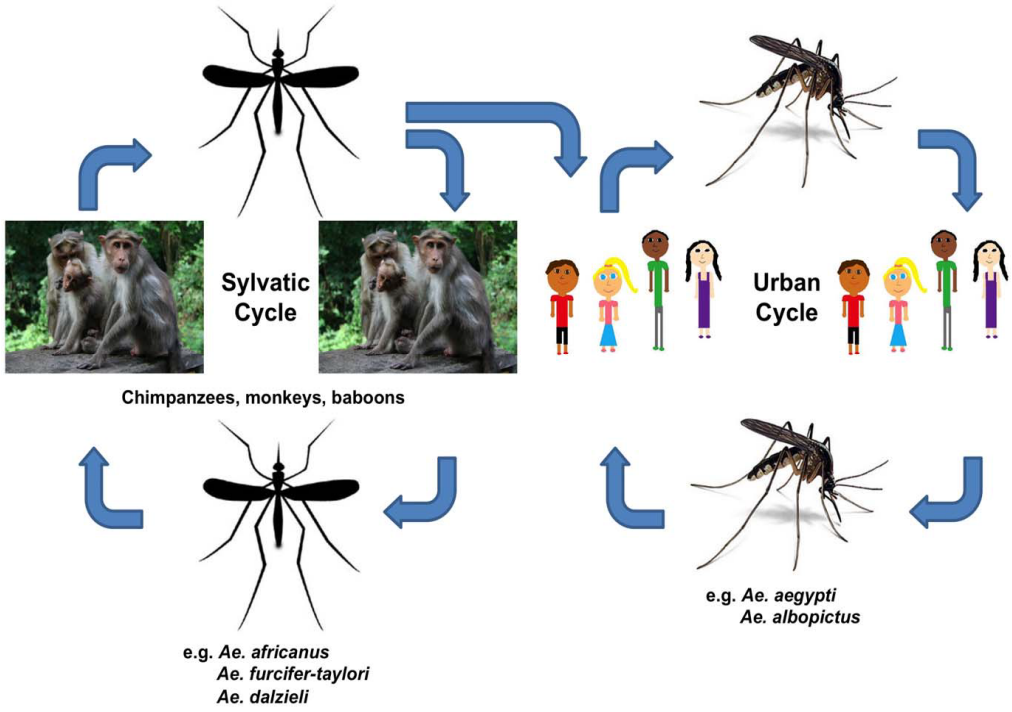

Figure 2.2: Transmission cycles of CHIKV (Adapted from Thiboutot *et al*., 2010)

2.1.4 Replication cycle of CHIKV

Viral replication is initiated from the moment the virus envelope attaches to the cellular host receptors (Strauss & Strauss, 1994). A study conducted by Bernard and colleagues in 2010 revealed that CHIKV replication in mammalian cells occurs via the epidermal growth factor receptor substrate 15 (Eps15)-dependent receptor mediated endocytosis. During viral entry, the virus fuses with the host membrane at low endosomal pH, upon which the viral nucleocapsid is released into the cytoplasm (Bernard *et al.,* 2010). Translation of nsP123 in the early stage of replication leads to formation of replication complex (RC) upon binding to free nsP4. The full length minus strand is formed from the RC for further production of the positive strand RNA (Singh & Unni, 2011).

During the late stage of replication, nsP123 is cleaved to yield mature non-structural proteins. Along with the host cell proteins, these proteins act as the plus strand replicase to produce the 26S subgenomic plus strand RNA. This RNA encodes the polyprotein precursor for the structural proteins, which upon production is further processed in the Golgi complex and transported to the plasma membrane. Viral RNA is packed into the nucleocapsid in the cytoplasm and mature virions bud out of the plasma membrane, the envelope proteins acquired during the budding process (Singh & Unni, 2011). Viral replication is rapid, each cycle completed within four hours (Edwards *et al.,* 2007). The schematic diagram in Figure 2.3 illustrates CHIKV replication in host cells.

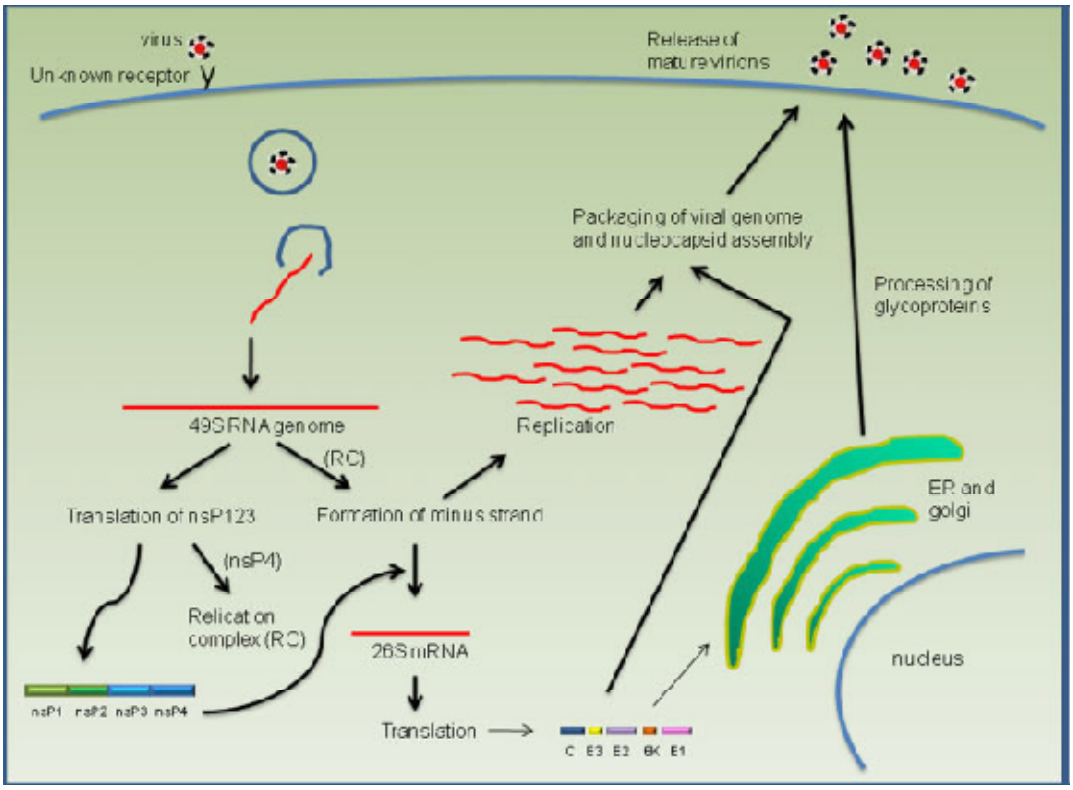

Figure 2.3: Replication cycle of CHIKV in mammalian host cells

(Adapted from Singh & Unni, 2011)

2.2 Epidemiology of CHIKV infection

CHIKV was first isolated from a febrile patient during a dengue outbreak in Newala district, Tanzania, in 1953 (Khan, *et al.*, 2002). Within the next five decades, recurring outbreaks and epidemics have been reported in Africa and Asia, the most recent being the epidemics and outbreaks in Congo (50,000 cases from 1999 to 2000) (Pastorino *et al.*, 2004), Indonesia (5821 cases from 2001 to 2003) (Laras *et al.*, 2005), India (1.4-6.5 million cases from 2006 to 2007) (Mavalankar *et al.*, 2007) and Thailand (42,000 cases in 2009) (Tiawsirisup, 2011). Increase in global travel, inadequate mosquito control and climatic conditions have also led to the spread of CHIKV to non-endemic regions including Europe, Australia and the United States (Thiboutot, *et al.*, 2010), as depicted in Figure 2.4. A debilitating outbreak struck the French Réunion Island from 2005 to 2006, infecting more than one third of its population and killing 284 people (Renault *et al.*, 2007). Meanwhile, small sporadic outbreaks were reported Italy in 2007, with over 200 reported CHIKV infection cases (Rezza *et al.*, 2007), and in Réunion Island again in 2010, with over 100 reported cases (D'Ortenzio *et al.*, 2011).

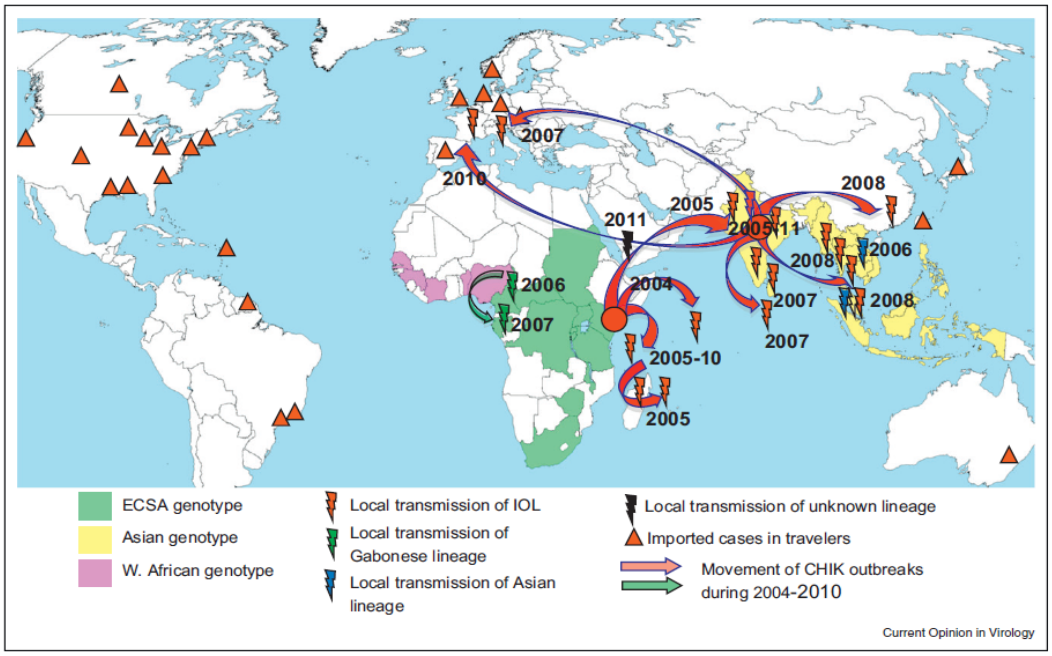

Figure 2.4: Geographic distribution of CHIKV genotypes

The movement and dissemination of CHIK outbreaks during 2004-2011 are depicted by the arrows, whereas countries with imported cases of CHIKV are denoted in triangles. (Adapted from Tsetsarkin *et al*., 2011)

In Malaysia, three separate outbreaks have been reported within the last 15 years. The first documented outbreak was in Klang district in Selangor in 1998 (51 cases) (Lam *et al.*, 2001), followed by a second outbreak in Perak in 2006 (49 confirmed cases) and the latest was in Tangkak, Johor in 2008 (2964 confirmed cases). Clusters of infection cases have also been reported all over the Peninsular and in Sarawak from 2008 onwards, believed to have spread from the Johor outbreak, with more than 6000 confirmed cases by the end of 2009 (Chua, 2010). From January 2010 to July 2011, the number of reported cases have declined to 823 cases (MOH, 2010, 2011). In February 2012, the virus resurfaced again, causing a small sporadic outbreak in Kuang, Selangor, involving 22 students and lecturers from a private college (MOH, 2012).

Phylogenetic analysis of the E1 glycoprotein sequence derived from CHIKV isolated during the three outbreaks revealed that strains from the Asian genotype were responsible for the Klang and the early 2006 Perak outbreaks. However, CHIKV isolated from patients during the late 2006 Perak and the 2008 to 2009 Johor outbreaks were of the ECSA genotype (Noridah *et al.*, 2007). The ECSA clustered strains responsible for the late 2006 Perak outbreak were imported from India, as contact tracing identified the patient who was the source of the virus to be from the Indian continent, whereas strains accountable for the Johor outbreak were believed to be introduced independently (Lim, 2010).

2.3 Clinical manifestation

The incubation period for CHIKV is short, requiring only two to six days, with symptoms showing on day four onwards (Ziegler *et al.*, 2008). CHIKV infection is mostly symptomatic, with asymptomatic infection reported in only 3-25% of patients (Chia *et al.*, 2010). Upon infection, CHIK tends to present itself in two phases. The first phase or the acute phase is heralded by sudden onset of high fever, maculopapular rash and arthralgia (Figure 2.5). The chronic phase occurs after infection is resolved, whereby more than 95% of patients are incapacitated by the disabling polyarthralgia, often from months to years (Thiboutot, *et al.*, 2010). Recurrent arthralgia and myalgia are typical long-term symptoms experienced by patients (Ozden *et al.*, 2007).

Atypical clinical presentations associated with CHIK infection have been observed in the recent outbreaks, including neurological complications such as encephalitis, myelopathy and myopathy (Chandak *et al.*, 2009), encephalopathy- and myelitis-associated central nervous system (CNS) infections (Arpino *et al.*, 2009), acute nephritis (Solanki *et al.*, 2007) and severe acute hepatitis (Garnier *et al.*, 2006). These severe complications were found to occur more prevalently in patients above 65 years of age and those with underlying medical conditions such as diabetes, alcoholic liver disease and ischemic heart disease (Chia, *et al.*, 2010).

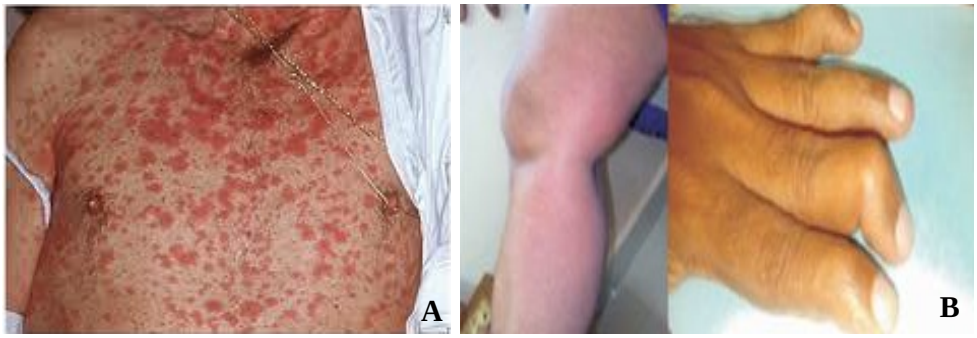

Figure 2.5: Typical symptoms experienced by patients (A: Maculopapular rash and B: Arthralgia)

Death is not a common characteristic of CHIK infection and has not been attributed directly to the virus infection, although mortalities associated with atypical complications caused indirectly by the infection have been reported in the recent Réunion Island outbreak (Economopoulou *et al.*, 2009). In Malaysia, the first death was reported in 2010, whereby the patient suffered from severe systemic infection involving the liver, leading to eventual circulatory collapse (Chua, 2010). The risk of death due to atypical complications is higher among neonates, the elderly and adults with pre-existing conditions due to their weakened immune system (Schwartz & Albert, 2010).

Mother-to-child-transmission of CHIKV was first reported in the Réunion Island outbreak. Ramful and colleagues discovered that vertical transmission rate is higher when delivery occurs during the viraemic period, with the risk of infection increasing to 50%. Foetuses were also susceptible to CHIKV infection during perinatal period. Transmission during birth was found to occur irrespective of the delivery method, and is postulated to take place transplacentally. Infected neonates displayed symptoms four days after birth, and while most suffered from typical infection which resolved within two weeks, some developed complications such as hemorrhagic syndromes, seizures and encephalopathy (Ramful *et al.*, 2007).

Association between blood group and susceptibility to CHIKV infection was recently investigated. Rhesus positive individuals, particularly those with O positive blood group were more vulnerable to CHIKV infection than their Rhesus negative counterparts (Lokireddy *et al.*, 2009). In a separate study, similar findings were obtained, although most infected Rhesus positive individuals were of the AB and A blood type (Kumar *et al.*, 2010). The role of blood group antigens in CHIKV disease development however, requires further investigation.

2.4 Prevention and treatment

There are currently no commercially licensed vaccines or antiviral therapies available to combat this infectious disease. Therefore, palliative treatment is administered to patients to relieve their symptoms. Analgesics, antipyretics and anti-inflammatory agents are given to treat the classic CHIK symptoms; fever and arthralgia. These pharmacological agents include paracetamol, non-steroidal anti-inflammatory drugs (NSAIDS) such as ibuprofen and indomethacin, as well as corticosteroids. Due to reports of possible haemorrhagic manifestations of the infection, aspirins are not prescribed to patients (Powers & Logue, 2007; Tesh, 1982). In cases where a patient's arthritis is unresolved or refractory to NSAIDs, administration of 250 mg of chloroquine was proven to be helpful (Brighton, 1984). Mild exercise is recommended to improve stiffness and morning arthralgia (Chhabra *et al.*, 2008), whereas bed rest and fluids promote faster recuperation (Cavrini *et al.*, 2009).

Due to the lack of cure, prevention remains the best weapon against CHIKV infection. Controlling mosquito vector breeding remains a challenge albeit being the most effective measure in reducing the spread of CHIKV, due in part to the ubiquitous nature of the *Aedes* mosquito species and the ability of CHIKV to adapt to different species through genetic evolution. Current control measures rely heavily in reducing the number of artificial water-filled container habitats that support mosquito breeding (Singh & Unni, 2011). Personal protection from mosquito bites via fogging, wearing long-sleeve clothes and the use of repellents and insecticides are also practiced to minimise exposure to infected mosquitoes (Her *et al.*, 2009). Epidemiological and vector surveillance should be intensified for early detection of new cases and monitoring of vector population and infestation, allowing effective and proper control measures to be implemented (Cavrini, *et al.*, 2009; Chhabra, *et al.*, 2008).

2.5 Current status of CHIKV research

In light of the aggressive outbreak in India and the French Réunion Island, researchers from various expertise and research fields are united in a multidisciplinary effort to understand the biology of CHIKV and its interaction with the human host and mosquito vector. Recent research highlights include findings pertaining virus tropism in human host cells, CHIKV genetic evolution, CHIKV-host immune interaction and development of vaccine and antiviral treatment.

2.5.1 CHIKV cellular and tissue tropism

In vitro studies in the 1960s to 1980s revealed CHIKV to be highly pathogenic in a wide array of non-human cell lines, including Vero monkey kidney cells, BHK21 hamster kidney cells, chick embryo cells and L292 mouse fibroblast-like cells (Hahon & Zimmerman, 1970; White *et al.*, 1972). Sourisseau and colleagues recently studied CHIKV tropism in a panel of human primary and non-primary cell lines to determine CHIKV tropism in human. Using four clinical strains from the Réunion Island outbreak, CHIKV was found to induce rapid apoptosis in most adherent human cell lines (ThBMEC bone marrow endothelial cells, MRC5 primary lung fibroblasts, BEAS-2B bronchial epithelial cells, HeLa cervical carcinoma cells, 293T kidney epithelial cells and Hs 789.Sk primary skin fibroblasts), but was refractory in monocytoid (THP-1 and U937 cells) and lymphoid (Jurkat cells) cell lines, lymphocytes (Primary $CD4^+$ T cells), monocytes (Primary $CD14^+$ cells) and monocytes-derived dendritic cells. The absence of infection was associated with poor binding of CHIKV to target cells. The observed findings are likely caused by the lack of receptors required for viral attachment to the cell surface, indicating that the unknown receptor is not ubiquitously found in all cell types (Sourisseau *et al.*, 2007).

In vivo study in neonates and type I interferon (IFN) deficient adult mice by Couderc and colleagues revealed that CHIKV primarily targets muscle, joint and skin fibroblast, as well as the liver, spleen and brain (Figure 2.6). Liver was found to be the main target organ for viral replication during early infection, as indicated by high viral titer within the first two days of infection. In fact, liver was determined to be the only organ infected during early infection, suggesting that this organ may serve as a reservoir for rapid viral replication before dissemination to other target organs. CNS infection was also observed in severe cases of infection, gaining access through the choroid plexuses. Their findings suggest that the classical symptoms of CHIK closely reflect CHIKV tissue tropism in contrast to other acute viral infections in which symptoms predominantly reflect the systemic immune response (Couderc *et al.*, 2008).

Immunohistological study of muscle biopsies from two patients exhibiting myositic syndrome during the acute and recurrent phases of CHIK found CHIKV exclusively inside the skeletal muscle progenitor cells (satellite cells), and not in muscle fibers. CHIKV persistence in the progenitor cells was demonstrated by detection of viral antigen in biopsied muscle specimens from a patient who developed the infection three months back and was suffering from recurrent myalgia. This suggests that these cells may serve as small reservoirs for the virus and virus-encoded components, plausibly accounting for the recurrent myalgia observed in many patients. Further *in vitro* study to determine CHIKV ability to replicate in the satellite cells showed that this arbovirus was selective towards undifferentiated satellite cells as differentiated myotube cultures were refractory (Ozden, *et al.*, 2007). Regardless, further studies are required to elucidate the role of viral persistence and selectivity towards satellite cells and its relation to the observed clinical symptoms.

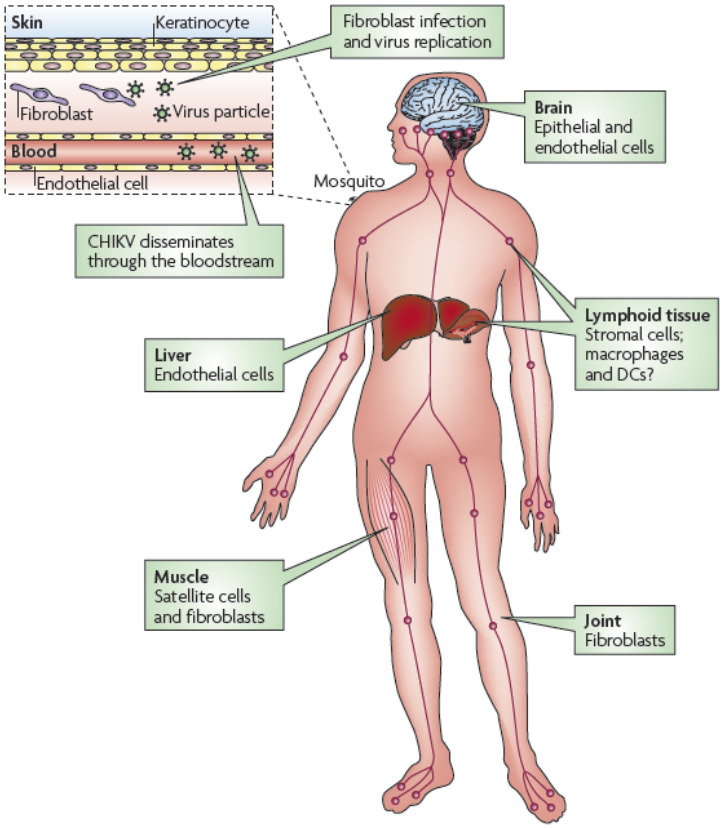

Figure 2.6: Dissemination of CHIKV in vertebrates

CHIKV transmission occurs immediately after the patient is bitten by CHIKV-infected mosquito. CHIKV replicates in the skin fibroblasts prior to dissemination to the target organs. The target cells are indicated for each tissue (Adapted from Pardigon, 2009)

2.5.2 CHIKV genetic mutation and evolution

Like most RNA viruses, the mutation rate of CHIKV genome is high, given the lack of proof-reading ability of the virus RNA polymerase (Elena & Sanjuan, 2005). Moreover, a single mutation can change the vector specificity, causing potential epidemics or outbreaks. Hence, studying the microevolution of the viral genome can provide important evidence to comprehend the atypical magnitude and virulence of previous outbreaks and to predict future outbreaks.

Genetic adaptation of CHIKV to new mosquito vectors is a probable factor facilitating recent CHIKV emergence (Weaver & Reisen, 2010). The most notable and widely studied mutation is the alanine to valine substitution at position 226 of the E1 glycoprotein (E1-A226V), in a region involved in fusion of viral particles with host endosomal membrane for viral entry. This mutation increased CHIKV adaptability in *Ae. albopictus*, the primary circulating vector in Europe that caused massive outbreaks in Indian Ocean Islands, mainly the Réunion Island (Cavrini, *et al.*, 2009). Strains carrying this mutation was subsequently identified in later outbreaks in India (Cherian *et al.*, 2009), Madagascar (Vazeille *et al.*, 2007) and Italy (Bordi *et al.*, 2008) in 2007, and the re-emerging outbreak in Réunion Island in 2010 (D'Ortenzio, *et al.*, 2011).

The relationship between the A226V mutation and virus adaptability in *Ae. albopictus* has been linked to the abrogation of cholesterol dependence of the virus for propagation in *Ae. albopictus*, which are cholesterol auxotrophs (Schuffenecker *et al.*, 2006). This adaptive mutation had no effect on CHIKV dissemination in the primary vector, *Ae. aegypti*, and only slightly increased its transmission in suckling mice model (Tsetsarkin, *et al.*, 2007). In contrast to the hypothesis that the A226V

mutation is responsible for the increase in symptom severity in patients, CHIKV carrying this mutation was recently determined to be more susceptible towards the innate immune response in non-human primate cells through antiviral action of IFN-α, although its replication kinetics are unaffected (Bordi *et al.*, 2011). Additional studies are required to explore the interplay between this point mutation and the innate defence system in human and its relation to disease severity.

The rapid genomic evolution of CHIKV also allows phylogenetic studies to distinguish different strains of the virus which is helpful in understanding its evolutionary potential and the geographic distribution and dissemination during outbreaks (Zheng *et al.*, 2010). Phylogenetic clustering of CHIKV strains from several outbreaks delineated the virus into three genotypes, while paraphyletic grouping of the African strains validated that CHIKV originated in Africa and subsequently disseminated to Asia (Powers, *et al.*, 2000). Strains and isolates from a particular outbreak have also been reported to show little genetic variation, forming a monophyletic clade. For instance, strains obtained from an outbreak in the Republic of Congo were found to be closely related to strains from previous outbreaks in Central Africa, indicating a strong phylogeographic structuring of CHIKV species (Powers & Logue, 2007).

2.5.3 CHIKV-host immune interaction

The study of CHIKV immune interaction with its human counterpart plays a vital role in understanding the pathophysiology of CHIKV. Chikungunya fever (CHIKF) has been attributed to cytokines such as interleukins (IL-1β, IL-6) and tumour necrosis factor-alpha (TNF-α), which are known pyretics. These inflammatory

cytokines are also postulated to be involved in the recurring arthralgia experienced by CHIKF patients, as they cause rheumatoid arthritis-like inflammation and tissue destruction, which are common symptoms of other alphavirus infections (Kam *et al.*, 2009). Type I IFNs (IFNα/β) have been associated with CHIK infection. A study on type I IFN-impaired mice revealed that severity of the infection depended on the level of IFN impairment, as mice with partially and totally abrogated IFN pathway contracted the mild and severe forms of the infection respectively, while healthy adult wild type mice were found to be resistant (Couderc, *et al.*, 2008). *In vitro* study by Sourisseau *et al.* also demonstrated that both type I and type II (IFN-γ) IFNs limited CHIKV, decreasing virus-induced cytopathic effect (CPE) (Sourisseau, *et al.*, 2007).

Recent *ex vivo* multiplex study involving 50 cytokines, chemokines and growth factor plasma has shed some light on the association between CHIKV infection and the human immune response. Kinetic studies on these inflammatory mediators revealed that CHIKV infection educed strong innate responses involving the production of high levels of antiviral IFN-α. This is followed by activation of the adaptive immune response, as characterised by high levels of IL-4, IL-10 and IFN-γ, and the production of $CD8^+$ T cells during early acute phase. Engagement of the $CD4^+$ T cells mediated response and the elevated levels of anti-inflammatory proteins IL-1 receptor antagonist (IL1rα) and IL-2 receptor alpha (IL2RA), as well as pro-inflammatory proteins such as IL-6, IL-8, regulated on activation, normal T cell expressed and secreted (RANTES), migration inhibitory factor (MIF) and macrophage inflammatory protein-1β (MIP-1β), were observed during the late phase of acute infection. Interestingly, evidence also suggested that CHIKV induced CD95-mediated apoptosis of $CD4^+$ T cells in the first two days of symptoms, as determined by the increased expression of $CD95^+$ in $CD4^+$ T cells (Wauquier *et al.*, 2011).

2.5.4 Vaccine and antiviral development

Development of potential CHIKV vaccine candidates dates back to 1967, where a group of researchers created the formalin-inactivated whole virus vaccine based on the African CHIK 168 strain. Potency test on this first generation vaccine however, generated controversial results (Harrison *et al.*, 1967). In the late 1980s, the second generation vaccine was developed through repeated passaging of CHIKV strain 15561 in MRC5 cells, producing attenuated vaccine TSI-GSD-218 which showed promising results in the phase I and II clinical trials (Edelman *et al.*, 2000; Levitt *et al.*, 1986).

Other alternative vaccine approaches currently being pursued are the chimeric, DNA and adenovirus vaccines. Both the chimeric alphavirus vaccine, which is based on recombination of CHIKV structural gene and alphaviruses such as eastern equine encephalitis virus as the backbone, and the DNA vaccine, provided immunity in mice (Mallilankaraman *et al.*, 2011; Wang, *et al.*, 2008). The recombinant CHIKV glycoprotein-encoded adenovirus vaccine, on the other hand, successfully protected mice against viraemia and also arthritis with a single immunisation (Wang *et al.*, 2011).

Weak base compounds such as chloroquine have been used traditionally to impair infectivity of alphaviruses (Her, *et al.*, 2009). Although chloroquine was shown to reduce CHIKV growth *in vitro*, it failed the Phase III clinical trial (Sourisseau, *et al.*, 2007). Another study on four compounds (ribavirin, IFN-α, glycyrrhizin and 6-azauridine) previously shown to elicit antiviral activities against flaviviruses, exhibited potent inhibition towards CHIKV *in vitro*. Moreover, combination of ribavirin and IFN-α showed synergistic effect, and warrants further investigation as a potential antiviral drug (Briolant *et al.*, 2004; Crance *et al.*, 2003).

2.6 Proteomics

The importance of studying proteins came to light following the advancement of genomic sequencing when researchers realised that having complete genome sequences is insufficient to elucidate biological function of cells as proteins are the active agents in cells (Pandey & Mann, 2000). Proteins play vital roles in living organisms, as they are the major components of the metabolic and regulatory pathways of cells, and cells rely on those pathways for survival (Tyagi *et al.*, 2010). Changes in their composition or expression, however minute, may lead to the onset of pathological diseases (Bodzon-Kulakowska *et al.*, 2007). Moreover, almost all drugs are directed against proteins. Ergo, the study of proteins directly contributes to drug development and pathway studies (Pandey & Mann, 2000).

Proteomics is defined as the study of total proteins, termed as 'proteome' by Marc Wilkins in 1994, expressed in a particular cell line, tissue or organism (Dove, 1999; Lee & Lee, 2004). The study of proteome consists of three main approaches, namely expression proteomics, structural/cell-map proteomics and functional proteomics. Expression proteomics, also known as differential expression proteomics, refer to the study of global changes in protein expression levels whereas structural proteomics involve determining the structure of protein complexes or specific proteins present in cellular organelles in attempts to identify all proteins within a complex or organelle, determine their subcellular location and characterise all protein-protein interactions. Meanwhile, functional proteomics serve to study the function of proteins to obtain important information such as protein signalling, disease pathogenesis and protein-drug interactions (Graves & Haystead, 2002). In general, proteomics provide a powerful set of tools aimed to characterise thousands of proteins within cells, tissues, and organisms (Issaq & Veenstra, 2008).

2.6.1 Tools of proteomics

Identification and characterisation of proteins were made possible by the development and integration of three imperative tools: i) Mass spectrometry (MS), ii) Analytical protein separation technology and iii) Bioinformatics tools (Liebler, 2002). The invention of MS is perhaps the most significant breakthrough in proteomics, as it extends analysis far beyond the mere display of proteins. MS is an analytic tool used to identify proteins, where the associated instrument (a mass spectrometer) measures the masses of molecules converted into ions via the mass-to-charge (m/z) ratio (Sellers & Miecznikowski, 2010). Development of mass spectrometry replaces the conventional Edman degradation method of identifying proteins, enabling high-throughput protein identification (Pandey & Mann, 2000).

Analytical separation techniques function to resolve complex protein mixtures into individual components, as well as allowing comparison of protein levels between two or more samples (Liebler, 2002). The main separation techniques used today are the conventional 2-DGE and gel-free based approaches such as multidimensional liquid chromatography (LC) (Monteoliva & Albar, 2004). Bioinformatics tools such as databases for protein identification, 2-D gels, as well as protein and genome-sequence databases, for example Swiss-Prot and the National Center for Biotechnology Information (NCBI), play essential roles in interpreting the massive amounts of data and expression information generated through proteomics analyses (Vihinen, 2001).

2.6.2 2-DGE

Introduced by O'Farrell in 1975, 2-DGE involves separating proteins based on two independent parameters; i) Isoelectric point (pI) in the first dimension via isoelectric focusing (IEF) and ii) Molecular mass (M_r) in the second dimension by sodium dodecyl sulphate-polyacrylamide gel electrophoresis (SDS-PAGE) (Beranova-Giorgianni, 2003). The resulting separations allow a complex protein mixture to be resolved into their respective protein represented as a single spot on the SDS-PAGE gel (Monteoliva & Albar, 2004). 2-DGE has been instrumental in changing the paradigm and boosting the development of proteomics in the 80's and early 90's with the advent of MS (Rabilloud *et al.*, 2010). Although it is no longer the exclusive separation tool given the introduction of alternate methods such as online liquid chromatography-mass spectrometry (LC-MS), 2-DGE remains a mainstay in differential expression proteomics (Shen *et al*., 2008).

2.6.2.1. Sample preparation

The classical 2-DGE workflow is illustrated in Figure 2.7. Sample preparation is a crucial step prior to 2-DGE, which requires meticulous selection of methods with proper optimisation to ensure superior results. There is no universal preparation method, as each choice depends largely on the type of sample at hand, which can be as simple and homogenous as cell culture to heterogenous and complex samples like tissue, blood, serum or plasma samples. Regardless, the general steps involved in preparing samples for 2-DGE serve the same objectives, first to extract the protein by lysing the cells, followed by removal of contaminants and protein solubilisation, and finally quantification of protein concentration (Canas *et al.*, 2007).

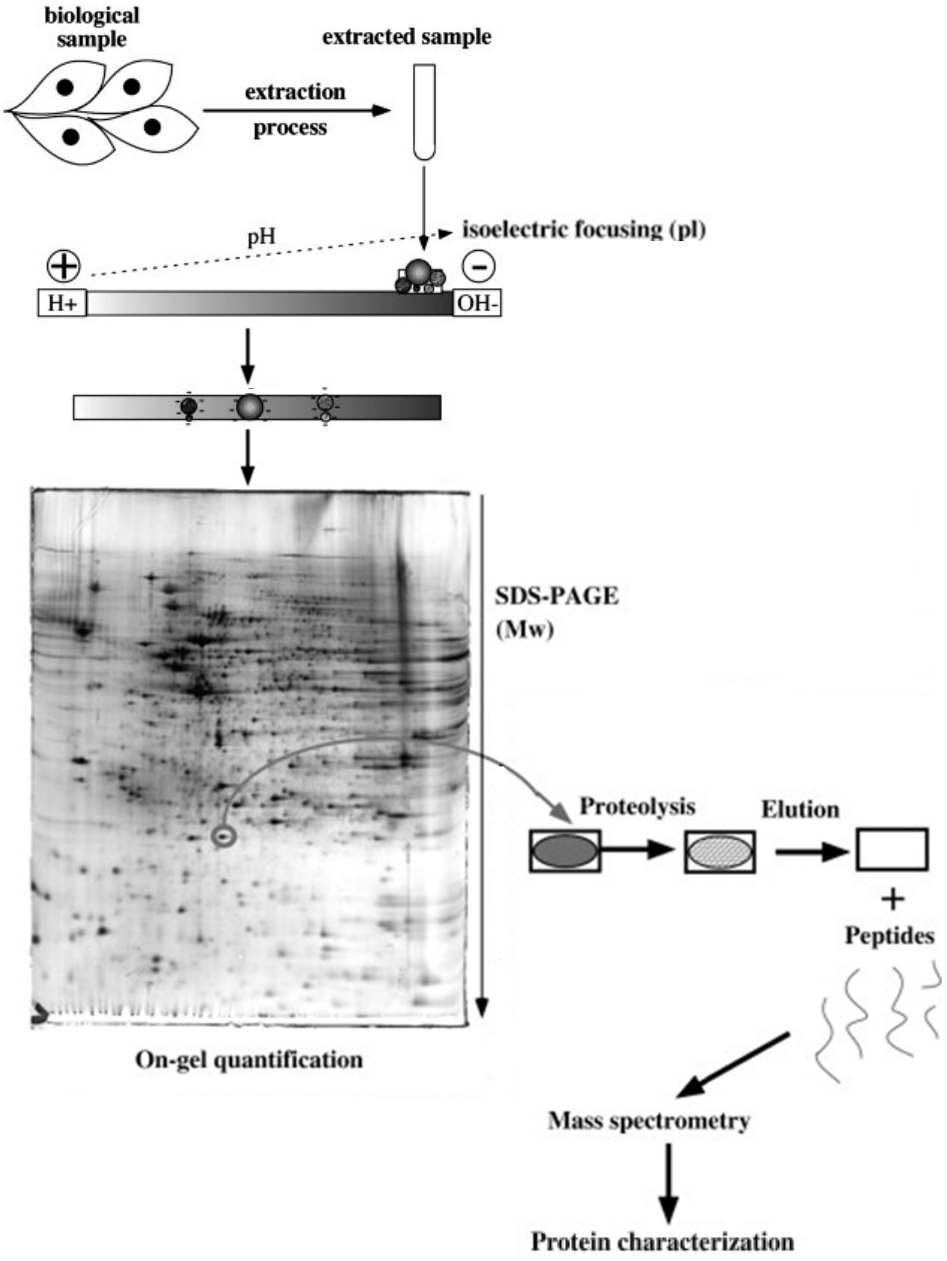

Figure 2.7: Schematic diagram of the conventional 2-DGE workflow

The 2-DGE workflow can be summarised into 5 main steps as follows; i) Protein extraction and processing of biological sample, ii) IEF separation according to the pI value, iii) SDS-PAGE separation according to the M_r, iv) Quantitative analysis of the gel image to determine protein spots of interest, v) In-gel digestion of gel plugs and extraction of the resulting peptides for MS identification and characterisation (Adapted and modified from Rabilloud and Leong, 2011).

Cellular disruption or homogenisation is the initial preparation step to extract proteins from cells, tissues or organs from various organisms. Depending on the complexity of the sample, homogenisation can be performed either by using the mechanical (eg. rotor-stator or open blade mills), ultrasonic (eg. sonication), pressure, freeze-thaw (eg. dry ice method), osmotic or detergent lysis method, or a combination of two or more of the aforementioned methods (Bodzon-Kulakowska, *et al.*, 2007). After cell disruption and prior to solubilisation, interfering compounds such as salts, polysaccharides, nucleic acids and lipids must be removed as they interfere with the first dimension run and can cause vertical or horizontal streaking on 2-D gels (Canas, *et al.*, 2007). Dialysis, ultrafiltration, protein precipitation (eg. acetone precipitation) and solid-phase extraction are commonly used methods to efficiently clean up samples from these contaminants (Bodzon-Kulakowska, *et al.*, 2007). Alternatively, several kits such as 2D clean up kit from GE Healthcare have been developed to effectively remove contaminants while minimising protein loss (Wells & Weil, 2003).

Proteins are held by multiple bonds; hydrogen bond, ionic bond, disulphide bridges and hydrophobic interactions, which confer their native conformation and allow quaternary structures to be formed between polypeptides. Successful solubilisation of a complex protein mixture requires disruption of all bonds. General solubilising solution contains a concoction of chaotropes to break hydrogen bonds and hydrophobic interactions (eg. urea and thiourea), reducing agents to reduce disulphide bonds (eg. dithiothreitol (DTT)), neutral or zwitterionic detergents to disrupt hydrophobic interactions (eg. 3-[(3-cholamidopropyl) dimethyl-ammonio]-1-propanesulfonate (CHAPS) and Triton-X), and buffer salts to prevent protein-protein interactions (eg. tris buffer) (Canas, *et al.*, 2007). Protease inhibitors are also added to prevent proteolysis by endogenous proteases liberated upon cell lysis (Bodzon-Kulakowska, *et al.*, 2007).

To ensure reproducibility of the gels, it is crucial to load equivalent amount of protein for each gel. Several techniques and kits have been established to accurately quantitate protein concentration, the most common being Bradford protein assay, bicinchoninic acid (BCA) assay and 2D Quant kit from GE Healthcare. Nonetheless, the choice of quantification protocol relies on the compatibility of the solubilising buffer with the selected method. High concentrations of chaotropes and detergents may cause interference, leading to deviation from linear response, hence, a method with higher tolerance towards these interference should be selected (Canas, *et al.*, 2007).

2.6.2.2. IEF

Prior to running IEF, the samples are rehydrated in immobilised pH gradient (IPG) drystrips to allow adsorption of proteins into the gel. Three techniques have been ascertained for effectual rehydration, the most common being rehydration loading (passive and active rehydration). The cup loading method is used for extreme pH and small volume of sample, while paper bridge rehydration is applied when rehydration loading is not feasible (Westermeiner & Naven, 2002). Proteins are then focused to their respective pI, which is the pH value of the protein at which the net charge is zero. A wide range of pH gradient drystrips are currently available, ranging from wide gradient (eg. pH 4-7, 3-10 and 3-12) to narrow gradient or zoom-in gels (eg. pH 5-6) (Gorg *et al.*, 2000). Low voltage (100 V) is used to initiate run to remove salts and allow ampholytes to reach their final position, as these interfering substances generate strong Joule heating if high field strength is applied immediately. This is followed by gradual increase of the field strength (500 V, 1000 V) to a final voltage of 8000 V (Gorg, *et al.*, 2000; Rabilloud & Lelong, 2011).

2.6.2.3. SDS-PAGE

Proteins separated in the isoelectric focusing are further equilibrated with SDS to confer the proteins a net negative charge, rendering them mobile in the second dimension. SDS-PAGE is then performed, first at low voltage (50 V) to allow the SDS front to re-solubilise the proteins while sweeping across the IPG strip, followed by high voltage (500 V) (Rabilloud & Lelong, 2011). Proteins are subsequently visualised by staining the gels with dyes such as Coomassie brilliant blue (CBB), silver stain and fluorescent stain (Patel *et al.*, 2005). Silver staining is the most commonly used method, due to its high detectability and sensitivity (detects up to ng). Despite its low sensitivity and narrow linear dynamic range, CBB is still widely used given the incompatibility of the silver staining protocol with MS unless modified (Monteoliva & Albar, 2004; Yan *et al.*, 2000). Gel images are then scanned and converted to digital data using a scanner and analysed with image analysis software tools such as ImageMaster™ (GE Healthcare), Progenesis SameSpots (Nonlinear Dynamics) and PDQuest™ (Bio-Rad Laboratories) (Sellers & Miecznikowski, 2010).

2.6.3 MS

Protein spots of interest are picked or excised from the gel and digested with sequence-specific proteases such as trypsin, which cleaves after lysine and arginine residues, into smaller peptides. The rationale for analysing peptides rather than proteins is that peptides can be eluted from the gel and analysed more easily than proteins. Furthermore, a subset of peptides from a protein provides sufficient data for identification, whereas analysis based on the molecular weight of proteins may result in ambiguous identification (Pandey & Mann, 2000). Digested peptides are then introduced into the mass spectrometer.

The two important modules in a mass spectrometer are the ion source and mass analyser. The ion source functions to ionise the charged and polar molecules to gas-phase ions, a pre-requisite prior to mass analysis, while the mass analyser separates and measures the m/z ratio of each ion, presenting the data in the form of a mass spectrum (Yates, 1998). To date, the two key ion sources for proteins and peptides analysis are matrix-assisted laser desorption/ionisation (MALDI) and electrospray ionisation (ESI)), both of which are soft ionisation techniques suitable for analysis of femtomole quantities of non-volatile and thermally labile analytes (Watson & Sparkman, 2007). Common mass analysers include time-of-flight (TOF), triple quadrupole and quadrupole ion trap analysers (Chen, 2008).

MS protein identification can be performed in two ways, i) 'peptide-mass mapping' which generates the 'peptide mass fingerprint' (PMF) of the studied protein, and ii) tandem MS (MS/MS). In peptide-mass mapping, different masses of the digested peptides of a particular protein are used to generate the peptide mass profile which is then compared with theoretical peptide libraries from existing databases to determine the protein identity (Barrett *et al.*, 2005). Tandem MS is a two-step procedure involving peptide-mass fingerprinting in the first step, and fragmentation of individual peptides in the second step to gain amino acid sequence information of each peptide fragment. Although more complex and less scalable than mass fingerprinting, tandem MS provides more specific sequence information which can be used to search both protein and nucleotide databases for unambiguous identification of proteins (Pandey & Mann, 2000).

2.6.3.1. Proteomic data analysis

Bioinformatics serve as an vital tool for analysis and interpretation of the mass spectra generated during MS analysis, without which protein identification and characterisation is virtually implausible. Each protein spot generates a unique digestion fingerprint that is searched against sequence databases for matching fingerprints to accurately identify the protein of interest. Various internet-based MS programs are available for interpretation of MS data, and can be grouped based on methods of analysis, such as peptide mass fingerprinting (Mascot, PeptIdent, MassSearch), protein molecular weight and sequence tags (PeptideSearch, PeptideMass) and peptide sequence tags (MS-Tag, MS-Seq). ExPASy (http://www.expasy.ch) is a bioinformatics resource portal operated by the Swiss Institute of Bioinformatics (SIB), providing a large selection of protein identification tools (Vihinen, 2001).

Online protein and complete genome-sequence databases such as expressed sequence tag (EST) and NCBI databases collectively provide a complete catalogue of proteins and genes expressed in organisms. This allows protein identification even with limited sequence information or raw mass spectral data by matching them with a database entry (Liebler, 2002). These databases also provide a platform for cross-species protein identification of organisms with incomplete databases against others with fully sequenced genomes (Barrett, *et al.*, 2005). Databases for 2-D reference maps are available as well to link identified spots to the images of the gels. The World-2DPAGE List houses an index of 2D databases such as SWISS-2DPAGE, to aid in spot selection and data analysis (Hoogland *et al.*, 2008).

2.6.4 Viral proteomics: Evaluation of virus-host interaction

Proteomic technologies have been widely employed in the discovery of novel drug targets, early disease biomarkers and in the elucidation of biopathomechanisms, especially in cancer research (Garbis *et al.*, 2005). In virology studies, proteomic approaches are extensively applied to study protein composition of virions, the structure and interactions of viral proteins, and the effects of viral infection on cellular proteome (Maxwell & Frappier, 2007). Both the gel-based and non-gel based approaches have been successfully used to study host responses towards a wide range of pathogenic viruses including dengue virus (Pattanakitsakul *et al.*, 2007), West Nile virus (Pastorino *et al.*, 2009), and hepatitis C virus infection (Jacobs *et al.*, 2005).

Despite extensive research on CHIKV and its interaction with the host and vector, little attention has been dedicated to proteomic study on this subject. Tchankouo-Nguetcheu and colleagues were the first to study protein modulation in midguts of *Ae. aegypti* mosquito vector in response to CHIKV by means of 2-DGE. Initial findings suggest alteration of proteins involved in cell protection and metabolic pathways subverted by the virus to favour their survival, replication and transmission in the vector (Tchankouo-Nguetcheu *et al.*, 2010). Another proteomic study was conducted by Dhanwani and colleagues in 2011, on the effect of virus infection in new-born mice tissues. Proteins related to stress, inflammation, apoptosis and metabolic pathways involved in nitrogen, iron and energy metabolism were found to be modulated upon infection (Dhanwani *et al.*, 2011). Meanwhile, proteomic analysis of CHIKV infection in microglial cells show down-regulation of the host cell antiviral responses as a possible target for host transcriptional shutoff (Abere *et al.*, 2012). Taken together, these studies provide plausible hypotheses as well as new insights in deciphering the mechanism involved in the pathogenesis of CHIK infection.

CHAPTER 3

MATERIALS AND METHODS

3.1 Cell culture and maintenance

3.1.1 Cell lines

The cell lines used in this research were WRL-68 human embryonic liver cell line, African green monkey kidney (Vero) cell line and C6/36 *Aedes albopictus* mosquito cell line. All cell lines were purchased from American Type Culture Collection (ATCC) and maintained at a low passage number.

3.1.2 Virus stock

CHIKV, clinical isolate CHIK06/08, of the ECSA genotype was obtained from Sungai Buloh General Health Laboratory, Selangor.

3.1.3 Cell culture media and solutions

i) Media for mammalian cell culture

A) 10× Dulbecco's Modified Eagle Medium (DMEM) stock

DMEM powder (Sigma-Aldrich®, USA)	2 packets
Sodium hydrogen carbonate (MERCK, Germany)	6.00g
4-(2-hydroxyethyl)-1-piperazineethanesulfonic acid (HEPES) (Promega, USA)	9.56 g
De-ionised water (ddH_2O)	Top up to 200.0 ml

The solution was stirred for 1 hour, filtered with 0.22 µM polyethersulfone (PES) filter (Nalgene®, USA) and stored at 4 °C.

B) 1× DMEM growth medium (Supplemented with 10% foetal bovine serum (FBS))

10× DMEM stock	10.0 ml
FBS (GIBCO®, USA)	10.0 ml
Sterile ddH_2O	80.0 ml

C) 1× DMEM maintenance medium (Supplemented with 2% FBS)

10× DMEM stock	10.0 ml
FBS	2.0 ml
Sterile ddH_2O	88.0 ml

D) 1× DMEM serum-free medium

10× DMEM stock	10.0 ml
Sterile ddH_2O	90.0 ml

ii) Media for C6/36 insect cell culture

A) 2× Leibovitz's L-15 medium stock

L-15 powder (Sigma-Aldrich®, USA)	1 bottle
ddH_2O	Top up to 500.0 ml

The solution was stirred for 1 hour, filtered with 0.22 µM PES filter and stored at 4 °C.

B) 1× L-15 growth medium (Supplemented with 10% FBS)

2× L-15 stock	50.0 ml
FBS	10.0 ml
Tryptose phosphate broth (TPB) (Sigma-Aldrich®, USA)	10.0 ml
ddH_2O	38.0 ml

C) 1× L-15 maintenance medium (Supplemented with 2% FBS)

2× L-15 stock	50.0 ml
FBS	2.0 ml
TPB	10.0 ml
ddH_2O	38.0 ml

iii) Cryopreserving medium

FBS	9.0 ml
100% dimethyl sulfoxide (DMSO) (Sigma-Aldrich®, USA)	1.0 ml

Cryopreserving medium was prepared fresh before use and kept in the dark.

iv) Phosphate buffered saline (PBS)

PBS (Sigma-Aldrich®, USA)	1 bottle
ddH_2O	1 L

PBS solution was autoclaved and stored at room temperature (25 °C).

v) Trypsin/0.25% ethylenediaminetetraacetic acid (EDTA) (GIBCO®, USA)

***NOTE:** All media were prepared under sterile conditions and stored at 4°C.

3.1.4 Cell culture and maintenance procedures

3.1.4.1 Cultivation of cell lines

Both WRL-68 and Vero mammalian cell lines were grown in DMEM growth medium at 37 °C in a humidified incubator with 5% carbon dioxide (CO_2). C6/36 mosquito cell line on the other hand was propagated in L-15 growth medium at 28 °C without 5% CO_2.

All cell lines were maintained in 25 cm^2 culture flask (NUNC™, USA) and sub-cultivated upon reaching 80% confluency. Briefly, spent medium was discarded and the adherent cells were washed twice with PBS and trypsinised in 1 ml trypsin/0.25% EDTA for 2 to 5 minutes at 37 °C. Cells were detached by gently tapping the flask. An equivalent amount of medium was added to stop trypsin activity. The cells were transferred to a 15 ml centrifuge tube and centrifuged at 250 × *g* for 5 minutes. The resulting cell pellet was resuspended in 1 ml of DMEM growth medium for mammalian cell lines and L-15 growth medium for C6/36 cell line. The cells were sub-cultivated at a ratio of 1:6 and 1:4 for mammalian and insect cell lines respectively with medium renewal of every two days.

3.1.4.2 Cryopreservation and thawing

All three cell lines were preserved in cryopreserving medium containing 10% DMSO and stored in liquid nitrogen. Briefly, confluent cells were trypsinised and centrifuged at 250 × *g* for 5 minutes. The supernatant was discarded and the cells were resuspended in 4 ml of cryopreserving medium and stored in 1.0 ml-aliquot in 1.5 ml cryovials (NUNC™, USA). The cells were incubated at 4°C for 30 minutes, -20°C for 4 hours and -80°C overnight prior to being transferred to liquid nitrogen for long term storage.

Cells were revived by rapid thawing at 37°C for 2 minutes followed by immediate transfer to a new 25 cm^2 culture flask containing fresh DMEM growth medium. The cells were incubated for 4 hours at 37 °C for mammalian cells and 28 °C for insect cells. Spent medium was then discarded and replaced with fresh medium to remove toxic DMSO and unattached cells. The cells were further incubated under their respective conditions and subjected to normal cell passaging upon reaching confluency.

3.2 CHIKV stock production

CHIKV was propagated twice in C6/36 cell line. Briefly, C6/36 cells were grown to 80% confluency in 25 cm^2 culture flask and infected with 100 µl of CHIKV stock for 2 hours at 28°C with gentle shaking at every 15 minutes interval. Viral inoculum was removed following incubation and infected cells were further incubated for 6 days in L-15 maintenance medium at 28 °C. Uninfected cells were cultured in parallel under the same conditions but without virus infection.

After 6 days incubation, the uninfected and CHIKV-infected cells were frozen at -80 °C and subsequently thawed at room temperature to lyse the cells for the release of virus particles. This process was repeated thrice for complete cell lysis. Lysed cells were transferred to a 2.5 ml microcentrifuge tubes in 2.0 ml-aliquots and spun at 1,000 × g for 5 minutes to remove cellular debris. The supernatant was harvested and stored in 1.0 ml-aliquot at -80 °C.

3.3 Cell counting and seeding

3.3.1 Chemicals and reagents

i) Trypan blue solution 0.4% (Sigma-Aldrich®, USA)

3.3.2 Procedure

Confluent cells were trypsinised and centrifuged at 250 ×*g* for 5 minutes. The supernatant was discarded and the cells were resuspended in 1 ml of DMEM growth medium. Ten µl of cells were mixed with 90 µl of trypan blue and 10 µl of the mixed cell suspension was loaded on one side of the haemocytometer chamber. Cells within the four side quadrants were viewed at 100× magnification and counted with a cell counter. The number of cells per ml of medium was calculated according to the formula below:

$$\text{Number of cells/ml} = \frac{\text{Total number of cells in 4 quadrants}}{4} \times 10\ (\text{Dilution factor}) \times 10^4$$

The cells were seeded at the appropriate density and incubated overnight at 37 °C in DMEM growth medium.

3.4 CHIKV titration: Plaque assay

3.4.1 Chemicals and reagents

i) 5% low melting point agarose

Type VII low melting point agarose (Sigma-Aldrich®, USA)	2.5 g
ddH_2O	50.0 ml

Solution was heated to dissolve the agarose powder and autoclaved.

ii) 0.5% agarose overlay

5% low melting point agarose	5.0 ml
ddH_2O	50.0 ml

Agarose overlay was prepared under sterile conditions and kept warm in 37 ℃ waterbath.

iii) Trichloroacetic acid (TCA)

TCA (MERCK, Germany)	20.0 g
ddH_2O	100.0 ml

iv) Crystal violet solution (Sigma-Aldrich®, USA)

3.4.2 Virus dilution

Ten-fold serial dilutions (10^{-1} to 10^{-8}) of the virus stock were prepared. Briefly, 900 µl of serum-free DMEM medium was added to eight microcentrifuge tubes (labelled 10^{-1} to 10^{-8}). One hundred µl of virus stock was added to the first tube and mixed well by inverting the tube repeatedly. Serial dilution was then performed by transferring 100 µl to the subsequent dilution and repeating the procedure.

3.4.3 Virus infection

Cells were seeded at a density of 5.0×10^5 cells per well in 6-well culture dish (NUNC™, USA) overnight at 37 °C. Prior to infection, DMEM growth medium was discarded and following that 200 µl of each virus dilution were added to the various well in duplicates. Supernatant of uninfected C6/36 cells were added to the negative control wells (mock control cells). Cells were incubated for 2 hours at 37 °C with gentle shaking every 15 minutes to prevent the cell sheets from drying. Viral inoculum was removed following incubation and 2 ml of 0.5% agarose overlay diluted in DMEM maintenance medium was added to each well. The agarose overlay was left to solidify at room temperature for 15 minutes. The cells were further incubated for 30 hours at 37 °C.

3.4.4 Plaque staining and counting

Cell sheets were fixed onto the plate by adding 2 ml of 20% TCA to each well with 5 minutes incubation. TCA solution was then removed and the agarose overlay was gently flicked off the plate. Cell sheets were rinsed with distilled water to remove residual TCA and agarose. Two ml of crystal violet solution was added to each well with 30 minutes incubation to stain the cells. Crystal violet was then rinsed off and

visible plaques were counted. The dilution that gives a plaque number of between 20 and 100 was used to determine the virus stock concentration. Virus stock concentration (pfu/ml) was counted using the formula below:

$$\text{Plaque forming unit (pfu)/ml} = \frac{\text{Number of plaques}}{\text{Dilution factor} \times \text{Inoculum volume}}$$

3.5 Determination of multiplicity of infection (MOI)

Virus titre (pfu/ml) was used to determine the MOI, defined as the average number of virus particles infecting a cell in a population subjected to infection. The MOI is calculated based on the formula below:

$$\text{MOI} = \frac{\text{Virus titre (pfu/ml)} \times \text{Inoculum volume (ml)}}{\text{Total number of seeded cells}}$$

3.6 Optimisation of infection condition

3.6.1 Confirmation of infection by indirect immunofluorescence assay (IIFA)

3.6.1.1 Chemicals and reagents

i) 3.7% formaldehyde in PBS

37% formaldehyde (MERCK, Germany)	100.0 µl
PBS	900.0 µl

ii) 0.15 M glycine in PBS

Glycine (MERCK, Germany)	56.30 g
PBS	50.0 ml

iii) 0.1% Triton X-100 in PBS

Triton X-100 (AppliChem, Sweden)	50.0 µl
PBS	49.95 ml

iv) 0.2% gelatin in PBS

Gelatin (Sigma-Aldrich®, USA)	0.2 g
PBS	50.0 ml

v) Anti-CHIK E2 monoclonal antibody (mAb) 3E4

Anti-CHIK E2 mAb 3E4 (82 µg/ml), a kind gift from Dr. Phillippe Després of Pasteur Institute, France, was diluted in PBS/0.2% gelatin at a ratio of 1:1000.

vi) Goat anti-mouse IgG secondary antibody (Novus Biologicals, USA)

The secondary antibody was diluted in PBS/0.2% gelatin at a ratio of 1:100.

vii) Fluoromount (Sigma-Aldrich®, USA)

3.6.1.2 Procedure

WRL-68 cells were seeded at a density of 1.5×10^5 cells per well in 24-well culture dish (NUNC™, USA) overnight at 37 °C. Spent medium was discarded and cells were washed twice with PBS to remove traces of FBS. Cells were infected in serum-free DMEM medium at the MOI of 0.5, 1.0, 5.0 and 10.0 for 2 hours at 37 °C with gentle shaking every 15 minutes. Viral inoculum was removed after incubation and cells were further incubated for 24 and 48 hours in 500 µl DMEM maintenance medium.

The medium was removed following incubation at the desired time-point and cells were rinsed with PBS and fixed with 300 µl of 3.7% formaldehyde in PBS for 20 minutes at room temperature. Cells were then washed with PBS and further incubated with 300 µl of 0.15 M glycine in PBS for 10 minutes to quench excess formaldehyde. The cells were washed again with PBS and permeabilised with 300 µl of 0.1% Triton X-100 in PBS for 5 minutes. Permeabilised cells were washed thoroughly and incubated with 150 µl of anti-CHIK E2 mAb 3E4 for 40 minutes at 37 °C.

Thereafter, the cells were washed extensively to remove unbound antibodies and incubated with 150 µl of goat anti-mouse IgG secondary antibody conjugated with fluorescein isothiocyanate (FITC) for 30 minutes at 37 °C in the dark. Cells were then rinsed with PBS and two drops of fluoromount were added to each well to reduce fluorochrome quenching during analysis. The cells were observed under an inverted microscope (Nikon Eclipse Ti-5, Japan) and fluorescence pictures were acquired using NIS-Elements imaging software (Nikon, Japan).

3.6.2 Quantitative analysis of cell infection via flow cytometry

3.6.2.1 Chemicals and reagents

i) 3.7% formaldehyde in PBS

ii) Staining buffer (0.1% Sodium azide, 1.0% FBS)

Sodium azide (w/v)	20.0 mg
FBS	200.0 µl
PBS	20.0 ml

iii) Anti-CHIK E2 mAb 3E4

Anti-CHIK E2 mAb 3E4 (82 µg/ml) was diluted in staining buffer at a ratio of 1:250.

iv) Goat anti-mouse IgG secondary antibody

The secondary antibody was diluted in staining buffer at a ratio of 1:100.

3.6.2.2 Procedure

WRL-68 cells were seeded at a density of 2.0×10^6 cells per 25 cm^2 culture flask (NUNC™, USA) overnight at 37 °C. The cells were infected with CHIKV at various MOI (MOI 0.5, 1.0, 5.0 and 10.0) in 1 ml DMEM serum-free medium for 2 hours at 37 °C with gentle shaking at every 15 minutes interval. Viral inoculum was removed after incubation and the cells were further incubated in 5 ml DMEM maintenance medium for 24 and 48 hours. Cells were harvested after incubation at their designated time-points and washed twice with PBS. Thereafter, 1.5×10^6 cells per sample were counted and fixed with 150 µl of 3.7% formaldehyde in PBS for 30 minutes. Permeabilised cells were pelleted at 6,000 × *g* for 3 minutes, washed twice with staining buffer and incubated with 50 µl of anti-CHIK E2 mAb antibody 3E4 for 90 minutes at 37 °C. After extensive washing with staining buffer, the cells were further incubated with 200 µl of FITC-conjugated secondary antibody for 60 minutes at 37 °C. Thereafter, the cells were washed thoroughly with staining buffer and resuspended in 500 µl PBS.

The cells were sorted using BD FACSCanto II flow cytometer (BD Bioscience, USA) and analysed with BD FACSDiva software (BD Bioscience, USA). Unstained control was used to adjust the forward scatter (FSC) and side scatter (SSC) voltages whereas cells stained with secondary antibody only was used to adjust the FITC voltage. Ten thousand events (representing 1.0×10^4 cells) were recorded for each sample and a dot plot was generated, using mock control sample to set the quadrant. Results were presented as percentage infection (%) ± standard deviation (SD) for three independent experiments.

3.6.3 Quantitative analysis of cell death by Annexin V (AV)/propidium iodide (PI) co-labelling

3.6.3.1 Kits and reagents

i) FITC AV apoptosis detection kit I (BD Pharmigen™, USA)

Components:

10× Annexin binding buffer	50.0 ml
FITC AV	0.5 ml
PI staining solution	2.0 ml

1× Annexin binding buffer was prepared by diluting 1 ml of 10× Annexin binding buffer in 9 ml PBS.

3.6.3.2 Procedure

Percentage of cell death was determined using FITC AV Apoptotic Detection Kit according to the manufacturer's protocol. Briefly, cells were seeded at the appropriate density in 25 cm^2 culture flask and infected at different MOI (MOI 0.5, 1.0, 5.0, 10.0) and time-points (24 and 48 hours). Following infection, the cells were harvested and washed twice with PBS. One million cells were counted for each sample and resuspended in 1 ml of 1× Annexin binding buffer. One hundred µl (equivalent to 1.0×10^5 cells) of the solution was transferred to a 5 ml round bottom test tube (BD Bioscience, USA). Five µl of AV and PI was added to each tube with 15 minutes incubation in the dark at room temperature. Four hundred µl of 1× Annexin binding buffer was then added to each tube and samples were analysed by flow cytometry within 1 hour.

Prior to analysing the samples, compensation controls were performed to detect and rectify spillover of the emission of one fluorochrome (FITC-AV or PI) into the detector designated to collect the emission of another fluorochrome (PI or FITC-AV). Three controls were used for the setup: i) unstained control; ii) cells stained with AV only; and iii) cells stained with PI only. Auto compensation was performed by adjusting the SSC, FSC, FITC-AV and PI voltages using unstained control, while manual compensation was performed thereafter for fine tuning. Ten thousand events (representing 1.0×10^4cells) were recorded for each sample and the dot plot was generated. Results were presented as percentage of cell death (%) ± SD for three independent experiments.

3.7 Optimisation of the condition for secretome sample preparation

3.7.1 Kits and reagents

i) CellTiter 96® Aqueous One Solution Cell Proliferation assay (MTS) (Promega, USA)

Components:

CellTiter 96® Aqueous One Solution Cell Proliferation reagent	50.0 ml

ii) CytoTox-Glo™ Cytotoxicity assay (Promega, USA)

Components:

AAF-Glo™ substrate	10.0 ml
Assay buffer	5.0 ml
Digitonin	0.175 ml

CytoTox-Glo™ Cytotoxicity assay reagent was prepared by mixing one bottle of AAF-Glo™ substrate with a bottle of assay buffer. Lysis reagent was prepared by adding 13 µl of digitonin to 2.75 ml of assay buffer.

3.7.2 MTS cell proliferation assay

For secretome study, the effect of serum deprivation on WRL-68 cell proliferation was determined using MTS cell viability assay. Briefly, cells were seeded at a density of 1.0×10^4 cells/well in 96-well dish overnight, followed by extensive washing with serum-free DMEM medium and incubation in either DMEM growth medium or serum-free DMEM medium at the selected time-point in triplicates. Twenty µl of CellTiter 96® Aqueous One Solution Cell Proliferation reagent was then added to

the cells, followed by 4 hours incubation at 37°C. The absorbance was read at 490 nm and cell viability graph was plotted based on the data from three independent experiments. All data were presented as mean ± SD.

3.7.3 Dead-cell protease release assay

Quantification of cellular disruption was determined using CytoTox-Glo™ Cytotoxicity assay according to the manufacturer's protocol. WRL-68 cells were seeded at a density of 1.0×10^4 cells/well in 96-well dish overnight, followed by extensive washing with serum-free DMEM medium and incubation in either DMEM growth medium or serum-free DMEM medium at the optimised time-point to determine the effect of serum deprivation on cell membrane integrity. The effect of CHIKV-infection at the optimised MOI on WRL-68 cellular disruption was evaluated concomitantly by infecting the cells for 2 hours with CHIKV, followed by extensive washing with serum-free DMEM medium and further incubation at the desired time-point.

After incubation, 50 µl of lysis reagent was added to the positive control wells for 1 minute to completely lyse the cells. Fifty µl CytoTox-Glo™ Cytotoxicity assay reagent was subsequently added to all wells, followed by 15 minutes incubation. Luminescence was measured using GloMax® 20/20 luminometer (Promega, USA) and the luminescence signals were quantified as relative luminescence unit (RLU). The relative percentage of cell lysis was calculated based on the maximum cellular disruption obtained from cells treated with lysis reagent. All data were presented as mean ± SD.

3.8 WRL-68 cell infection for 2-DGE

3.8.1 Infection protocol of WRL-68 cells for whole cell proteome study

WRL-68 cells were seeded at a density of 4.5×10^6 cells in 75 cm^2 culture flasks overnight at 37°C. Cells were infected with CHIKV in serum-free DMEM medium at the optimised MOI and incubated for 2 hours at 37 °C with gentle shaking at every 15 minutes interval. Viral inoculum was then removed and the cells were further incubated at the optimised time-point in DMEM maintenance medium. Mock control cells were cultured in parallel as control.

3.8.2 Infection protocol of WRL-68 cells for secretome study

WRL-68 cells were seeded at a density of 4.5×10^6 cells in 75 cm^2 culture flasks overnight at 37 °C. Cells were infected with CHIKV in serum-free DMEM medium at the optimised MOI and incubated for 2 hours at 37 °C with gentle shaking at every 15 minutes interval. Viral inoculum was then removed and the cells were washed extensively with serum-free medium to remove traces of FBS from the virus supernatant. Infected cells were further incubated at the optimised time-point in serum-free DMEM medium. Mock control cells were cultured in parallel as control.

3.9 Protein sample processing

3.9.1 Protein extraction

3.9.1.1 Chemicals and reagents

i) Lysis buffer stock solution (7 M Urea, 2 M Thiourea, 4% CHAPS, 2% IPG buffer, 40 mM DTT)

Urea (GE Healthcare, Uppsala, Sweden)	10.5 g
Thiourea (Invitrogen, USA)	3.8 g
CHAPS (Invitrogen, USA)	1.0 g
DTT (Gold Biotechnology®, USA)	0.154 g
IPG buffer pH 3-10 (GE Healthcare, Uppsala, Sweden)	500.0 µl
ddH_2O	Top up to 25.0 ml

Lysis buffer was stored in 1.0 ml-aliquots at -20°C. Ten µl of nuclease mix (GE Healthcare, Uppsala, Sweden) and protease cocktail inhibitor (GE Healthcare, Uppsala, Sweden) were added to the aliquots fresh before use.

ii) Rehydration buffer stock solution (7 M Urea, 2 M Thiourea, 2% CHAPS, 0.5% IPG buffer)

Urea	10.5 g
Thiourea	3.8 g
CHAPS	0.5 g
IPG buffer pH 3-10	125.0 µl
1% bromophenol blue stock solution	50.0 µl
ddH_2O	Top up to 25.0 ml

Rehydration buffer stock solution was stored in 0.6 ml-aliquots at -20°C. 10.8 µl of 1M DTT were added to the aliquots fresh before use. Bromophenol blue was omitted from the stock used to re-dissolve proteins after clean-up.

iii) 1 M DTT stock solution

DTT	0.1542 mg
ddH_2O	1.0 ml

DTT stock solution was stored in 25µL-aliquots at -20°C.

iv) Bromophenol blue stock solution (1% Bromophenol blue, 50 mM Tris base)

Bromophenol blue (GE Healthcare, Uppsala, Sweden)	100.0 mg
Tris base (MERCK, Germany)	60.0 mg
ddH_2O	10.0 ml

3.9.1.2 Extraction procedure for whole cell proteins

Mock control and CHIKV-infected cells were trypsinised and the cell suspensions were centrifuged at 3,000 × *g* for 5 minutes. Supernatants were discarded and the cell pellets were washed with PBS and centrifuged again. Cell pellets were harvested and 200 µl of lysis buffer was added to lyse the cells. The samples were incubated on ice for 30 minutes with brief vortexing at every 15 minutes interval. Extracted protein was then centrifuged at 17,000 × *g* to remove cellular debris and stored at -80 °C.

3.9.1.3 Extraction procedure for secretome

The supernatant of and CHIKV-infected WRL-68 cells were collected in 50 ml centrifuge tubes and centrifuged at 3,000 × *g* for 5 minutes to remove dead cells and cellular debris. The supernatants were filtered through 0.22 µm syringe filters (Sartorius Stedim Biotech, Germany) and further concentrated using Vivaspin® 20 centrifugal concentrator with a 3,000 kDa molecular weight cut-off membrane (Sartorius Stedim Biotech, Germany) and stored at -80 °C.

3.9.2 Protein clean-up and quantification

3.9.2.1 Kits and reagents

i) 2-D Clean-Up kit (GE Heathcare, Uppsala, Sweden)

Components:

Precipitant	15.00 ml
Co-precipitant	17.00 ml
Wash buffer	50.00 ml
Wash additive	0.25 ml

ii) Quick Start Bradford Protein assay kit I (Bio-Rad, USA)

Bradford dye reagent	1.0 L
Bovine serum albumin (BSA) (2.0 mg/ml)	5 × 1.0 ml

3.9.2.2 Protein clean-up: 2-D Clean-Up kit

Protein samples were cleaned up using 2-D Clean-Up kit according to the manufacturer's protocol. Briefly, 300 µl of precipitant was added to 100 µl of samples with 15 minutes incubation on ice, followed by the addition of equal volume of co-precipitant. The samples were vortexed and centrifuged at full speed (17,000 × g) for 5 minutes at 4 °C. The supernatants were decanted and 40 µl of co-precipitant was added to each pellet with 5 minutes incubation prior to centrifugation at full speed for 5 minutes. A cocktail of 10 µl Milli-Q, 5 µl wash additive and 1 ml wash buffer wash then added to the samples with vortexing to disperse the protein pellets. The pellets were incubated at -20 °C for 30 minutes with vigorous vortexing every 10 minutes and

centrifuged at full speed for 5 minutes. The pellets were then re-dissolved in 100 µl rehydration buffer without bromophenol blue.

3.9.2.3 Protein estimation: Bradford assay

The concentrations of whole cell proteins and secretome were estimated using Bradford Protein assay kit I, with BSA as the protein standard. BSA stock (2 mg/ml) was first diluted to 1 mg/ml in ddH_2O. 200 µl of Bradford dye reagent was pipetted into each well of the 96-well dish. The BSA stock (1 mg/ml) was added to the wells in triplicates to produce a range of amounts from 1 µg to 5 µg. One µl of each protein sample was added to the wells in triplicates. The mixture was equilibrated for 5 minutes at room temperature and the absorbance was read at 595 nm. The protein concentration for each sample was calculated from the BSA standard curve generated using Microsoft Excel.

3.10 First dimensional electrophoresis: Isoelectric focusing (IEF)

3.10.1 Chemicals and reagents

i) Rehydration buffer stock solution (7 M Urea, 2 M Thiourea, 2% CHAPS, 0.5% IPG Buffer)

Rehydration buffer containing 1% bromophenol blue was prepared according to the recipe described in section 3.9.1.1.

ii) Drystrip cover fluid (GE Healthcare, Uppsala, Sweden)

3.10.2 Passive rehydration

Prior to running the first dimension, the protein samples were rehydrated for 16 hours to allow proteins to absorb into the gel. Briefly, 40 µg (for analytical gels) or 80 µg (for preparative gels for MS analysis) of proteins were mixed with rehydration buffer (with bromophenol blue) to a final volume of 250 µl per drystrip and loaded onto the Immobiline® DryStrip reswelling tray (GE Healthcare, Uppsala, Sweden). Immobiline™ drystrip pH 3-10 linear, 13 cm gels (GE Healthcare, Uppsala, Sweden) were gently slid into the sample solution with the gel side facing down to avoid trapping bubbles and overlaid with 2 ml of drystrip cover fluid to prevent the drystrips from drying out.

3.10.3 IEF

Following 16 hours incubation, the rehydrated drystrips were transferred onto the ceramic strip holder and placed on the IPGphor electrode platform. Damped paper wicks (GE Healthcare, Uppsala, Sweden) were placed on both ends of the strips and platinum wire electrodes were placed on top of the paper wicks. Six ml of drystrip cover fluid was added onto the drystrips and focusing was performed at 20 °C using the protocols tabulated in Tables 3.1 (for whole cell proteins) and 3.2 (for secretome). The drystrips were stored individually in screw-capped glass tubes in -80 °C after focusing.

Table 3.1: IEF protocol for whole cell proteome samples

Steps	Voltage (V)	Voltage-hour (Vhr)	Approx. time
Step-and-hold	500	550	1h 15min
Gradient	1000	1000	1h
Gradient	8000	12000	3h
Step-and-hold	8000	11000	1 h 20 min
Total:		24550	**6 h 35 min**

Table 3.2: IEF protocol for secretome samples

Steps	Voltage (V)	Voltage-hour (Vhr)	Approx. time
Step-and-hold	500	600	1 h 30 min
Gradient	1000	1000	1 h
Gradient	8000	12000	3h
Step-and-hold	8000	16000	2 h
Total:		30000	**7 h 30 min**

3.11 Second dimensional electrophoresis: SDS-PAGE

3.11.1 Chemicals and reagents

i) SDS equilibration buffer solution (6 M Urea, 75 mM Tris-HCl pH 8.8, 29.3% Glycerol, 2% SDS, 0.002% Bromophenol blue)

Urea	72.1 g
Tris-HCl, pH 8.8	10.0 ml
87% glycerol (w/w) (MERCK, Germany)	69.0 ml
SDS (GE Healthcare, Uppsala, Sweden)	4.0 g
1% bromophenol blue stock solution	400.0 µl
ddH_2O	Top up to 200.0 ml

ii) 10× Laemmli SDS electrophoresis buffer

Tris base	30.3 g
Glycine (MERCK, Germany)	144.1 g
SDS	10.0 g
ddH_2O	Top up to 1.0 L

iii) 1× Laemmli SDS electrophoresis buffer

10× Laemmli SDS electrophoresis buffer	100.0 ml
ddH_2O	Top up to 1.0 L

iv) 10% SDS solution

SDS	5.0 g
ddH_2O	Top up to 50.0 ml

v) 30% T, 2.6% C monomer stock solution

Acrylamide (GE Healthcare, Uppsala, Sweden)	150.0 g
N,N'-methylenebisacrylamide (GE Healthcare, Uppsala, Sweden)	4.0 g
ddH_2O	Top up to 500.0 ml

The solution was filtered through 0.45 µM PES filter and stored at 4°C.

vi) 4× Resolving gel buffer solution (1.5 M Tris-HCl, pH 8.8)

Tris base	181.7 g
ddH_2O	Top up to 500.0 ml

The pH of the solution was adjusted to 8.8, and the solution was stored at 4°C.

vii) 10% ammonium persulfate (APS) solution

APS (MERCK, Germany)	0.1 g
ddH_2O	1.0 ml

APS solution was prepared fresh before use.

v) Agarose sealing solution

1× Laemmli SDS electrophoresis buffer	100.0 ml
Agarose (Invitrogen, USA)	0.5 g
1% bromophenol blue stock solution	200.0 µl

vi) DTT

vii) Iodoacetaminde (IAA) (MERCK, Germany)

3.11.2 Polyacrylamide gel casting

The gel caster was set up and 12.5% polyacrylamide gel solution was prepared following the recipe in Table 3.3. The solution was mixed well and pipetted into the gel casting chamber until the height of 1 cm below the top of the glass plates. Isopropanol (MERCK, Germany) was overlaid on top of each gel to remove bubbles and the gels were left to polymerize for 1 hour prior to being stored at 4 °C overnight.

Table 3.3: Recipe for casting two 12.5% polyacrylamide gels

Solutions	Amount (ml)
ddH_2O	15.80
4× Resolving buffer	12.50
Monomer solution	20.85
10% SDS	0.60
10% APS	0.25
Tetramethylethylenediamine (TEMED) (MERCK, Germany)	0.0167

3.11.3 Drystrip equilibration

Equilibration was performed on focused drystrips in two steps. The drystrips were first reduced in equilibration buffer containing 1% DTT for 15 minutes. The equilibration buffer was discarded and the drystrips were further alkylated in equilibration buffer containing 2.5% IAA for another 15 minutes. The equilibration buffer was decanted and the equilibrated strips were rinsed with 1× Laemlli electrophoresis running buffer to remove residual DTT and IAA.

3.11.4 SDS-PAGE

Equilibrated strips were gently laid on top of the polymerized gels with the plastic backing pushed against the back plate. The strips were sealed into place with agarose sealing gel which was previously melted in the microwave and left to cool down to 60 °C. The sealing gel was left to solidify for 2 minutes and second dimensional separation was performed using SE600 Ruby™ vertical electrophoresis unit (GE Healthcare, Uppsala, Sweden) in two steps as tabulated in Table 3.4.

Table 3.4: SDS-PAGE running protocol

Voltage (V)	Current (mA/gel)	Time (min)
50	40	30
500	40	165
Total run time:		195

3.11.5 Silver staining

3.11.5.1 Silver staining solutions (For 2 gels)

i) Fixing solution

Absolute ethanol (Hmbg, Germany)	200.0 ml
Acetic acid (MERCK, Germany)	50.0 ml
Distilled water (dH_2O)(Analytical gels)/ddH_2O(Preparative gels)	250.0 ml

ii) Sensitising solution

Absolute ethanol	150.0 ml
Sodium acetate (MERCK, Germany)	34.0 g
Sodium thiosulfate (MERCK, Germany)	1.0 g
25% glutaraldehyde (Calbiochem®, USA)*	2.5 ml
dH_2O (Analytical gels)/ddH_2O (Preparative gels)	Top up to 500.0 ml

* Glutaraldehyde was omitted when staining preparative gels.

iii) Silver nitrate solution

Silver nitrate (MERCK, Germany)	1.25 g
37% formaldehyde*	0.2 ml
dH_2O (Analytical gels)/ddH_2O (Preparative gels)	Top up to 500.0 ml

* 37% Formaldehyde was omitted when staining preparative gels.

iv) Developing solution

Sodium carbonate anhydrous (Amresco, USA)	12.5 g
37% formaldehyde	0.2 ml
dH_2O (Analytical gels)/ddH_2O (Preparative gels)	Top up to 500.0 ml

v) Stopping solution

EDTA disodium salt (Calbiochem®, USA)	7.3 g
dH_2O (Analytical gels)/ddH_2O (Preparative gels)	Top up to 500.0 ml

vi) Preserving solution

Absolute ethanol	150.0 ml
87% glycerol	23.0 ml
dH_2O (Analytical gels)/ddH_2O (Preparative gels)	Top up to 500.0 ml

3.11.5.2 Procedure

The gels were fixed overnight in fixing solution with constant shaking at room temperature. Fixing solution was poured off the next day and the gels were sensitised with sensitising solution for 30 minutes, followed by washing with distilled (for analytical gels) or de-ionised water (for preparative gels) thrice, 15 minutes each wash. The gels were subsequently stained with silver nitrate solution for 20 minutes and washed twice with distilled or de-ionised water for 2 minutes. The spots were developed in developing solution for 2 to 4 minutes and the reaction was stopped with stopping solution for 10 minutes. Developing and stopping solution were washed off with distilled or de-ionised thrice, 10 minutes each wash. Gels were stored in preserving solution at 4 °C or scanned directly with ImageScanner™ III (GE Healthcare, Uppsala, Sweden).

3.11.6 Differential image analysis

Scanned images were analysed using ImageMaster™ 2D Platinum v7.0 software (Amersham Biosciences, Sweden). A total of ten gels (Five gels from five individual flasks for each group) were used for analysis of both whole cell proteins and secretome. The parameters used for spot detection were (i) minimal area: 5.0; (ii) smooth factor: 3.0; and (iii) saliency: 200.0. Quantitative comparison was performed based on normalised percentage spot volume, which is the ratio between each spot and the sum of all spot intensities in the gel, calculated by the software. Manual matching was then performed to eliminate artefacts and rectify incorrectly matched spots.

For statistical analysis, significance of the differential expression was determined by analysis of variance (ANOVA) and Student's t-tests. All data were presented as mean ± SD. Protein spots having p-value <0.05 and a fold-change of at least 1.3 were deemed statistically significant.

3.12 MS analysis

3.12.1 Chemicals and reagents

i) 100 mM ammonium bicarbonate

Ammonium bicarbonate (MERCK, Germany)	1.582 g
ddH_2O	200.0 ml

ii) 50% acentonitrile (ACN)

100% ACN (MERCK, Germany)	50.0 ml
ddH_2O	50.0 ml

iii) 10 mM DTT in 100 mM ammonium bicarbonate

DTT	0.0154 g
100 mM ammonium bicarbonate	10.0 ml

iv) 55 mM iodoacetamide in 100 mM ammonium bicarbonate

IAA	0.10175 g
100 mM ammonium bicarbonate	10.0 ml

v) 50 mM ammonium bicarbonate in 50% ACN

100% ACN	10.0 ml
100 mM Ammonium bicarbonate	10.0 ml

vi) 50 mM sodium thiosulphate

Sodium thiosulphate	0.0791 g
ddH_2O	10.0 ml

vii) Destaining solution (15 mM Potassium ferricyanate in 50 mM Sodium thiosulphate)

Potassium ferricyanate (MERCK, Germany)	0.0494 g
50 mM sodium thiosulphate	10.0 ml

viii) 1000 ng/µl trypsin in 50 mM acetic acid (Stock)

Trypsin powder (Promega, USA)	1 bottle
Glacial acetic acid	2.8 µl
ddH_2O	100.0 µl

ix) 10 ng/µl trypsin in 50 mM ammonium bicarbonate

1000 ng/µl trypsin stock	1.0 µl
100 mM ammonium bicarbonate	99.0µl

x) 0.1% formic acid

Formic acid (MERCK, Germany)	1.0 µl
ddH_2O	1.0 ml

xi) 0.1% formic acid in 50% ACN

Formic acid	1.0 µl
100% ACN	500.0 µl
ddH_2O	499.0 ml

xii) Buffer A (2% ACN, 0.1% Trifluoroacetic Acid (TFA))

TFA	100.0 µl
100% ACN	2.0 ml
ddH_2O	97.9 ml

xiii) Buffer B (98% ACN, 0.1% TFA)

TFA	100.0 µl
100% ACN	98.0 ml
ddH_2O	1.9 ml

xiv) α-Cyano-4-Hydroxycinnamic Acid (CHCA) matrix

CHCA matrix (Sigma-Aldrich®, USA)	10.0 mg
Buffer A	400.0 µl
Buffer B	600.0 µl

3.12.2 In-gel trypsin digestion/peptide extraction

Significantly expressed spots were picked from five gels and pooled together in a microcentrifuge tube and stored at -20 ℃ in de-ionised water. Samples ready to be digested were thawed and the water was removed. Gel pieces were washed with 150 µl of 100 mM ammonium bicarbonate for 15 minutes with constant shaking. The gel plugs were destained with 150 µl of destaining solution twice, 10 minutes each wash, and reduced at 60 ℃ for 30 minutes with 150 µl of 10 mM DTT in 100 mM ammonium bicarbonate. The gel plugs were cooled to room temperature for 5 minutes, spun down for 1 minute at 1,000 × *g* and subsequently alkylated with 150 µl of 55 mM IAA in 100 mM ammonium bicarbonate in the dark for 20 minutes. Washing was performed thrice with 500 µl of 50 mM ammonium bicarbonate in 50% ACN, 20 minutes each

wash with shaking, followed by dehydration of the gel pieces with 50 µl of 100% ACN for 15 minutes with shaking. The gel plugs were dried in a HetoVac VR-1 vacuum concentrator (Birkercd, Denmark) at medium speed for 20 minutes and proteins were digested for 16 hours with 25 µl of 10 ng/µl MS grade trypsin in 50 mM ammonium bicarbonate at 37 °C.

Digested peptides spun at 1,000 ×g for 1 minute to spin down the contents, followed by first extraction with 50 µl of 50% ACN for 15 minutes with constant shaking. The extracted peptides were transferred to a new microcentrifuge tube and a second extraction was performed with 50 µl of 100% ACN for another 15 minutes with shaking. Both extractions were pooled into the same tube and dehydrated with HetoVac VR-1 vacuum concentrator for 1 to 2 hours. Dried peptides were stored at -20°C.

3.12.3 Desalting with ZipTip®

Dried peptides were dissolved in 10 µl of 0.1% formic acid. Ten µl of wetting solution (50% ACN) was aspirated into a ZipTip®C18 micropipette tip (Millipore, USA) to wet the C18 column and discarded onto tissue. This was repeated twice, followed by equilibration of the ZipTip® C18 column with 10 µl of equilibration solution (0.1% formic acid) thrice. The sample was aspirated and pipetted up and down repeatedly 10 times and discarded onto the tissue. Ten µl of washing solution (0.1% formic acid) was aspirated and discarded thrice and 2 µl of elution solution (50% ACN in 0.1% formic acid) was pipetted up and down repeatedly 5 times to elute the peptides. Equivalent amount of CHCA matrix solution was added to the eluted peptides and 0.7 µl of the solution was spotted onto the MALDI stainless-steel plate in duplicates. Another 0.7 µl of peptides was subsequently spotted after the spots have dried.

3.12.4 MALDI-TOF/TOF analysis

The peptide mass spectra and MS/MS spectra for each protein spot were obtained on a MALDI-TOF/TOF mass spectrometer (ABI 4800 Plus, Applied Biosystems™, USA) in the positive ion reflector mode. The MS and MS/MS data were searched using internal MASCOT (Matrix Science, UK) against Swiss-Prot database information, whereby seven parameters were set for searching; i) trypsin enzyme; ii) one missed cleavage; iii) variable modifications of carbamidomethyl and oxidation of methionine; iv) peptide charge of 1+; v) monoisotropic mass values; vi) peptide mass tolerance of ± 50 ppm and; vii) fragment mss tolerance of ± 0.1 Da.

3.12.5 Bioinformatics

Identified proteins were searched against UniProt (Swiss-Prot/TrEMBL) Knowledgebase to determine their main biological functions in the cell. Protein-protein interactions were predicted using Search Tool for the Retrieval of Interacting Genes/Proteins (STRING) database v9.0 (www.string-db.org/).

3.13 Western blot

3.13.1 Chemicals and reagents

i) RIPA buffer (25mMTris pH 7.6, 150 mM Sodium chloride (NaCl), 1.0% Triton-X, 1.0% Sodium deoxycholate, 0.1% SDS)

Tris base	0.03 g
NaCl	0.088 g
Triton-X	0.1 ml
Sodium deoxycholate	0.1 g
SDS	0.01 g
ddH_2O	Top up to 10.0 ml

The pH of the solution was adjusted to 7.6, and the solution was stored at -20 °C.

ii) Bicinchoninic Acid (BCA) Protein assay kit (Pierce, USA)

BCA reagent A	500.0 ml
BCA reagent B	25.0 ml
BSA (2.0 mg/ml)	10 x 1.0 ml

iii) Stacking gel buffer (0.5 M Tris-HCl, pH 6.8)

Tris base	18.17 g
ddH_2O	Top up to 50.0 ml

The pH of the solution was adjusted to 8.8, and the solution was stored at 4°C.

iv) 5× Sample buffer (10.0% SDS, 10 mM DTT, 20% Glycerol, 0.2 M Tris-HCl pH 6.8, 0.05% Bromophenol blue)

SDS	5.0 g
DTT	0.078 g
87% glycerol	11.49 ml
0.5 M Tris-HCl, pH 6.8	20.0 ml
0.05% bromophenol blue	0.025 g
ddH_2O	Top up to 50.0 ml

v) 1× Tris-buffered saline with 0.05% Tween-20 (TBST)

Tris base	2.4 g
NaCl	8.8 g
Tween-20	0.5 ml
ddH_2O	Top up to 1.0 L

The pH of the solution was adjusted to 7.6, and the solution was stored at 4°C.

vi) 1× Laemmli SDS electrophoresis buffer

Refer to Section 3.11.1 for the recipe.

vii) 10×Towbin buffer (without methanol)

Tris base	30.3 g
Glycine	144.4 g
ddH_2O	Top up to 1.0 L

The 10× Towbin buffer was diluted to 1× buffer before use.

viii) Blocking buffer (5% Non-fat dry milk)

Blotting grade blocker non-fat dry milk (Bio-Rad, USA)	1.0 g
TBST buffer	20.0 ml

ix) Mouse mAbs specific to β-actin (ACTB), glyceraldehyde-3-phosphate dehydrogenase (GAPDH), cyclin dependent kinase 1 (CDK1),pyruvate dehydrogenase E1 (PDHA1) and GTP-binding nuclear protein ran (RAN)

All primary antibodies were diluted in TBST buffer at a ratio of 1:500.

x) Goat anti-mouse IgG secondary antibody conjugated to horseradish peroxidase (HRP)

The secondary antibody was diluted in TBST buffer at a ratio of 1:2,500.

xi) 2-D Clean-Up kit

xii) PageRulerPrestained protein ladder (Fermentas, Lithuania)

xiii) TMB Stabilised Substrate for HRP (Promega, USA)

xiv) Methanol, absolute (MERCK, Germany)

3.13.2 Protein extraction and quantification

The whole cell protein samples for mock control and CHIKV-infected WRL-68 cells were extracted following the protocol described in section 3.9.1.2, but lysis buffer was replaced with 600 µl of RIPA buffer per flask. Extracted protein samples were quantified using BCA protein assay kit, following manufacturer's protocol. Briefly, a series of BSA standards of eight different concentrations (2.0 mg/ml, 1.5 mg/ml, 1.0 mg/ml, 0.75 mg/ml, 0.50 mg/ml 0.25 mg/ml and 0.125 mg/ml) were prepared. BCA working reagent was prepared by mixing 50 parts of BCA reagent A with 1 part of BCA reagent B. Two-hundred µl of BCA working reagent was pipetted into each well of the 96-well dish. Ten µl of each BSA concentration and sample was added to each well in triplicate. The mixture was equilibrated for 30 minutes at 37 °C and the absorbance was read at 570 nm. The protein concentration for each sample was calculated from the BSA standard curve generated using Microsoft Excel.

The secretome of mock control and CHIKV-infected cells were processed according to the protocols described in sections 3.9.1.2 (Protein sample processing), 3.9.2.2 (Protein clean-up) and 3.9.2.3 (Protein estimation).

3.13.3 1-D Western blot

3.13.3.1 Gel casting

Proteins were resolved on 12% polyacrylamide gels that were cast fresh before use. Briefly, the resolving gel solution (see Table 3.5 for recipe) was prepared and pipette into the gel casting chamber until the height of 1 cm below the top of the glass plates. Isopropanol was overlaid on top of each gel to remove bubbles and the gels

were left to polymerize at room temperature. The isopropanol layer was subsequently removed and the polymerized gel was rinsed with ddH_2O. Thereafter, the stacking gel solution (see Table 3.6 for recipe) was prepared and pipetted on top of the resolving gel. An 8-well comb was inserted into the gel sandwich to form the wells. The stacking gel layer was left to solidify at room temperature.

3.13.3.2 SDS-PAGE

Twenty µg of whole cell proteins for each sample was mixed with 5× sample buffer at a ratio of 4 volume of protein sample to 1 volume of 5× sample buffer. The protein mixture was denatured at 95 °C for 5 minutes, and loaded into each lane. Seven µl of PageRuler Prestained protein ladder was loaded into the last lane on both ends of the gel. Proteins were resolved using the dual vertical mini-gel electrophoresis system (C.B.S. Scientific, USA), at a constant voltage of 100 V. Three biological replicates for each group (mock control and CHIKV-infected) were resolved on the same gel.

Table 3.5: Recipe for casting the resolving gel solution (12% polyacrylamide gel)

Solutions	Amount (ml)
ddH_2O	3.1
Stacking gel buffer	1.25
Monomer solution	0.67
10% SDS	0.05
10% APS	0.025
TEMED	0.005

Table 3.6: Recipe for casting the stacking gel solution (4% polyacrylamide gel)

Solutions	Amount (ml)
ddH_2O	10.2
4× Resolving buffer	7.5
Monomer solution	12.0
10% SDS	0.30
10% APS	0.15
TEMED	0.02

3.13.3.3 Protein transfer

Prior to protein transfer, the polyvinylidene fluoride (PVDF) membrane was soaked in absolute methanol for 2 minutes to activate the membrane, followed by simultaneous equilibration with electrophoresed gel in Towbin buffer for at least 5 minutes. The membrane and gel were positioned side by side, sandwiched in between two pre-wet filter papers and sponges, and clamped tightly to ensure no air bubbles have formed between the gel and membrane. The sandwich was submerged in Towbin buffer and protein transfer was performed using the EBU-200 mini-electrophoresis blotting system (C.B.S. Scientific, USA) at a constant current of 100 mA, with a maximum voltage of 80 V for 1 hour 30 minutes at 4 °C. After transfer, the membrane was blocked overnight in blocking buffer containing 5% non-fat dry milk at 4°C.

3.13.3.4 Antibody staining

After overnight blocking, the membrane was washed thrice with TBST buffer, 10 minutes per wash. The membrane was probed with two antibodies, the endogenous control (either ACTB or GAPDH), and the target protein (CDK1 or PDHA1), without stripping, by making a straight cut from one end of the protein marker to another, thus separating the target protein from the endogenous control. The cut membranes were incubated separately with the respective mouse mAb for 1 hour 30 minutes at room temperature. The membranes were rinsed thrice with TBST buffer, 5 minutes each rinse, and subsequently incubated with HRP-conjugated goat anti-mouse IgG secondary antibody for 1 hour at room temperature. Thereafter, the membranes were rinsed again with TBST buffer and stained with TMB stabilised substrate for HRP for until the intended bands develop. The membrane was rinsed with water and stored dry at room temperature, protected from light.

3.13.3.5 Image analysis

The blot was scanned using ImageScanner™ III in reflective mode, and densitometric quantification was performed using ImageJ v1.45 (http://rsb.info.nih.gov/ij). The mean relative density for each target band was normalised against ACTB or GAPDH and the significance of the expression changes was determined by using Student's t-test.

3.13.4 2-D Western blot

3.13.4.1 2-DGE

2-DGE was performed to resolve secretome sample prior to protein transfer. Sixty µg of secretome sample was rehydrate in Immobiline™ drystrip pH 3-10 linear, 7 cm gels (GE Healthcare, Uppsala, Sweden), as previously described in section 3.10.2. IEF was performed following the protocol in Table 3.7.

Table 3.7: IEF protocol for secretome samples

Steps	Voltage (V)	Voltage-hour (Vhr)	Approx. time
Step-and -hold	200	200	1 h 15 min
Gradient	500	500	1 h
Gradient	1000	1000	2 h
Step-and -hold	4000	17000	4 h
Total:		18700	**8 h 15 min**

Following IEF, the focused strip was equilibrated according to the protocol described in section 3.11.3, and resolved on 12.5% polyacrylamide gel (which was cast following the recipe in Table 3.3) at a constant voltage of 100 V.

3.13.4.2 Protein transfer, staining and image analysis

The blotting sandwich was assembled according to section 3.13.3.2. Protein transfer was carried out at a constant current of 80 mA, with a constant voltage of 80 V, for 1 hour at 4 °C. After transfer, the membrane was blocked overnight in blocking buffer containing 5% non-fat dry milk at 4°C. Protein staining was carried out according to the detailed protocol in section 3.13.3.3, without cutting the membrane as the membrane was stained with the target protein only. The membrane was scanned using the ImageScanner™ III in reflective mode.

3.14 Real-time qPCR

3.14.1 Chemicals, reagents and kits

i) RNeasy Mini kit (Qiagen, USA)

Components:

Buffer RLT	45.0 ml
Buffer RW1	45.0 ml
Buffer RPE	55.0 ml
RNase-free water	10.0 ml
RNeasy mini spin columns	50 pieces
Collection tube (1.5 ml)	50 pieces

ii) RNase-free DNase set (Qiagen, USA)

Components:

DNase I, RNase-free	1,500 Kunitz unit
Buffer RDD	2.0 ml
RNase-free water	1.5 ml

DNase I incubation mix was prepared before use by adding 10 µl of DNase I to 70 µl of buffer RDD.

iii) Preparation of 1% agarose gel

Agarose powder (Invitrogen, USA)	0.5 g
1× Tris/Borate/EDTA (TBE) buffer (Promega, USA)	50.0 ml
Ethidium bromide (EtBr)	1.0 µl

The mixture was heated to dissolve the agarose powder. The agarose gel solution was cooled down to 60 °C prior to addition of 1 µl EtBr. The gel was cast and allowed to polymerize for 1 hour.

iv) High Capacity RNA-to-cDNA kit (Applied Biosystems™, USA)

2× RT buffer	1.0 ml
20× Enzyme mix	100.0 µl

v) Fast SYBR® Green Master Mix (Applied Biosystems™, USA) 2 × 5 ml

vi) QIAshredder mini spin column (Qiagen, USA)

vii) 6× RNA loading dye (Fermentas, Lithuania)

3.14.2 RNA extraction

Total RNA from mock control and CHIKV-infected C6/36 cells was extracted using Qiagen RNeasy Mini kit according to the manufacturer's protocol. All centrifugation steps were performed at full speed. C6/36 cell pellet was lysed in 350 µl of buffer RLT and centrifuged in a QIAshredder mini spin column for 2 minutes. An equal volume of 70% ethanol (HMBG, Germany) was mixed with the flow-through and transferred to an RNeasy spin column placed in a 2 ml collection tube and further centrifuged for 15 seconds. The flow-through was discarded and 350 µl of buffer RW1 was added to the spin column which was then centrifuged for another 15 seconds. The flow-through was discarded and 80 µl of DNase I incubation mix was added to the spin column, followed by 15 minutes incubation at room temperature. The column was subsequently spun for 15 seconds and the flow-through was discarded. Another 350 µl

of buffer RPE was added to the spin column followed by 15 seconds centrifugation. The flow-through was discarded and 500 µl of buffer RPE was added and the spin column was centrifuged for 2 minutes. The flow-through was discarded and the spin column was centrifuged again for 1 minute with the column cap opened to remove residual ethanol and buffer. The spin column was transferred to a new 1.5 ml centrifuge tube. Fifty µl of RNase-free water was pipetted directly onto the RNeasy membrane and the spin column was centrifuged for 1 minute to elute the RNA.

3.14.3 RNA quantitation

RNA quantitation and quality determination was performed using GeneQuant™ 1300 spectrophotometer (GE Healthcare, Uppsala, Sweden). Purified RNA was diluted 40 times in RNase-free water to a final volume of 80 µl and pipetted into a quartz cuvette. The absorbance was read using the spectrophotometer which was previously blanked with 80 µl of RNase-free water. Pure RNA would give an A260/280 absorbance reading between 1.8 and 2.0 and an A230/260 reading above 2.0.

3.14.4 Determination of RNA integrity

RNA integrity was determined via agarose gel electrophoresis. One µg of RNA sample was diluted with nuclease-free water to a final volume of 5 µl. Diluted RNA was mixed well with 1 µl of 6× RNA loading dye and pipetted into the wells of the 1% agarose gel. Electrophoresis was performed at 100V and 100 mA for 45 minutes. Gel image was visualised by Bio-Rad Quantity One software.

3.14.5 Conversion of RNA to cDNA

Conversion of total RNA to cDNA was performed using High Capacity RNA-to-cDNA kit (Applied Biosystems™, USA) following the manufacturer's protocol. One µg of RNA sample was converted per 20 µl reaction following the recipe in Table 3.8. RT reaction mix was aliquot to 0.2 ml PCR tubes. The tubes were briefly centrifuged to spin down the contents and eliminate air bubbles. Reverse transcription was performed using a PCR thermal cycler (PTC-100® Programmable Thermal Controller) in 3 steps. RNA to cDNA conversion was first performed at 37 °C for 60 minutes, followed by 5 minutes run at 95 °C to stop the reaction and the product was cooled to 4 °C. Converted cDNA was stored at -80 °C until qPCR was performed.

Table 3.8: Volume of components required per reaction

Components	Amount (µl)
2X RT buffer	10.0
20X Enzyme mix	1.0
RNA sample	Up to 9.0
Nuclease-free water	Top up to 20.0
Total per Reaction:	20.0

3.14.6 Primer amplification efficiency test

All primers were designed using Primer3 Input (Version 0.4.0) online software at http://frodo.wi.mit.edu/primer3/ and purchased from 1st Base Laboratories, Malaysia. Primer specificity was also confirmed using Basic Local Alignment Search Tool (BLAST) prior to purchase. Each primer pair was then subjected to an efficiency test to determine their amplification efficiency and specificity to the gene product. Five-fold dilutions of the cDNA product were performed to give a range of amounts from 25 ng to 0.04ng. Both the forward and reverse primers were diluted 100 times. Two µl of each cDNA product dilution was mixed with 4 µl each of the forward and reverse primers and 10 µl of Fast SYBR® Green Master Mix to a final volume of 20 µl in a MicroAmp® optical 8-cap strips (Applied Biosystems™, USA). The strips were spun briefly to spin down the content and real-time PCR was performed using the StepOnePlus™ Real-Time PCR System (Applied Biosystems™, USA), following manufacturer's protocol as shown in Table 3.9. All dilutions were assayed in triplicates. The amplification plot was generated and the slope of the curve was determined to calculate the efficiency of the primer whereas primer specificity was evaluated by determining the number of peaks in the dissociation curve.

Table 3.9: Real-time qPCR protocol

Steps	Number of cycles	Temperature (°C)	Duration
i) cDNA synthesis	1	60	30 min
ii) Pre-denaturation	1	94	2 min
iii) cDNAamplification	40		
- Denaturation		94	15 sec
- Annealing		55-65	30 sec
- Elongation		72	1 min
iv) Final extension	1	72	10 min

3.14.7 Quantitation of mRNA expression

For each reaction, 2 µl containing 1ng of template cDNAwas mixed with 4 µl each of the 100X diluted forward and reverse primers, and 10 µl of Fast SYBR® Green Master Mix.Non-template control (NTC) was prepared by substituting 2 µl of template cDNA with de-ionised water. Real-time PCR quantitation was performed using StepOnePlus™ Real-Time PCR System and all reactions were analysed in triplicates using StepOnePlus™ software v2.1 (Applied Biosystems™, USA). The expression level for each gene was normalised against the expression of the internal control, ACTB, and fold-change of CHIKV-infected sample relative to the mock control was calculated based on the delta-delta Ct (ddCt) algorithm, $2^{(-\Delta\Delta Ct)}$. Significance of expression was determined statistically using Student's t-test where significance was defined as $p < 0.05$.

CHAPTER 4

RESULTS

4.1 Determination of virus titer by plaque assay

Following propagation, the titer of each virus stock was determined via plaque assay method using Vero cells. CHIKV was found to be highly infectious in Vero cells, with visible plaques forming shortly after 24 hours post-infection. The earliest incubation time-point to obtain clear and distinct plaques was determined to be 30 hours post-infection (Figure 4.1). To minimise error, each dilution was performed in duplicate and the dilution producing a range of 20 to 100 plaques was chosen to determine the virus titer. Based on plaque titration, CHIKV stock titer was found to be between 2.0×10^8 and 5.0×10^8 pfu/ml.

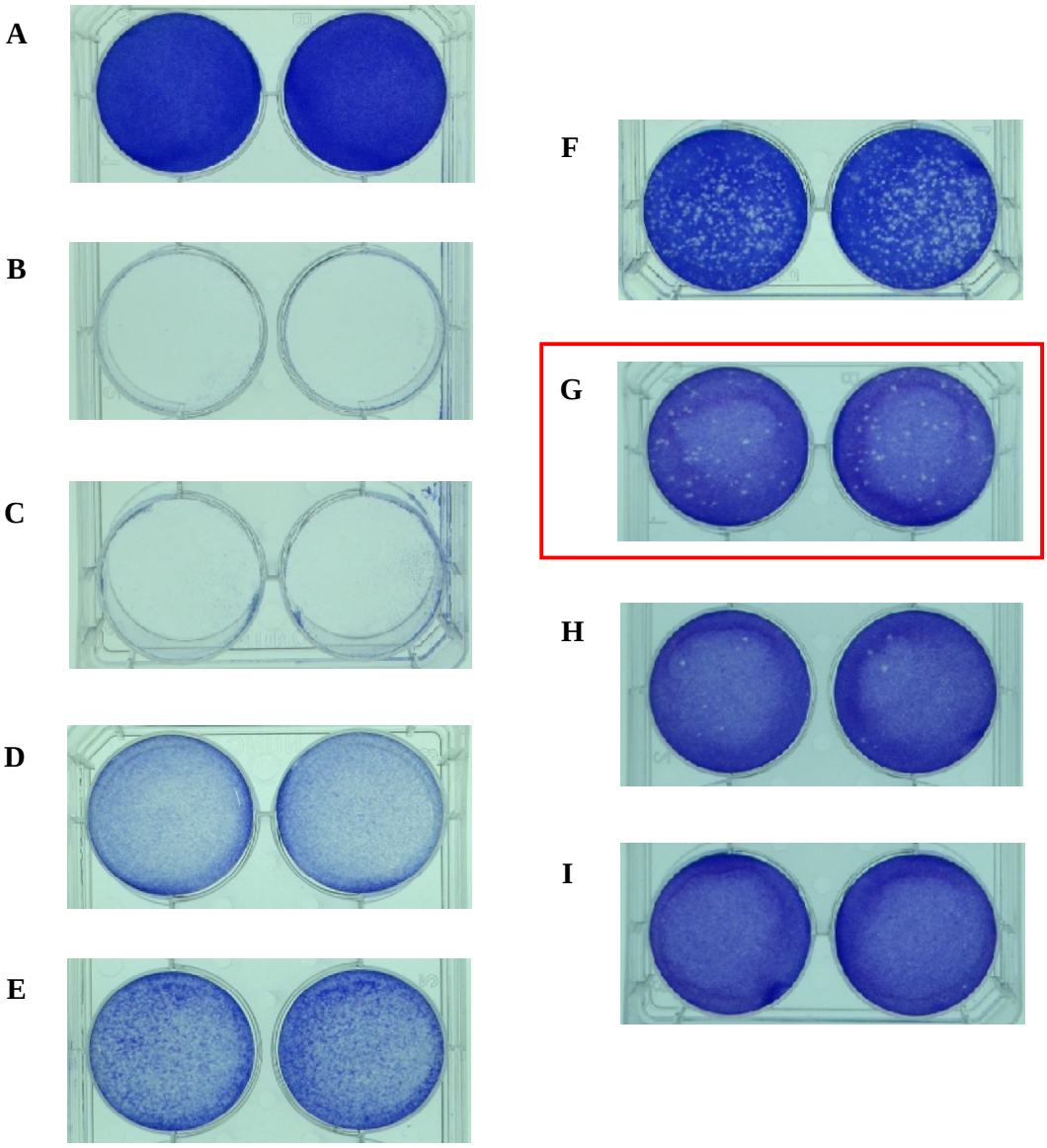

Figure 4.1 Plaque titration of CHIKV in Vero cells at different dilutions

CHIKV stock was subjected to 10-fold serial dilution to a total of 8 dilutions (Panels **B**: 10^{-1} dilution, **C**: 10^{-2} dilution, **D**: 10^{-3} dilution, **E**: 10^{-4} dilution, **F**: 10^{-5} dilution, **G**: 10^{-6} dilution, **H**: 10^{-7} dilution, **I**: 10^{-8} dilution), each plated in duplicate. Mock control Vero cells (Panel **A**) served as negative control. The 10^{-6} dilution (boxed in red) was selected to calculate the titer of the virus using the formula mentioned in section 3.4.4. The virus titer for this batch was determined to be 2.5×10^{8} pfu/ml.

4.2 Optimisation of infection condition for early host response study

Optimisation of the MOI and time-point for early infection study was performed by using four approaches;

i) Morphological analysis

ii) IIFA

iii) Flow cytometric quantification of infected cells

iv) AV/PI staining to quantify cell death

4.2.1 Morphological changes of WRL-68 cells upon CHIKV infection

WRL-68 cells were infected at four different MOIs, ranging from low (MOI of 0.5 and1.0) to high (MOI of 5.0 and 10.0) MOI, and incubated for 24 and 48 hours. The effect of CHIKV infection on the morphology of the cells was observed under inverted microscope at 100× magnification. At 24 hours post infection, morphology of WRL-68 cells infected at the MOI of 0.5, 1.0 and 5.0 was indistinguishable from mock control cells while slight CPE was apparent at the MOI of 10.0. However, marked CPE was observed at 48 hours post-infection, as characterised by cell shrinkage, rounding and detachment. CPE was also found to be more profound with increasing MOI, indicating that cytopathogenicity was time- and MOI-dependent (Figure 4.2).

Figure 4.2: Morphological changes of WRL-68 cells infected with CHIKV

WRL-68 cells were infected with CHIKV at four different MOI (Panels **II**: MOI = 0.5, **III**: MOI = 1.0, **IV**: MOI = 5.0, **V**: MOI = 10.0) and incubated for 24 (Panel **A**) and 48 hours (Panel **B**). Mock control cells (Panel **I**) served as negative control. At 24 hours post-infection, cells infected with CHIKV at the MOI of 0.5, 1.0 and 5.0 exhibited no apparent morphological changes while slight CPE could be seen at the MOI of 10.0. However, CPE was observed in CHIKV-infected cells at all four MOIs at 48 hours post-infection, and was more profound at the MOI of 5.0 and 10.0. All images were captured at 100× magnification.

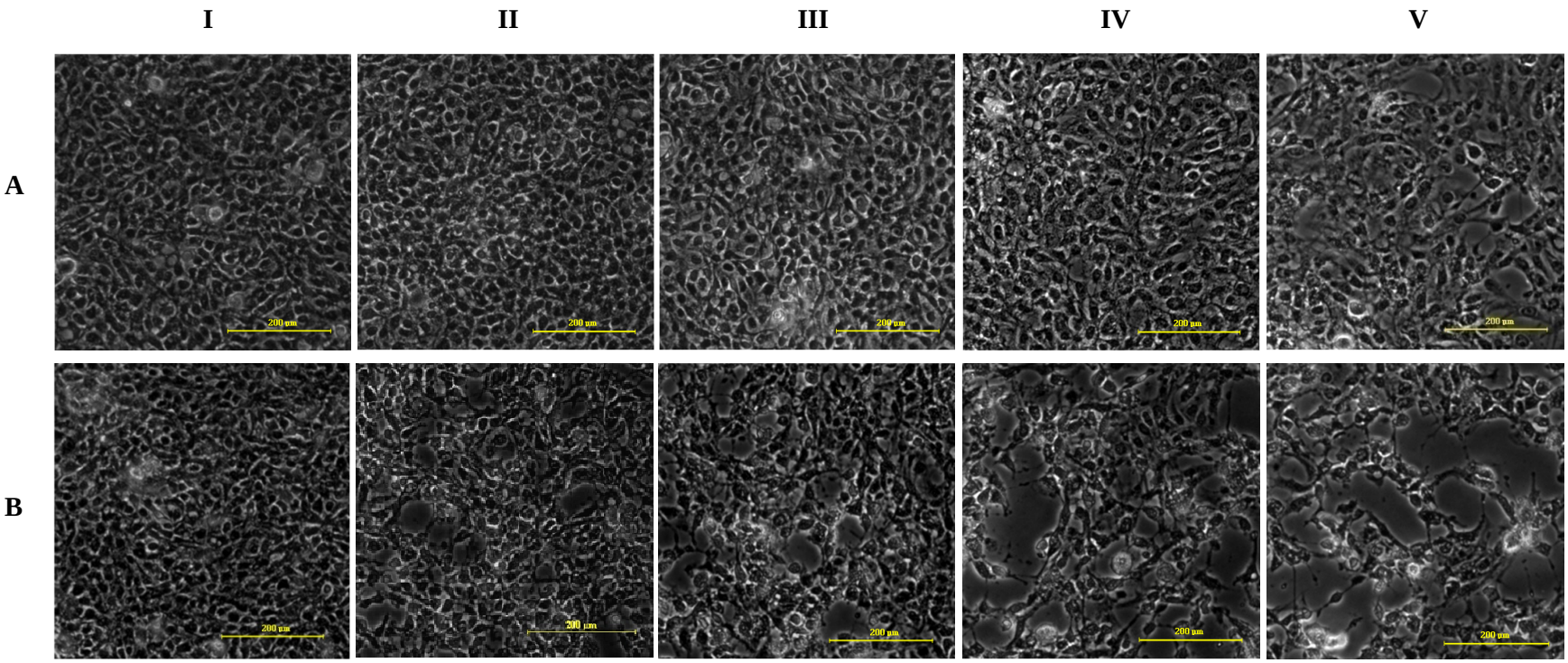
I
II
III
IV
V
A
B
200 µm

4.2.2 Confirmation of CHIKV infection in WRL-68 cells via IIFA

Infection of CHIKV in WRL-68 cells was confirmed by indirect immunostaining of cells with anti-CHIK mAb 3E4 specific to the viral E2 structural protein, as shown in Figure 4.3. CHIKV was found to be highly infectious in WRL-68 cells, as viral antigens were detected in the cells at the lowest MOI (MOI of 0.5) at 24 hours post-infection. Fluorescence intensity, however, was found to be higher at the MOI of 5.0 and 10.0 as compared to lower MOI (MOI of 0.5 and 1.0). At 48 hours post-infection, intense cytoplasmic staining was observed in all infected cells regardless of the MOI used. Conversely, no fluorescence signals were detected in mock control cells at either time-point, indicating no infection.

Figure 4.3: Confirmation of CHIKV infection through anti-CHIK mAb 3E4 immunostaining

Fluorescence detection of CHIKV antigen was performed on WRL-68 cells infected at four different MOI (Panels **II**: MOI = 0.5, **III**: MOI = 1.0, **IV**: MOI = 5.0, **V**: MOI = 10.0) and incubated for 24 (Panel **A**) and 48 hours (Panel **B**). Mock control cells (Panel **I**) served as negative control. Fluorescence intensity of WRL-68 cells infected at low MOI (MOI of 0.5 and 1.0) were lower than that of cells infected at high MOI (MOI of 5.0 and 10.0) at 24 hours post-infection. At 48 hours post-infection however, fluorescence intensity of infected cells appeared similar, irrespective of the MOI used. Cells were visualised under Nikon Eclipse Ti-5 fluorescence inverted microscope and images were captured at 100× magnification.

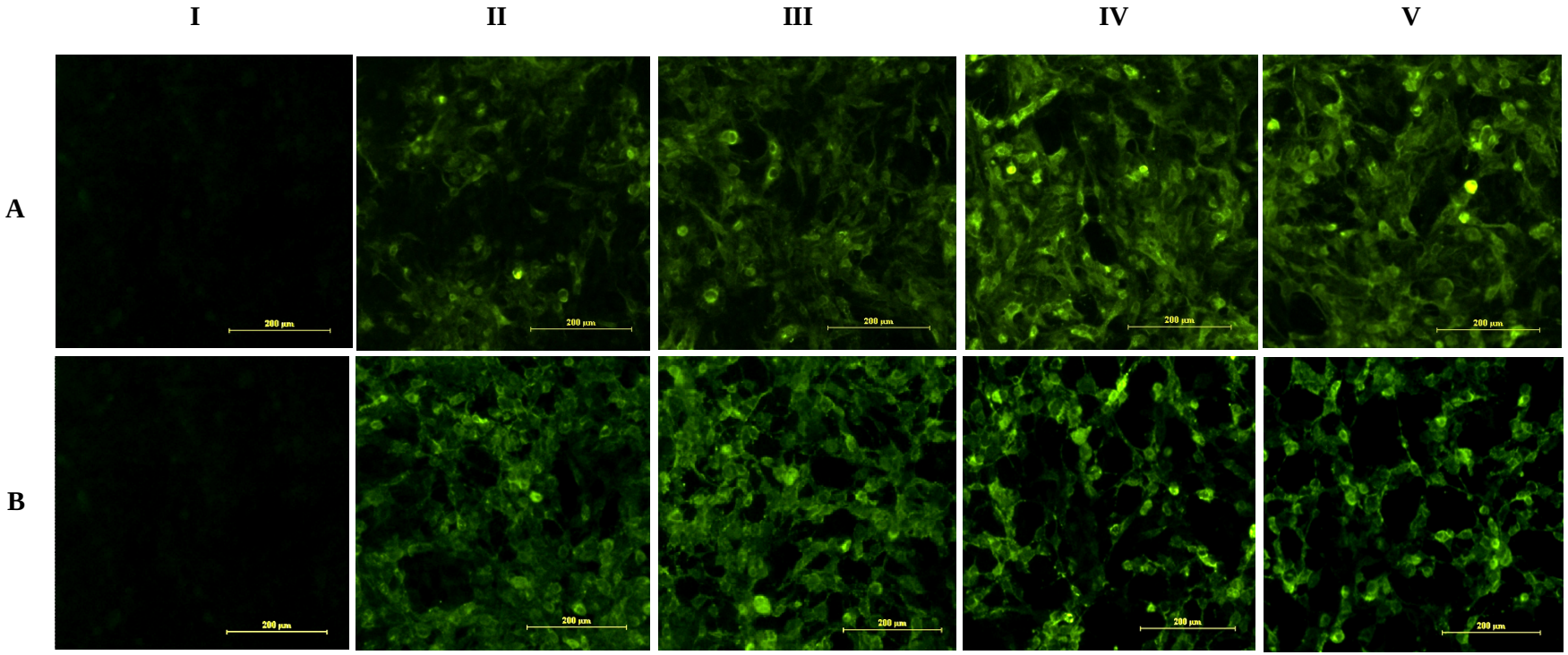
I
II
III
IV
V
A
B
200 µm

4.2.3 Quantitative analysis of infection via flow cytometry

IIFA per se does not provide sufficient proof for accurate selection of the optimal MOI and infection time-point due to the lack of quantitative data. Therefore, the number of infected cells (presented as percentage of infection) was further quantified by flow cytometry. Infected cells were distinguished from uninfected cells based on the relative fluorescence intensity, measured in terms of signal area (FITC-A). The quadrants were defined in such a way that the uninfected population, having minimal or no fluorescence emission (low FITC-A value), appears in the third quadrant (Q3), whereas infected population emits a high fluorescence signal (high FITC-A value) and thus appears in Q4. The dot plots from one of the triplicates are depicted in Figure 4.4.

Figure 4.5 shows the mean percentage of infected cells from three independent experiments. The percentage of infected cells was found to be greater with increasing MOI and incubation period. At 24 hours post-infection, both the MOI of 5.0 and 10.0 showed similarly high percentage of infection at 74.77% ± 9.83 and 75.53% ± 7.43, respectively, while a lower percentage of infection was recorded for the MOI of 0.5 (35.53% ± 3.38) and 1.0 (56.57% ± 6.81). There was a significant increase in the percentage of infected cells at 48 hours post-infection, with more than 70% infection recorded for cells infected at the MOI of 0.5 (74.75% ± 9.30) and 1.0 (80.50% ± 12.63), and more than 90% of cells infected at the MOI of 5.0 (92.43% ± 4.01) and 10.0 (93.10% ± 0.10). Conversely, mock control cells showed no infection at both time-points.

Figure 4.4: Representative flow cytometric dot plots of mock control and CHIKV-infected WRL-68 cells at different MOI at 24 and 48 hours post-infection

The percentage of infected cells was determined by calculating the number of infected cells (Q4)/total number of cells (Q3+Q4) × 100%. The percentage of infected cells was determined for CHIKV-infected cells at four different MOI (Panels **II**: MOI = 0.5, **III**: MOI = 1.0, **IV**: MOI = 5.0 and **V**: MOI = 10.0) at 24 (Panel **A**) and 48 hours (Panel **B**) post-infection. Mock control cells served as negative control (Panel **I**). The uninfected population is gated in Q3 whereas infected population is gated in Q4. A shift in the population from Q3 to Q4 could be observed when the MOI was increased and when the incubation time was longer, indicating an increase in the number of infected cells.

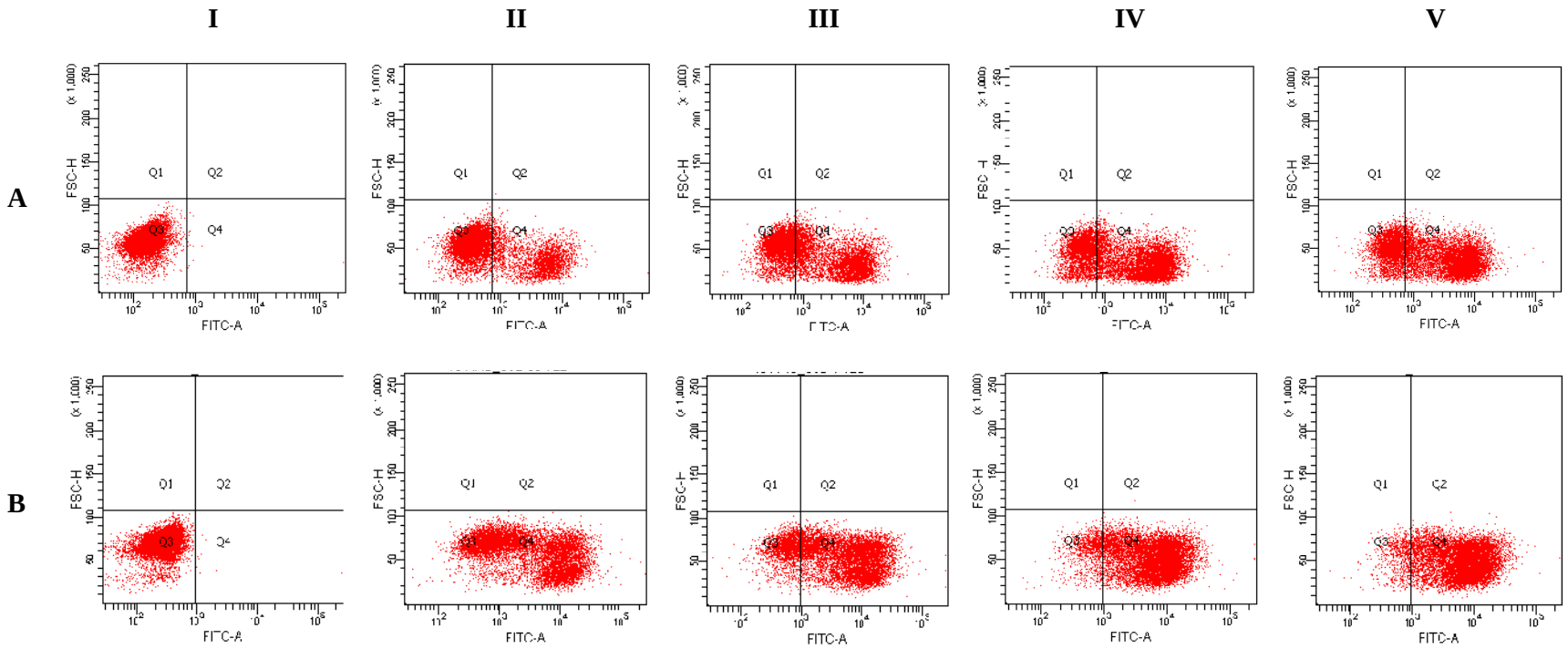
I
II
III
IV
V
A
B
FSC-H
FITC-A
Q1
Q2
Q3
Q4

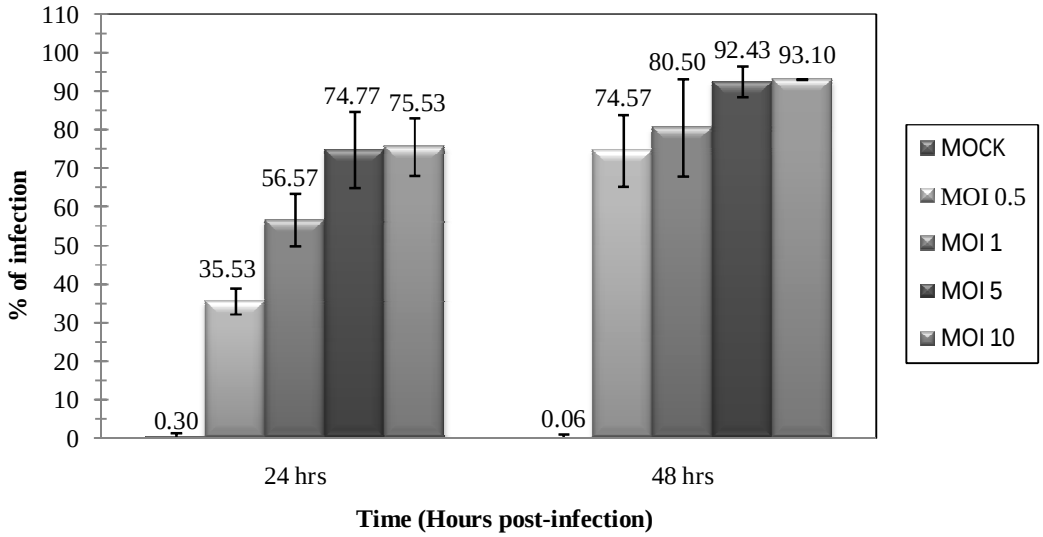

Figure 4.5: Mean percentage of infection of WRL-68 cells infected at different MOI at 24 and 48 hours post-infection

The percentage of infection was determined to increase in a MOI and time-dependent manner. At 24 hours, infection was highest at the MOI of 5.0 (74.77% ± 9.83) and 10.0 (75.53% ± 7.43). At 48 hours post-infection, infection at all four MOI resulted in more than 70% infection. Percentage of infection in mock control cells remained zero at both time-points, indicating no infection. Data presented are representative of three independent experiments and the error bars represent standard deviation.

4.2.4 Quantitative analysis of cell death via AV/PI co-labelling

Measurement of cell death was performed by flow cytometric quantification of CHIKV-infected cells co-labelled with AV and PI, which stains apoptotic and necrotic cells, respectively. Viable cells would not take up any dye (AV^-/PI^-) and will appear in Q3 of the dot plot, as illustrated in Figure 4.6. Cells undergoing early apoptosis will be stained with AV only (AV^+/PI^-), thus appearing as a population in Q4. Meanwhile, late apoptotic cells gated in Q2 are positively stained with both AV and PI (AV^+/PI^+), whereas Q1 population represents dead or necrotic cells stained with PI only (AV^-/PI^+).

To avoid the effects of apoptosis and necrosis in cellular proteome alteration, cell death was defined as cells undergoing both early and late apoptosis, as well as necrosis. Hence, cell populations in Q1, Q2 and Q4were considered as dead cells in determining cell death percentage. Based on the graph shown in Figure 4.7, cell death was observed even for mock control (14.33% ± 3.72 and 17.63% ± 8.15 at 24 and 48 hours respectively). At 24 hours post-infection, cells infected at all four MOI showed slightly higher cell death percentage than mock control cells. Cell viability was considerably lower after 48 hours post-infection, with over 50% cell death regardless of the MOI used. Conversely, percentage of cell death for mock control cells at 48 hours incubation remained similar to that of 24 hours.

Based on the results, the MOI of 5.0 and 24 hours incubation was selected as the optimal condition for early infection study. A high percentage of infection (74.77%) was achieved under this condition, while the percentage of cell death (25.90%), albeit higher than mock control cells (14.33%), was similar to infection at other MOI at 24 hours incubation. Furthermore, infection under this condition did not induce any CPE.

Figure 4.6: Representative AV/PI flow cytometric dot plots of mock and CHIKV-infected WRL-68 cells at different MOI at 24 and 48 hours post-infection

The percentage of infected cells was determined by calculating the number dead cells (Q1+Q2+Q4)/Total number of cells (Q1+Q2+Q3+Q4) × 100%. The percentage of cell death was determined for WRL-68 cells infected at four different MOI (Panels **II**: MOI = 0.5, **III**: MOI = 1.0, **IV**: MOI = 5.0 and **V**: MOI = 10.0) at 24 (Panel **A**) and 48 hours (Panel **B**) post-infection. Mock control cells served as negative control (Panel **I**). Live cells are gated in Q3 (Red dots), while cells undergoing early and late apoptosis are gated in Q4 (Blue dots) and Q2 (Green dots), respectively. Necrotic cells are represented by the red dots in Q1. The percentage of cell death was observed to increase in a MOI and time-dependent manner.

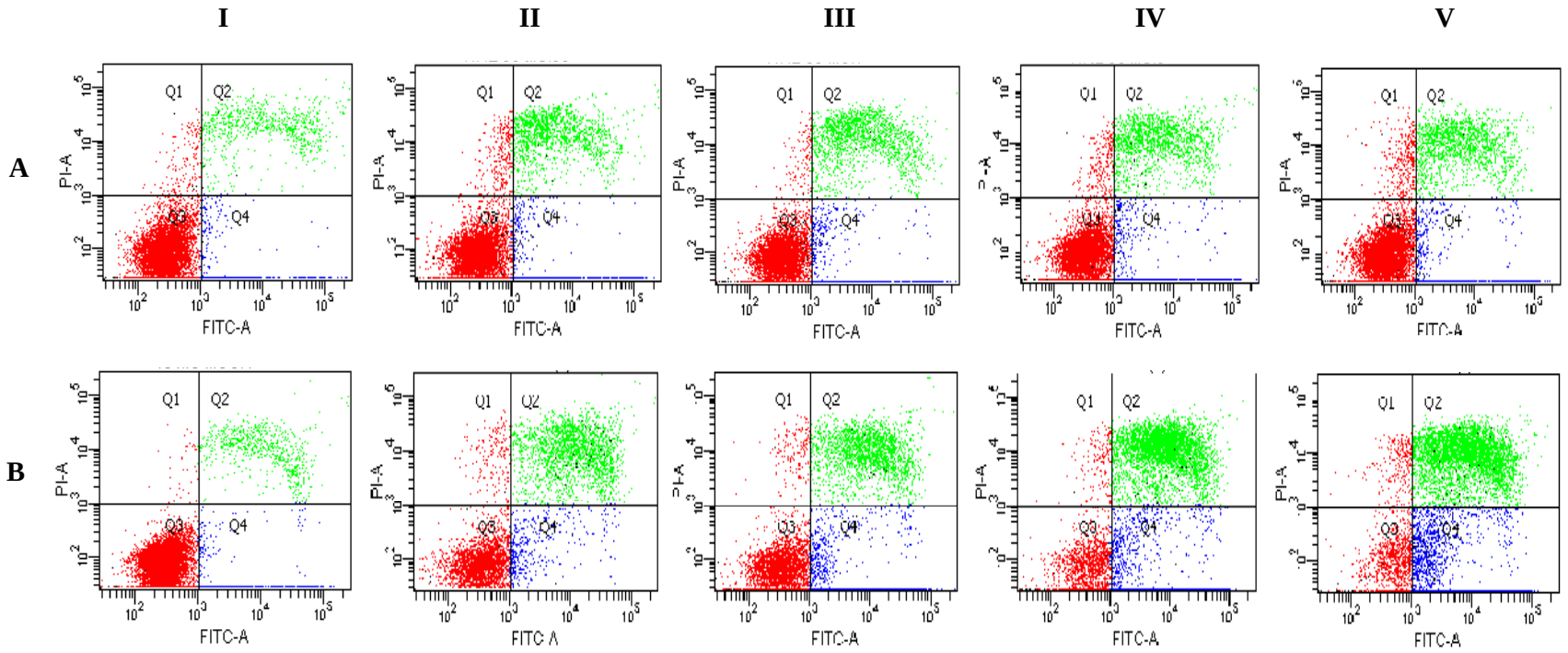
I
II
III
IV
V
A
B
Q1
Q2
Q3
Q4
PI-A
FITC-A

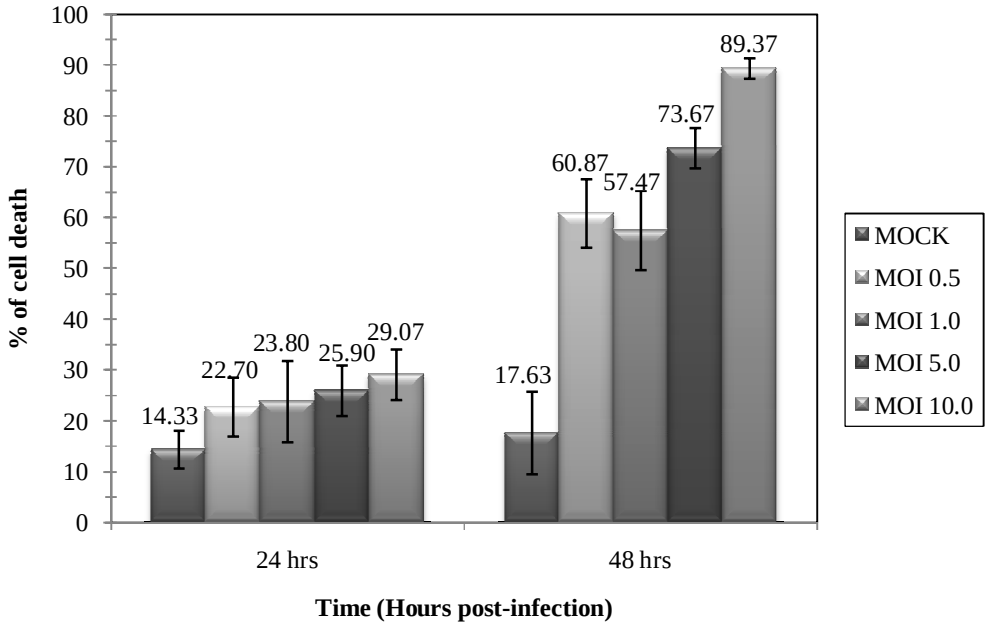

Figure 4.7: Mean percentage of cell death (%) of WRL-68 cells infected at different MOI at 24 and 48 hours post-infection

The percentage of cell death was found to increase in a MOI and time-dependent manner. At 24 hours post-infection, cell death was below 30% for all the MOI used, and 14.33% for mock control cells. A significant increase in percentage of cell death by at least 2.5-fold was observed in cells infected at all four MOI, at 48 hours post-infection. Cell death for mock control cells, however, remained similar to that of 24 hours. Data presented are representative of three independent experiments and the error bars represent standard deviation.

4.3 Optimisation of sample harvesting for analysis of the secretome

For the purpose of analysing the secretome, the effects of serum deprivation and CHIKV infection (at the optimised condition) on cell integrity and viability were evaluated using two assays:

i) MTS cell proliferation assay

ii) Dead-cell protease assay

4.3.1 Effect of serum deprivation on cell viability

MTS was used to investigate the viability of serum-starved WRL-68 cells at the chosen time-point, which was 24 hours. Figure 4.8 shows the relative viability between cells grown in normal DMEM medium (10% FBS) and serum-free medium. No significant difference in cell viability was observed between the two conditions.

4.3.2 Effect of serum deprivation and CHIKV infection on cell membrane integrity

Figure 4.9 depicts the relative percentage of cell lysis between uninfected WRL-68 cells incubated in DMEM growth medium, serum-free medium and CHIKV-infected cells (MOI of 5.0) incubated in serum-free medium for 24 hours. Cells lysed with digitonin were used as the positive control, normalised to 100%. A low percentage of cellular disruption (7.64% ± 0.29) was observed in cells cultured in growth medium. Only a slight increase in the percentage of lysed cells was detected in serum-free cultured cells (9.11% ± 0.46) and CHIKV-infected cells (9.08% ± 0.42), as compared to cells incubated in growth medium.

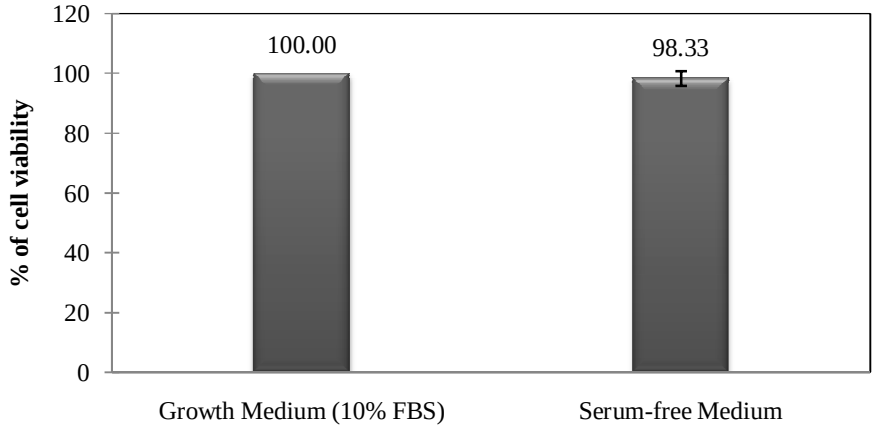

Figure 4.8: Relative cell viability of WRL-68 cells grown in DMEM growth medium (10% FBS) and serum-free medium for 24 hours

Cell viability of WRL-68 cells grown in DMEM growth medium was normalised to 100%, and the relative viability of serum-starved cells was determined. At 24 hours incubation, the absence of serum did not significantly reduce cell viability as percentage viability was above 98%. Data presented are representative of three independent experiments and the error bars represent standard deviation.

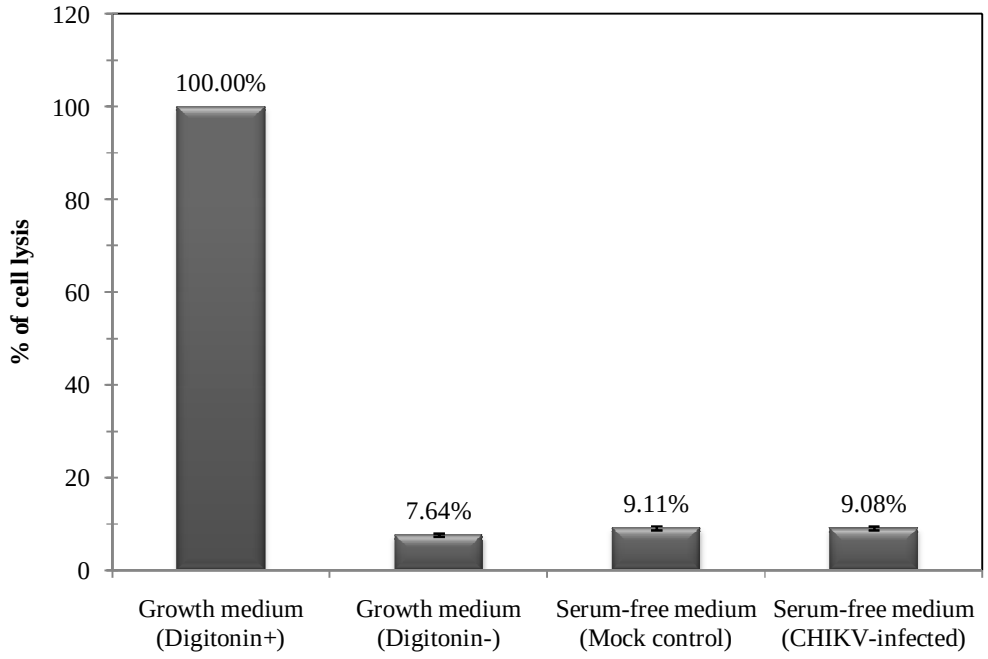

Figure 4.9: Relative percentage of cell lysis between WRL-68 cells incubated in DMEM growth medium, serum-free medium and CHIKV-infected cells incubated in serum-free medium for 24 hours

Percentage of cell lysis for digitonin-lysed cells (positive control) was normalised to 100%. The absence of serum in the culture medium was found to have no significant effect on cellular disruption. Similarly, WRL-68 cells infected with CHIKV at the MOI of 5.0 showed similar percentage as the mock control cells. Data presented are representative of three independent experiments and the error bars represent standard deviation.

4.4 Comparative proteomic study

WRL-68 cells were infected with CHIKV at the MOI of 5.0 at 24 hours post-infection. After infection, the cells were lysed to obtain whole cell proteome or cell lysate while the medium was harvested for the secretome. 2-DGE was employed to resolve and compare the whole cell proteome and secretome of mock control and CHIKV-infected cells to identify the proteins and potential pathways involved during early CHIKV infection. Differentially modulated protein spots were further identified with MALDI-TOF/TOF MS analysis and the expression of three proteins was validated using Western blot. The obtained results are presented in the sections that follow.

4.4.1 Differential protein expression of CHIKV-infected WRL-68 whole cell proteome and secretome

Forty µg of proteins was first separated based on the isoelectric point (pI) on a 13 cm, pH3-10 linear Immobiline™ DryStrip, followed by a second separation on the basis of the molecular weight (M_r) on a 12.5% SDS-PAGE gel. The resulting gel was silver stained and analysed with ImageMaster™ gel analysis software. Figures 4.10 and 4.12 show the representative whole cell proteome and secretome gels of mock control WRL-68 cells, respectively. The expanded views show the spot number of differentially expressed proteins between mock control and CHIKV-infected whole cell proteome (Figures 4.11A and 4.11B) and secretome (Figure 4.13A and 4.13B).Five biological replicates (from five individual flasks) were used for analysis for each group (mock control and CHIKV-infected).

The gel analysis software detected and matched approximately 1,700 and 1,300 spots for whole cell proteome and secretome samples, respectively. Quantitative

analysis of normalised spot volume revealed 53 differentially expressed protein spots for the whole cell proteome sample, and 34 spots with significant modulation for the secretome sample. All proteins were differentially expressed by at least 1.3-fold and were statistically significant ($p<0.05$), as determined by ANOVA and Student's t-test.

Overall, majority of the protein spots were found to be down-regulated in both studies (44 and 25 spots for the whole cell proteome and secretome samples, respectively). Only nine spots were up-regulated in both samples. For the whole cell proteome sample, most protein spots had a fold difference lower than 2.0, and only one spot (UL8) showed a 3.1 fold increase upon infection. The secretome sample, on the other hand, showed higher overall fold-change, with 24 spots having at least a 2.0 fold difference. These protein spots were further subjected to MALDI-TOF/TOF MS for identification.

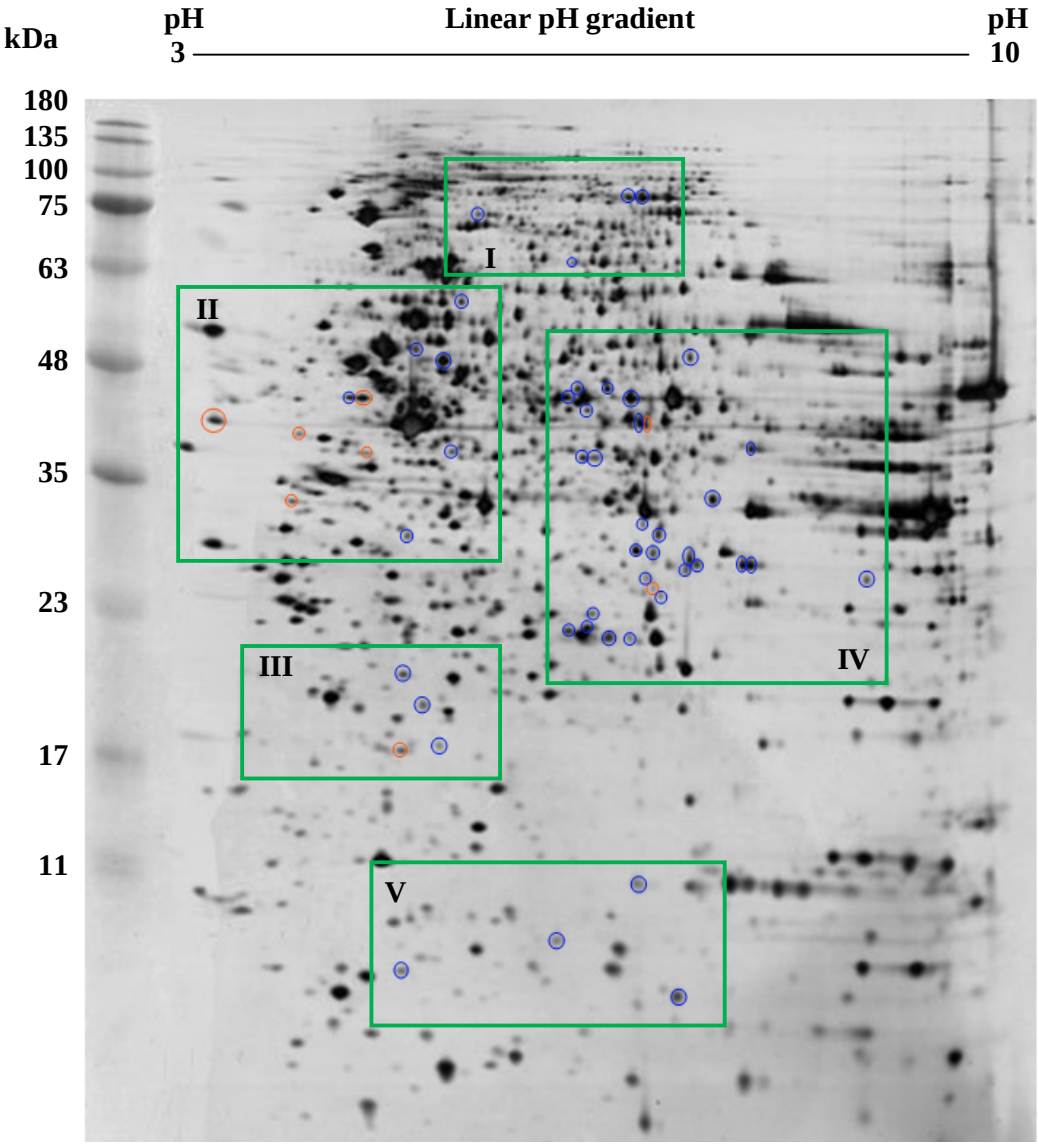

Figure 4.10: Representative proteome map of WRL-68 whole cell proteome

Forty µg of mock control and CHIKV-infected WRL-68 whole cell proteome were resolved on 13 cm linear Immobiline™ DryStrip of pH 3-10 in the first dimension and 12.5% SDS-PAGE gel in the second dimension. The silver stained gels were analysed using ImageMaster™ gel analysis software. A total of 53 protein spots were determined to be differentially expressed, nine of which were up-regulated (circled orange) whereas 44 were down-regulated (circled blue). Boxed areas (I, II, III, IV and V) show the locations of the expanded views illustrated in Figure 4.11.

Figure 4.11: Expanded views showing the location of differentially expressed spots on the mock control and CHIKV-infected WRL-68 whole cell proteome gels

Expanded view of five sections (**I**, **II**, **III**, **IV** and **V**) showing differentially expressed proteins in mock control (**A**) and CHIKV-infected (**B**) 2-D gels. UL1 to UL9 refer to up-regulated protein spots, whereas DL10 to DL53 refer to down-regulated protein spots. Five biological replicates per group (n=5) were used for analysis.

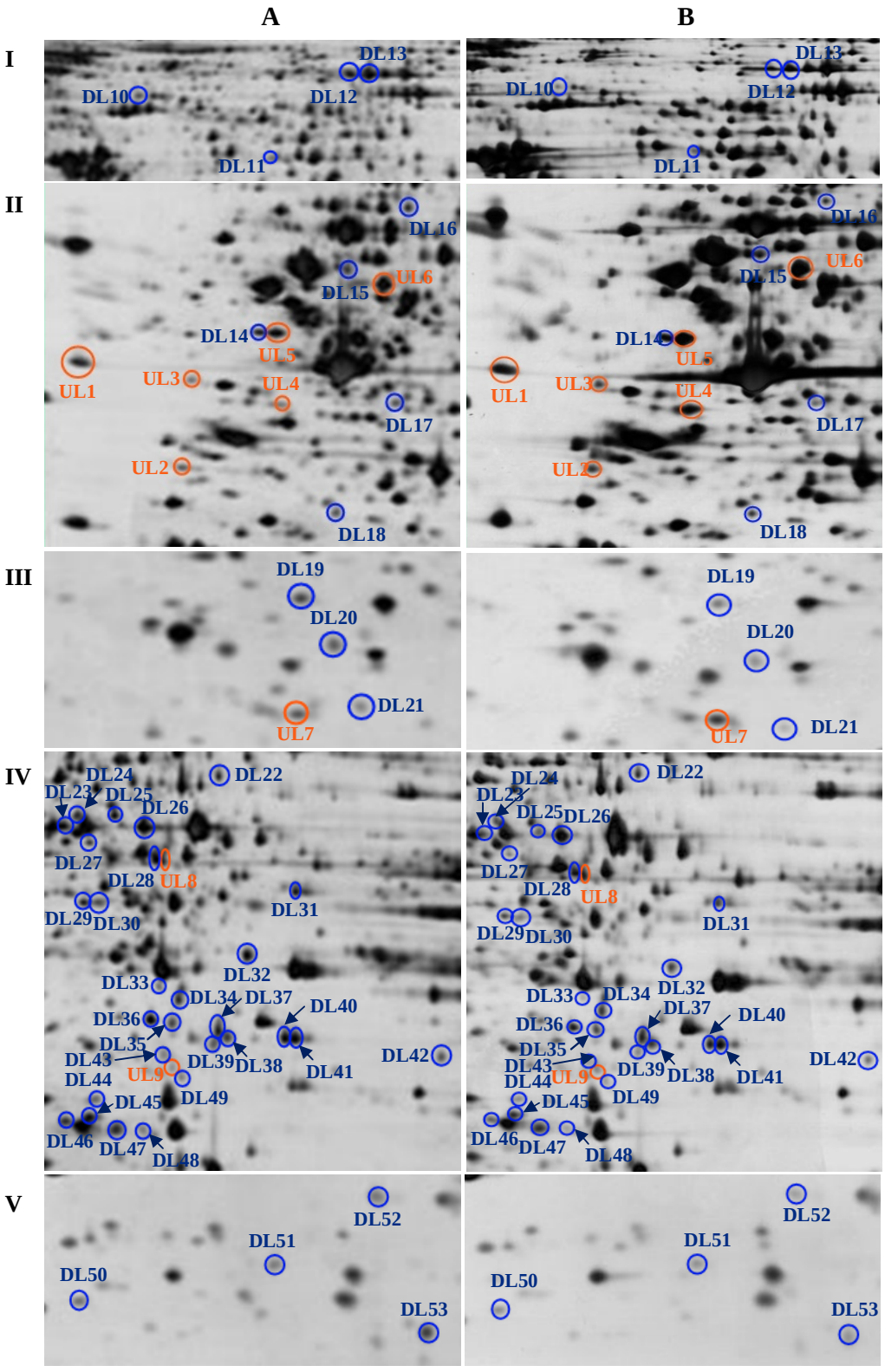
A
B
I
II
III
IV
V
DL10
DL11
DL12
DL13
DL14
DL15
DL16
DL17
DL18
DL19
DL20
DL21
DL22
DL23
DL24
DL25
DL26
DL27
DL28
DL29
DL30
DL31
DL32
DL33
DL34
DL35
DL36
DL37
DL38
DL39
DL40
DL41
DL42
DL43
DL44
DL45
DL46
DL47
DL48
DL49
DL50
DL51
DL52
DL53
UL1
UL2
UL3
UL4
UL5
UL6
UL7
UL8
UL9

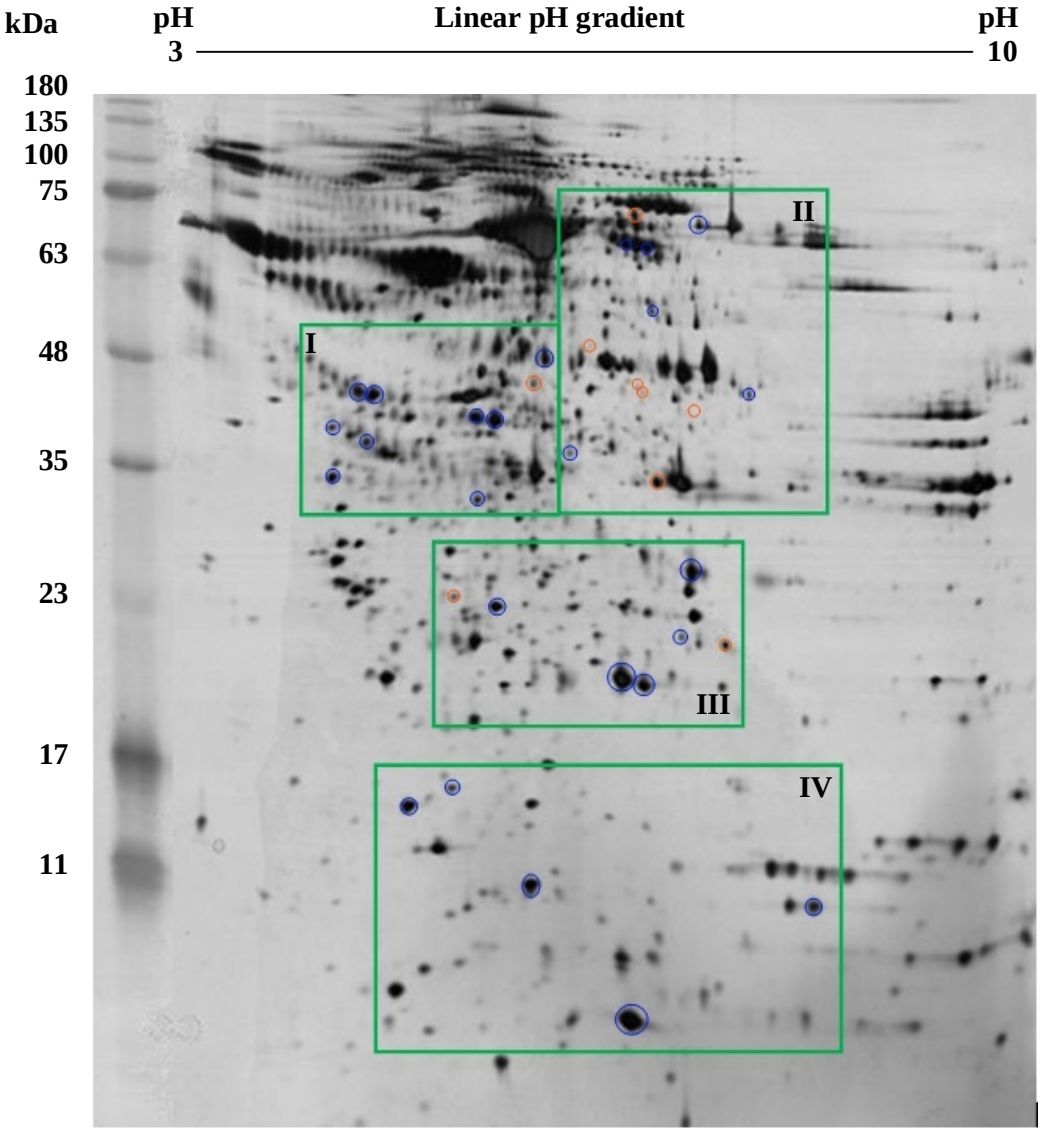

Figure 4.12: Representative proteome map of WRL-68 secretome

Forty µg of mock control and CHIKV-infected WRL-68 secretome were resolved on 13 cm linear Immobiline™ DryStrip of pH 3-10 in the first dimension and 12.5% SDS-PAGE gel in the second dimension. The silver stained gels were analysed using ImageMaster™ gel analysis software. A total of 34 protein spots were determined to be differentially expressed, nine of which were up-regulated (circled orange) whereas 25 were down-regulated (circled blue). Boxed areas (I, II, III and IV) show the location of the expanded images illustrated in Figure 4.13.

Figure 4.13: Expanded views showing the location of differentially expressed spots on the mock control and CHIKV-infected WRL-68 secretome gels

Expanded view of five sections (**I**, **II**, **III** and **IV**) showing differentially expressed proteins between mock control (**A**) and CHIKV-infected (**B**) 2-D gels. US1 to US9 refer to up-regulated protein spots, whereas DS10 to DS34 refer to down-regulated protein spots. Five biological replicates per group (n=5) were used for analysis.

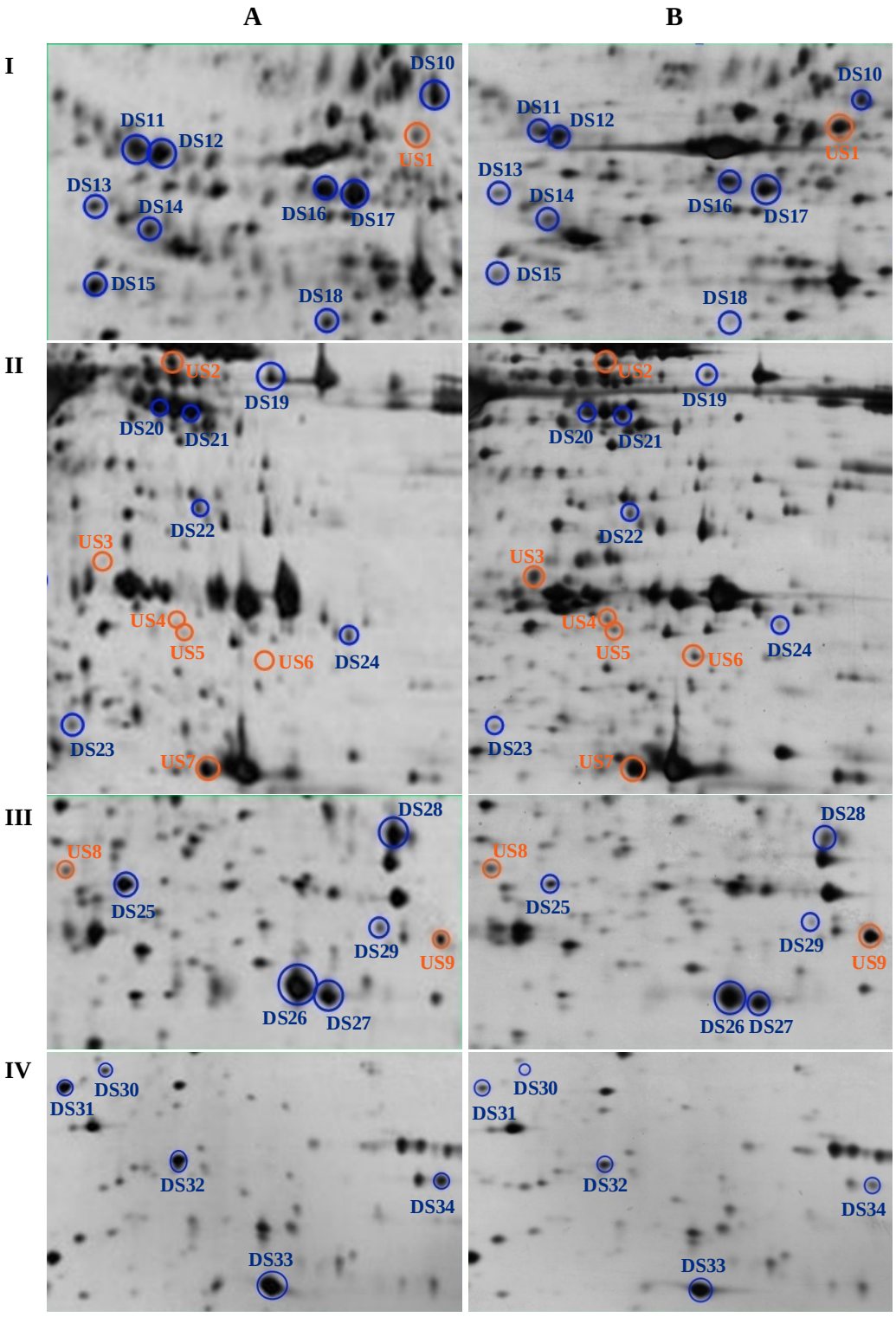
A
B
I
II
III
IV
DS10
DS11
DS12
US1
DS13
DS14
DS16
DS17
DS15
DS18
US2
DS19
DS20
DS21
DS22
US3
US4
US5
US6
DS24
DS23
US7
DS28
US8
DS25
DS29
US9
DS26
DS27
DS30
DS31
DS32
DS34
DS33

4.4.2 MS identification of differentially expressed proteins

The 87 differentially expressed protein spots from the whole cell proteome and secretome samples were excised from five preparative gels each and pooled together. The proteins were digested with MS grade trypsin and subjected to MALDI-TOF/TOF MS analysis. The MS/MS spectra were then queried against Mascot's databases of known sequences and the top 10 protein hits were ranked based on their MOWSE score. Protein identification was considered successful if the MOWSE score was greater than the significant threshold of the Mascot algorithm, and if the protein was the top match. In addition to MOWSE score, the percentage sequence coverage, pI and molecular mass values of the identified protein were taken into consideration in determining the confidence level of identification.

Fifty spots (94.3% identified) from the whole cell proteome sample and 25 spots (73.5% identified) from the secretome sample were successfully identified, as listed in Tables 4.1 and 4.2. These proteins were functionally categorised based on the information obtained from Uniprot (SWISS-PROT/TrEMBL) Knowledgebase. A total of 12 spots (Spots UL9, DL17 and DL53 from the whole cell proteome sample and spots US3, US4, US5, US6, DS11, DS12, DS13, DS14 and DS23 from the secretome sample) failed to be identified. In addition, several spots were identified as the same protein. For instance, spots DL39, DL40 and DL41 were identified as guanine nucleotide-binding protein (GNB2L1), while spots DS26 and DS27 were identified as tissue inhibitor of matrix metalloproteinase 2 (TIMP2). Hence, the 50 and 25 successfully identified spots corresponded to identification of 45 and 20 proteins, respectively.

Of the 45 identified proteins from the whole cell proteome sample, eight exhibited an increase in spot intensity upon CHIKV infection. These proteins include PDHA1 (UL8), chromobox protein homolog 3 (CBX3) (UL7), heterogeneous nuclear ribonucleoprotein C1/C2 (hnRNP C1/C2) (UL4), protein SET (SET) (UL1), cytokeratin-7 (KRT7) (UL5), cytokeratin-17 (KRT17) (UL6), nucleophosmin (NPM1) (UL2), and reticulocalbin-1 (RCN1) (UL3). The other 37 proteins showed reduced spot intensity, including proteins involved in metabolism, protein translation, protein ubiquitination, as well as protein transport and trafficking.

Conversely, for the secretome fraction, five of the identified proteins showed an increase in spot intensity whereas 15 proteins exhibited a decrease in spot intensity. Three of the up-regulated proteins are transport proteins, namely glutamate receptor subunit 3A precursor (GRIN3A) (US1), Ran-specific GTPase-activating protein (RANBP1) (US8) and GTP-binding nuclear protein Ran (RAN) (US9), whereas the other two up-regulated proteins are moesin (MSN) (US2) and aldose reductase (AKR1B1) (US7). Percentage spot volume for proteins involved in the immune and defence response, cell adhesion, protein repair and metalloproteinase inhibition, were all found to be significantly reduced during early CHIKV infection, as shown in Table 4.2.

Table 4.1: List of differentially expressed proteins in the whole cell proteome sample identified by MALDI-TOF/TOF MS

All identified proteins have significant MOWSE scores ($p < 0.05$) of at least 55 and are categorised according to their respective biological functions in the cells.

Spot no.	Protein ID	MOWSE Score/ Coverage (%)	Theoretical pI/ M_r (Experimental pI/ M_r)	Mock-control (Mean ± SD)	CHIKV-infected (Mean ± SD)	Fold-change (*p*-value)	Peptides matched
	RNA/DNA/protein synthesis						
	Transcription						
UL7	Chromobox protein homolog 3	88 (27)	5.23/20.8 (4.6/17.3)	0.0360 ± 0.007	0.0501 ± 0.009	1.39 (0.022)	5
DL33	Pirin	107 (33)	6.42/32.1 (6.8/30.2)	0.0198 ± 0.002	0.0126 ± 0.011	-1.57 (0.005)	15
	Translation						
DL12	Elongation factor 2	497 (37)	6.42/95.3 (6.7/75.0)	0.1986 ± 0.017	0.1470 ± 0.045	-1.35 (0.043)	46
DL13	Elongation factor 2	338 (20)	6.42/95.3 (6.8/75.0)	0.1261 ± 0.023	0.0774 ± 0.030	-1.63 (0.022)	17
DL29	Eukaryotic translation initiation factor 3 subunit H	174 (11)	6.09/39.9 (6.3/36.9)	0.0702 ± 0.015	0.0444 ± 0.015	-1.58 (0.028)	4
DL43	Translation initiation factor eIF-2B subunit alpha	94 (34)	6.90/33.7 (6.8/25.4)	0.0375 ± 0.007	0.0243 ± 0.004	-1.54 (0.008)	11
	mRNA processing						
UL4	Heterogeneous nuclear ribonucleoproteins C1/C2	278 (27)	4.95/33.7 (4.4/37.1)	0.0292 ± 0.018	0.0905 ± 0.022	3.10 (0.0028)	21
DL25	La ribonucleoprotein	101 (23)	6.68/46.8 (6.5/43.1)	0.0886 ± 0.022	0.0128 ± 0.053	-1.67 (0.015)	16

Table 4.1: Continue

DL30	Poly(rC)-binding protein1	116 (29)	6.66/37.5 (6.4/37.0)	0.0698 ± 0.009	0.0492 ± 0.016	-1.42 (0.039)	17
	Metabolism						
	Carbohydrate metabolism						
UL8	Pyruvate dehydrogenase E1	126 (19)	8.35/43.3 (6.8/39.1)	0.0395 ± 0.019	0.0773 ± 0.023	1.96 (0.024)	14
DL11	Phosphoglucomutase 2	197 (26)	6.28/68.2 (6.2/63.9)	0.0269 ± 0.007	0.0118 ± 0.003	-2.29 (0.004)	16
DL14	Gamma-enolase	215 (36)	4.91/47.2 (4.2/42.8)	0.0873 ± 0.011	0.0592 ± 0.010	-1.47 (0.003)	17
DL26	Alpha-enolase	113 (28)	7.01/47.1 (6.7/42.8)	0.2530 ± 0.020	0.1909 ± 0.026	-1.32 (0.003)	18
DL28	Isocitrate dehydrogenase (NADP)	176 (24)	6.53/46.6 (6.7/39.1)	0.1428 ± 0.032	0.0910 ± 0.019	-1.57 (0.015)	16
DL35	Glucosamine-6-phosphate isomerase	95 (27)	6.42/32.7 (6.9/26.1)	0.0652 ± 0.014	0.0455 ± 0.008	-1.43 (0.027)	16
DL44	Phosphoglycerate mutase 1	347 (44)	6.28/68.2 (6.2/23.1)	0.0450 ± 0.004	0.0327 ± 0.008	-1.37 (0.019)	14
DL47	Triosephosphateisomerase	141 (55)	6.45/26.7 (6.5/21.6)	0.1147 ± 0.013	0.0778 ± 0.008	-1.81 (0.000)	15
DL48	Triosephosphateisomerase	129 (33)	6.45/26.7 (6.7/21.6)	0.0416 ± 0.010	0.0230 ± 0.003	-1.47 (0.005)	9
	Nucleotide metabolism						
DL20	Inosine triphosphate pyrophosphatase	97 (27)	5.50/21.4 (6.8/19.8)	0.0391 ± 0.003	0.0296 ± 0.005	-1.32 (0.012)	6
DL21	Adenine phosphoribosyltransferase	239 (57)	5.78/19.6 (7.0/18.2)	0.0214 ± 0.005	0.0141 ± 0.003	-1.52 (0.035)	12
DL22	Nicotinamide phosphoribosyltransferase	164 (15)	6.69/55.5 (7.2/48.2)	0.0527 ± 0.008	0.0365 ± 0.006	-1.44 (0.010)	14
DL27	Adenylosuccinate synthetase isozyme 2	486 (46)	6.13/50.0 (6.3/40.9)	0.0503 ± 0.016	0.0223 ± 0.012	-2.25 (0.014)	28
DL34	Ribose-phosphate pyrophosphokinase I	104 (38)	6.51/34.8 (7.0/28.3)	0.0668 ± 0.007	0.0504 ± 0.002	-1.33 (0.001)	14
DL49	S-methyl-5-thioadenosine phosphorylase	303 (53)	6.75/31.2 (7.0/24.5)	0.0261 ± 0.004	0.0182 ± 0.005	-1.44 (0.039)	25

Table 4.1: Continue

	Lipid metabolism						
DL15	Hydroxymethylglutaryl-CoA synthase , cytoplasmic	62 (17)	5.22/57.3 (3.8/49.3)	0.0655 ± 0.014	0.0405 ± 0.003	-1.62 (0.005)	14
DL32	Aldo-ketoreductase family 1 member C2	250 (40)	7.13/36.7 (7.4/33.1)	0.0873 ± 0.016	0.0541 ± 0.017	-1.62 (0.015)	15
DL46	Isopentyl-diphosphate Delta-isomerase 1 (IPP isomerase)	129 (14)	5.93/26.3 (6.1/22.1)	0.0643 ± 0.007	0.0395 ± 0.007	-1.63 (0.001)	4
	Amino acid metabolism						
DL31	Phosphoserine aminotransferase	81 (14)	7.56/40.4 (7.8/38.0)	0.0956 ± 0.026	0.0553 ± 0.015	-1.73 (0.018)	10
	Detoxification						
DL36	S-formylglutathione hydrolase	68 (31)	6.54/31.4 (6.7/26.1)	0.1085 ± 0.011	0.0737 ± 0.015	-1.47 (0.004)	14
	Cell cycle and apoptosis						
UL1	Protein SET	303 (38)	4.23/33.5 (3.0/39.1)	0.0953 ± 0.025	0.1363 ± 0.017	1.43 (0.017)	20
DL39	Guanine nucleotide-binding protein	64 (18)	7.60/35.1 (7.2/25.5)	0.0417 ± 0.007	0.0162 ± 0.003	-2.58 (0.002)	8
DL40	Guanine nucleotide-binding protein	400 (58)	7.60/35.1 (7.7/25.8)	0.1428 ± 0.048	0.0758 ± 0.036	-1.88 (0.038)	24
DL41	Guanine nucleotide-binding protein	606 (67)	7.60/35.1 (7.8/25.8)	0.1226 ± 0.011	0.0871 ± 0.018	-1.40 (0.006)	30
DL42	Cell division control protein 2 homolog (Cyclin dependent kinase 1)	335 (58)	8.37/34.0 (8.8/25.4)	0.0426 ± 0.011	0.0240 ± 0.005	-1.77 (0.010)	28
	Cell structure						
UL5	Keratin, type I cytoskeletal 17	760 (47)	4.97/48.1 (4.3/42.8)	0.1510 ± 0.017	0.2054 ± 0.024	1.36 (0.004)	40
UL6	Keratin, type II cytoskeletal 7	751 (52)	5.50/51.4 (5.0/47.9)	0.2186 ± 0.019	0.3065 ± 0.055	1.40 (0.010)	36
DL37	Actin-related protein 2/3 complex subunit 2 (p34-ARC)	192 (42)	6.84/34.3 (7.2/25.9)	0.1003 ± 0.013	0.0710 ± 0.011	-1.41 (0.007)	20

Table 4.1: Continue

	Transport and trafficking						
DL16	Copine-1	147 (4)	5.52/59.0 (5.2/60.0)	0.0436 ± 0.015	0.0249 ± 0.003	-1.75 (0.030)	3
DL23	Rab GDP dissociation inhibitor beta	441 (42)	6.11/50.6 (6.1/42.8)	0.0894 ± 0.015	0.0382 ± 0.022	-2.34 (0.003)	25
DL24	Rab GDP dissociation inhibitor beta	132 (34)	6.11/50.6 (6.2/43.1)	0.0575 ± 0.013	0.0381 ± 0.010	-1.51 (0.036)	16
DL38	Electron transfer flavoprotein subunit alpha	129 (22)	8.62/35.1 (7.3/25.7)	0.0639 ± 0.013	0.0450 ± 0.012	-1.42 (0.047)	8
DL51	Fatty-acid binding protein, epidermal	100 (52)	6.60/15.2 (6.0/9.1)	0.0389 ± 0.008	0.0268 ± 0.002	-1.46 (0.012)	12
	Protein ubiquitination and degradation						
DL19	Ubiquitin-conjugating enzyme E2	215 (39)	5.33/22.4 (5.7/20.9)	0.0420 ± 0002	0.0290 ± 0.003	-1.45 (0.001)	16
DL45	Proteasome subunit alpha type-6	215 (50)	6.34/27.4 (6.3/22.7)	0.0964 ± 0.012	0.0635 ± 0.017	-1.52 (0.008)	21
	Immune response						
DL52	Peptidyl-prolylcis-trans isomerase A (Cyclophilin A)	158 (41)	7.68/18.0 (6.8/10.7)	0.0543 ± 0.003	0.0399 ± 0.006	-1.36 (0.003)	22
	Chaperone						
UL2	Nucleophosmin (B23)	100 (22)	4.64/32.6 (3.7/33.1)	0.0307 ± 0.006	0.0426 ± 0.005	1.38 (0.011)	8
	Binding						
UL3	Reticulocalbin-1 precursor	299 (30)	4.86/38.9 (3.8/38.5)	0.0226 ± 0.002	0.0319 ± 0.004	1.41 (0.004)	17
	Signalling						
DL50	Thioredoxin-like protein 5	103 (22)	5.40/13.9 (4.7/8.0)	0.0366 ± 0.003	0.0268 ± 0.006	-1.37 (0.020)	4
	Miscellaneous						
DL10	Spartin	80 (7)	5.66/72.8 (5.3/73.4)	0.0256 ± 0.007	0.0154 ± 0.005	-1.67 (0.035)	5
DL18	Spermidine synthase	228 (23)	5.30/33.8 (4.7/28.6)	0.0390 ± 0.007	0.0290 ± 0.006	-1.35 (0.036)	12

Table 4.2: List of differentially expressed proteins in the secretome sample identified by MALDI-TOF/TOF MS

All identified proteins have significant MOWSE scores ($p < 0.05$) of at least 55 and are categorised according to their respective biological functions in the cells.

Spot no.	Protein ID	MOWSE Score/ Coverage (%)	Theoretical pI/ M_r (Experimental pI/ M_r)	Mock-control (Mean ± SD)	CHIKV-infected (Mean ± SD)	Fold-change (*p*-value)	Peptides matched
	Immune and defence response						
DS10	Cathepsin D	395 (38)	6.10/44.5 (6.1/48.2)	0.1655 ± 0.028	0.0610 ± 0.031	-2.72 (0.001)	23
DS16	Cathepsin L1	109 (5)	5.31/37.5 (6.5/39.8)	0.1904 ± 0.048	0.1072 ± 0.027	-1.78 (0.010)	2
DS17	Cathepsin L1	109 (5)	5.31/37.5 (6.6/39.8)	0.3237 ± 0.067	0.1280 ± 0.051	-2.53 (0.001)	2
DS19	Complement C3 precursor	224 (10)	6.02/187.0 (7.4/73.0)	0.0786 ± 0.033	0.0245 ± 0.011	-3.21 (0.009)	28
DS33	β-2 microglobulin	68 (8)	6.06/13.7 (6.8/7.3)	0.9748 ± 0.157	0.5797 ± 0.125	-1.68 (0.002)	1
DS34	Cystatin-3	179 (47)	9.00/15.8 (8.5/9.5)	0.1393 ± 0.025	0.0512 ± 0.013	-2.72 (0.000)	14
	Transport proteins						
US1	Glutamate receptor subunit 3A precursor	44 (11)	7.81/125.5 (6.0/42.2)	0.0308 ± 0.013	0.0941 ± 0.046	3.05 (0.014)	18
US8	Ran-specific GTPase-activating protein	102 (19)	5.19/23.3 (5.3/23.0)	0.0243 ± 0.003	0.0438 ± 0.012	1.80 (0.011)	9
US9	GTP-binding nuclear protein Ran	227 (51)	7.01/24.4 (7.7/22.1)	0.0594 ± 0.010	0.2185 ± 0.036	3.68 (0.000)	19
DS18	Vesicular integral-membrane protein VIP36 precursor	473 (44)	6.46/40.2 (5.5/33.7)	0.0307± 0.018	0.0136 ± 0.003	-2.25 (0.050)	23
DS22	Tubulointerstitial nephritis antigen-like precursor	85 (16)	6.54/52.4 (7.0/55.4)	0.0475± 0.009	0.0170 ± 0.010	-2.79 (0.001)	11

Table 4.2: Continue

	Cell adhesion						
DS15	Collagen alpha-1(V) chain precursor	199 (9)	4.94/183.4 (4.2/34.8)	0.1119 ± 0.036	0.0356 ± 0.013	-3.14 (0.002)	25
DS32	Cadherin-2 precursor	405 (11)	4.64/99.7 (5.9/10.4)	0.2778 ± 0.060	0.0935 ±0.042	-2.97 (0.001)	18
	Metalloproteinases inhibitor						
DL26	Tissue inhibitor of metalloproteinases 2	282 (35)	7.45/24.4 (6.7/21.3)	0.2858 ± 0.105	0.1357 ± 0.059	-2.11 (0.024)	15
DL27	Tissue inhibitor of metalloproteinases 2	360 (39)	7.45/24.4 (7.0/21.3)	0.7474 ± 0.105	0.4013 ± 0.140	-1.86 (0.002)	20
DL28	Tissue inhibitor of metalloproteinases 1	498 (67)	8.46/23.2 (7.4/23.7)	0.2818 ± 0.079	0.0817 ± 0.033	-3.45 (0.001)	18
	Carbohydrate and lipid metabolism						
US7	Aldose reductase	212 (45)	6.51/35.8 (7.1/34.5)	0.1718 ± 0.051	0.3167 ± 0.050	1.84 (0.002)	28
DS20	Kexin type 9 precursor	288 (9)	6.09/74.3 (6.8/66.9)	0.2072 ± 0.046	0.0482 ± 0.020	-4.30 (0.001)	11
DS21	Kexin type 9 precursor	67 (6)	6.09/74.3 (7.0/66.5)	0.0336 ± 0.015	N/A	N/A (0.001)	6
DS30	Kexin type 9 precursor	428 (34)	6.09/74.3 (5.3/16.2)	0.1723 ± 0.045	0.0493 ± 0.027	-3.50 (0.002)	29
DS31	Kexin type 9 precursor	460 (19)	6.09/74.3 (4.9/13.1)	0.1423 ± 0.008	0.0599 ± 0.013	-2.41 (0.001)	22
	Protein repair						
DS29	Protein-L-isoaspartate O-methyltransferase	98 (35)	6.70/24.6 (7.3/22.3)	0.0238 ± 0.005	0.0104 ± 0.002	-2.29 (0.002)	12
	Regulation of MAPK cascade						
DL25	Renin receptor precursor(ATPase H(+)-transporting lysosomal accessory protein 2)	104 (380)	5.76/39.0 (5.6/22.7)	0.1632 ± 0.064	0.0370 ± 0.015	-4.42 (0.003)	18
	Miscellaneous						
US2	Moesin	86 (22)	6.08/67.8 (6.9/74.5)	0.0829 ± 0.025	0.1272 ± 0.022	1.53 (0.021)	22
DS24	Plasminogen activator inhibitor 1 precursor	88 (23)	6.68/45.0 (7.9/42.1)	0.0294 ± 0.010	0.0120 ± 0.005	-2.46 (0.009)	14

4.4.3 Functional classification and sub-cellular location distribution of altered proteins

Figures 4.14A and 4.14B show functional distribution of identified proteins from the whole cell proteome and secretome samples, respectively. Whole cell proteins were clustered into 10 main groups whereas proteins from the secretome sample were categorised into seven functional classes, based on the information obtained from UniProt (SWISS-PROT/TrEMBL) Knowledgebase. Early CHIKV infection had major impact on the expression changes of metabolic enzymes, which constituted 42.22% of the total altered whole cell proteins, followed by proteins involved in DNA/RNA/protein synthesis (17.78%). On the contrary, a major proportion of differentially modulated proteins from the secretome sample were involved in transport as well as in immune and defence response (25.00% for both).

The percentage breakdown of the sub-cellular protein distribution is shown in Figures 4.15A and 4.15Bfor the whole cell proteome and secretome samples, respectively. More than half of the whole cell proteins were found in the cytoplasm (56.90%). Nevertheless, proteins located in the nucleus (17.24%), cell membrane (8.62%), mitochondrion (5.17%), cytoskeleton/intermediate filament (5.17%), endoplasmic reticulum (ER) (3.45%) and peroxisome (3.45%), were also differentially expressed upon CHIKV infection. Conversely, only 50.00% of proteins identified in the secretome fraction were secreted proteins, while other modulated proteins, albeit detected in the culture medium, were intracellular proteins located primarily in the cellular membrane (15.38%), lysosome (11.54%), cytoplasm (11.54%), nucleus (7.69%) and ER (3.85%).

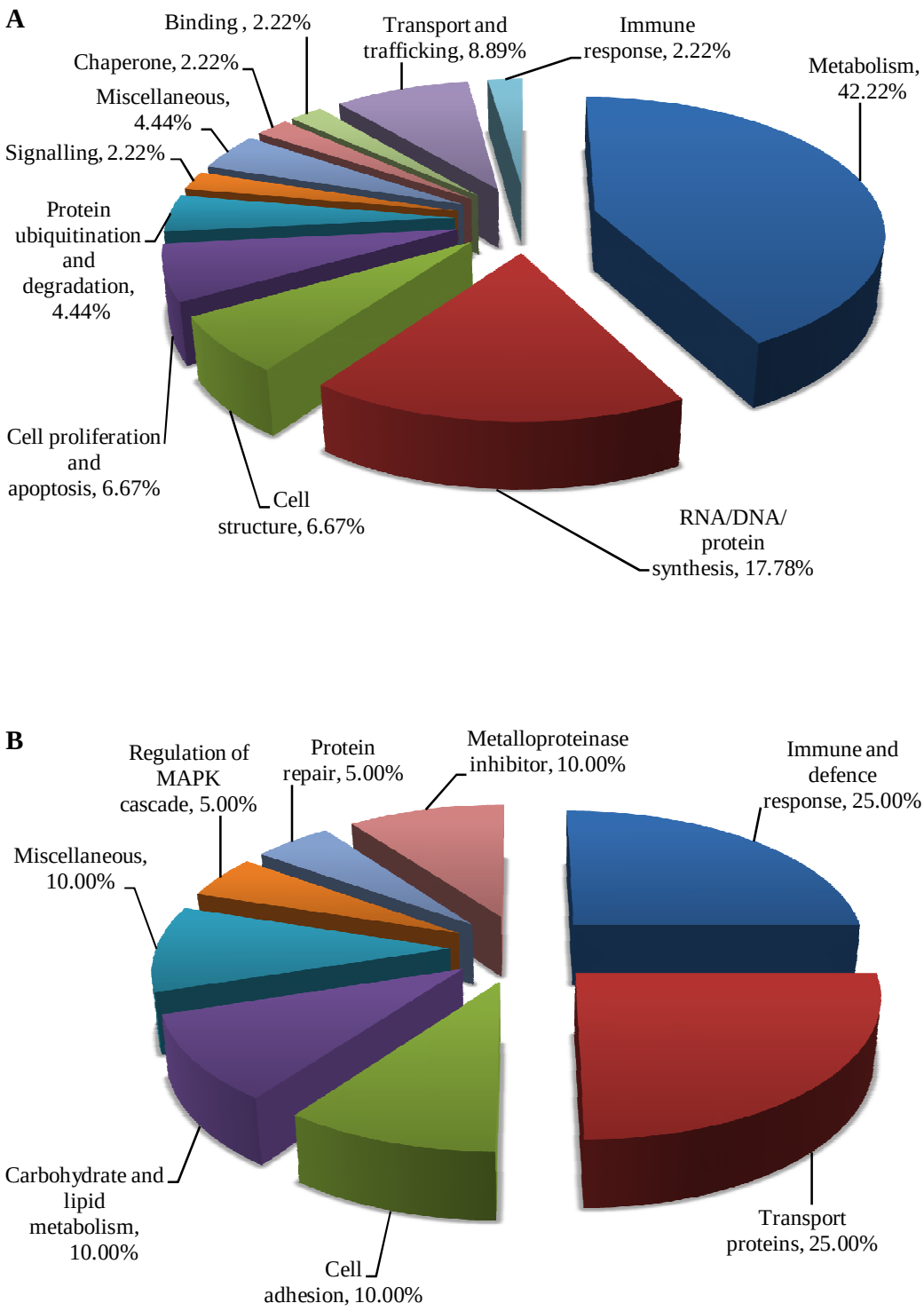

Figure 4.14: Functional classification of differentially expressed proteins from the whole cell proteome (A) and secretome (B) samples.

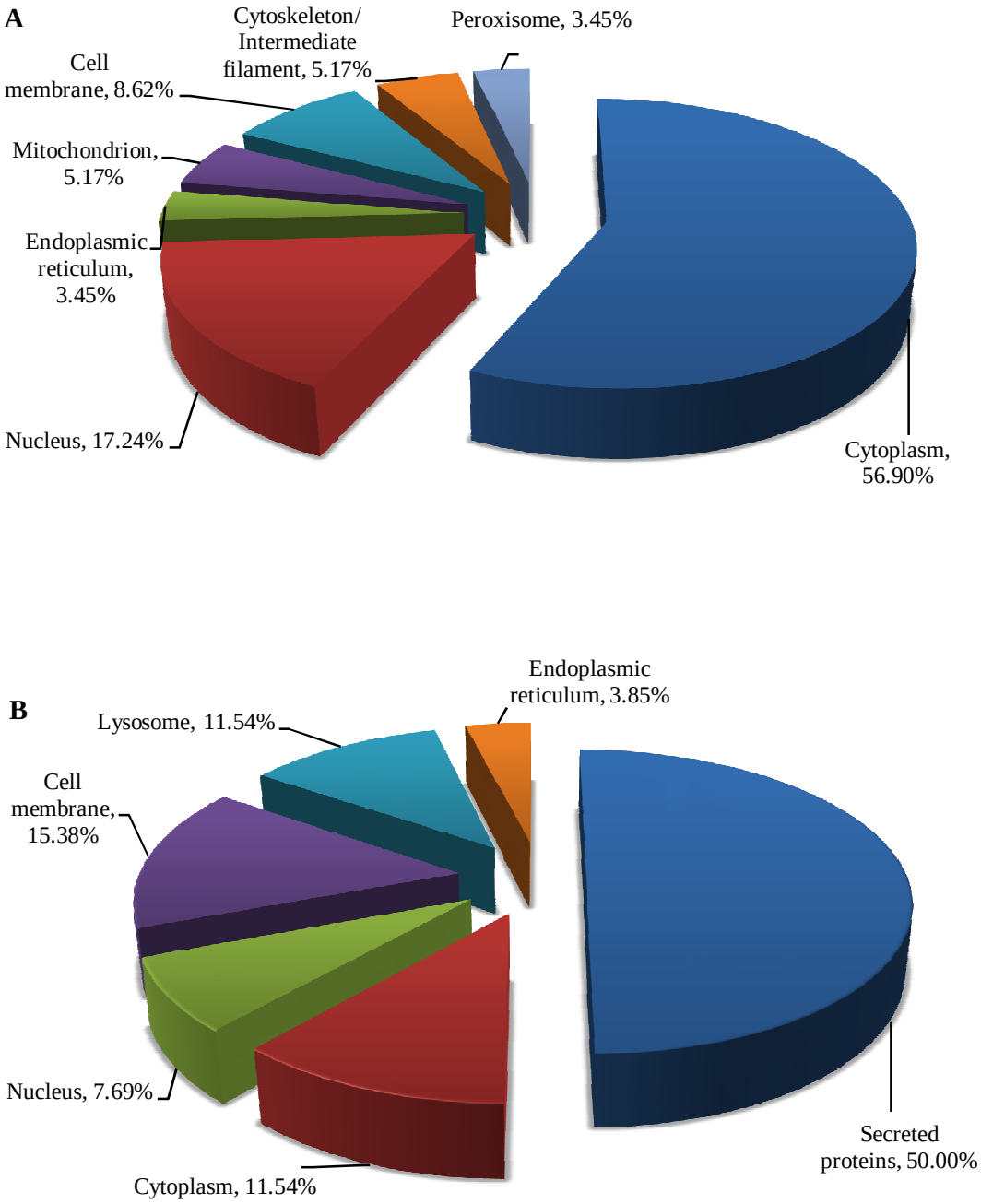

Figure 4.15: Sub-cellular distribution of differentially expressed proteins from the whole cell proteome (A) and secretome (B) samples.

4.4.4 Protein network analysis

Prediction of protein-protein interactions was performed using STRING database v9.0 to illustrate the connections between differentially expressed proteins. Proteins were linked based on seven criteria; neighbourhood, gene fusion, co-occurrence, co-expression, experimental evidences, existing databases and textmining. Medium stringency (STRING score = 0.4) was used to analyse the network. Proteins were represented as nodes and their functional links were defined by solid lines. The thickness of the lines signifies the level of confidence of the reported association. Twenty additional interacting proteins were also added to the interaction map to provide a more comprehensive overview of the biological processes affected during CHIKV infection. The protein names and gene symbols used in the networks are listed in Appendices A1 (Whole cell proteome) and A2 (Secretome).

STRING network analysis of altered whole cell proteins revealed 37 interlinked proteins (Figure 4.16A), while 17 of the 20 proteins from the secretome sample were connected by at least one criterion (Figure 4.16B). Gene ontology (GO) enrichment analysis of biological process was further evaluated using STRING database to identify significant biological processes associated with the network. False discovery rate (FDR) correction was the default statistical method used to determine the significance of each process. Eight and five processes were found to be significant in the predicted whole cell proteome and secretome networks, respectively, as shown in Table 4.3. Analysis of the whole cell proteome network revealed involvement of energy production, cell cycle regulation, gene expression, mRNA metabolism, protein metabolism and modification, DNA replication and ubiquitin-protein ligase activity. Signal transduction, cellular component and extracellular matrix (ECM) organisation, regulation of cytokine stimulus and immune response were shown to be involved in the secretome network.

Figure 4.16: Whole cell proteome (A) and secretome (B) networks showing functional linkages between identified proteins

STRING interaction maps were generated using default settings (Medium confidence of 0.4 and 7 criteria for linkage: neighbourhood, gene fusion, co-occurrence, co-expression, experimental evidences, existing databases and textmining). Twenty additional interplay proteins were also added to each network.

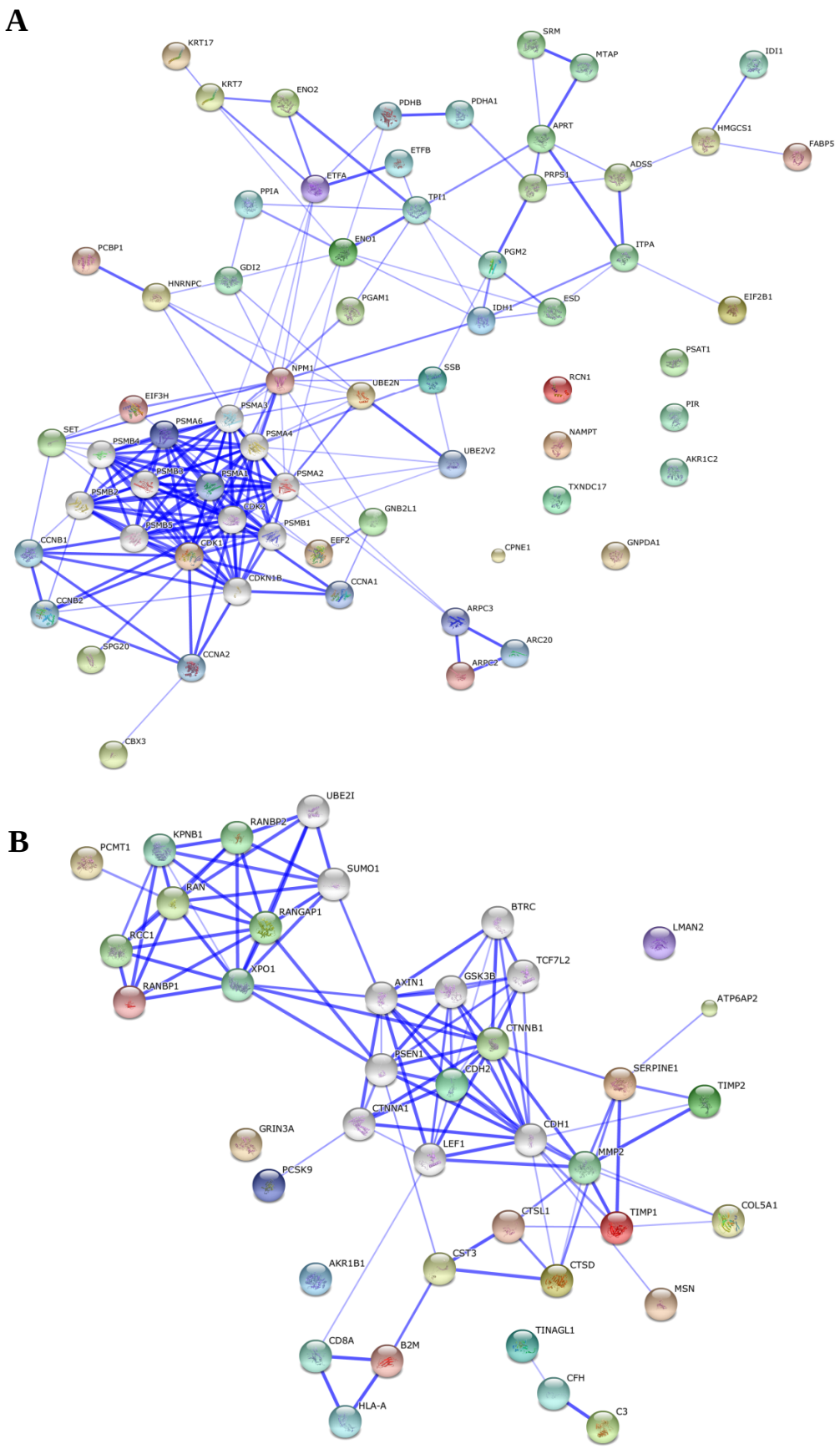
A
KRT17
KRT7
ENO2
PDHB
PDHA1
SRM
MTAP
IDI1
APRT
HMGCS1
FABP5
ETFB
ETFA
PRPS1
ADSS
PPIA
TPI1
ENO1
PCBP1
GDI2
PGM2
ITPA
HNRNPC
PGAM1
IDH1
ESD
EIF2B1
PSAT1
NPM1
SSB
RCN1
UBE2N
EIF3H
PSMA3
PIR
PSMA6
SET
PSMB4
PSMA4
NAMPT
UBE2V2
AKR1C2
PSMB3
PSMA1
PSMA2
TXNDC17
PSMB2
CDK2
GNB2L1
PSMB5
PSMB1
CCNB1
CDK1
EEF2
CPNE1
GNPDA1
CDKN1B
CCNA1
CCNB2
ARPC3
ARC20
SPG20
CCNA2
ARPC2
CBX3
B
UBE2I
RANBP2
KPNB1
PCMT1
SUMO1
RAN
RANGAP1
BTRC
LMAN2
RCC1
TCF7L2
XPO1
AXIN1
GSK3B
RANBP1
ATP6AP2
CTNNB1
PSEN1
CDH2
SERPINE1
TIMP2
CTNNA1
GRIN3A
CDH1
LEF1
MMP2
PCSK9
COL5A1
CTSL1
TIMP1
AKR1B1
CST3
CTSD
MSN
TINAGL1
CD8A
B2M
CFH
HLA-A
C3

Table 4.3: GO enrichment analysis of biological processes involved in the whole cell proteome and secretome networks

The significance of the GO biological processes was determined by FDR analysis ($p< 0.05$).

GO Biological process	*p*-value
Whole cell proteome network	
Regulation of ubiquitin-protein ligase activity	4.34×10^{-14}
Gene expression	1.14×10^{-6}
mRNA metabolic process	8.06×10^{-6}
Protein modification	1.75×10^{-5}
Regulation of cell cycle	1.63×10^{-5}
Protein metabolic process	1.02×10^{-5}
Generation of energy and precursor metabolite	1.35×10^{-2}
DNA replication	4.98×10^{-2}
Secretome network	
Regulation of cellular component organisation	7.03×10^{-3}
Response to cytokine stimulus	1.11×10^{-2}
Regulation of signal transduction	1.24×10^{-2}
ECM organisation	1.70×10^{-2}
Regulation of immune process	3.53×10^{-2}

4.4.5 Protein validation by Western blot analysis

One-dimensional (1-D) Western blot was applied to validate the expression of two selected whole cell proteins, CDK1 (Figure 4.17A) and PDHA1 (Figure 4.17B), which were normalised against the endogenous controls, ACTB and GAPDH, respectively. Densitometric analysis revealed down-regulation of CDK1 and up-regulation of PDHA1 by 1.42 and 1.72 folds, respectively (Figures 4.17C and 4.17D), confirming the directions of the fold changes. The fold-differences obtained for both proteins were also comparable to that of the fold differences determined by 2-DGE analysis, which showed down-regulation by 1.77 for CDK1 and up-regulation by 1.96 for PDHA1.

Conversely, 2-D Western blot was used to validate the position of RAN, which was identified to be up-regulated in the secretome sample. Although the protein expression level cannot be accurately determined, 2-D Western blot analysis allows confirmation of protein location on the gel based on molecular weight and pI/pH values. Figure 4.17E shows the position and spot intensity of RAN protein in mock control (I) and CHIKV-infected (II) 2-Dimmunoblots. The location of RAN on both immunoblots was similar to that of 2-DGE gel (Figure 4.12), confirming the identity of the protein spot. RAN protein exhibited a molecular weight of slightly below 26 kDa (Theoretical value: 24,408 kDa) and apI/pH of around 7 to 8 (Theoretical value: 7.01). Furthermore, comparison between the immunoblots also showed a similar increase in spot intensity upon CHIKV infection, as was observed with 2-DGE analysis.

Figure 4.17: Western blot validation of CDK1, PDHA1 and RAN proteins

Down-regulation of CDK1 (**A**) and up-regulation of PDHA1 (**B**) was validated by 1-D Western blot. Densitometric analysis of the mean relative intensity (n=3) for each target protein showed a 0.70 (or 1.42 fold decrease) and 1.72 fold differences for CDK1 (**C**) and PDHA1 (**D**), respectively. The band intensities of CDK1 and PDHA1 were normalized against ACTB and GAPDH, respectively. Error bars indicate standard deviation of three biological replicates. Student's t-test was employed to determine the significance of the fold-differences, where * indicates p-value<0.05. Panel **E** shows the position of RAN protein spot in mock control (**I**) and CHIKV-infected (**II**) immunoblots, whereby an increase in spot intensity was observed in the CHIKV-infected blot as compared to the mock control blot.

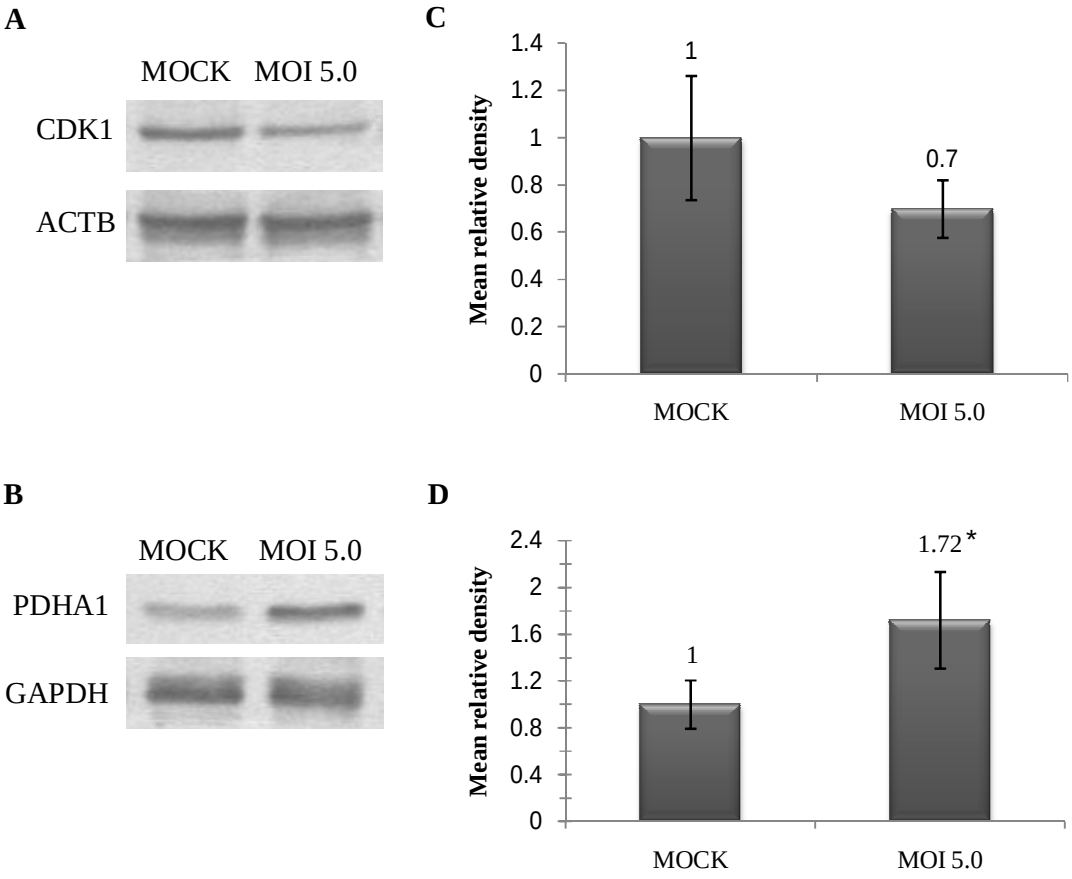
A
MOCK
MOI 5.0
CDK1
ACTB
C
Mean relative density
1.4
1.2
1
0.8
0.6
0.4
0.2
0
1
0.7
MOCK
MOI 5.0
B
MOCK
MOI 5.0
PDHA1
GAPDH
D
Mean relative density
2.4
2
1.6
1.2
0.8
0.4
0
1
1.72*
MOCK
MOI 5.0

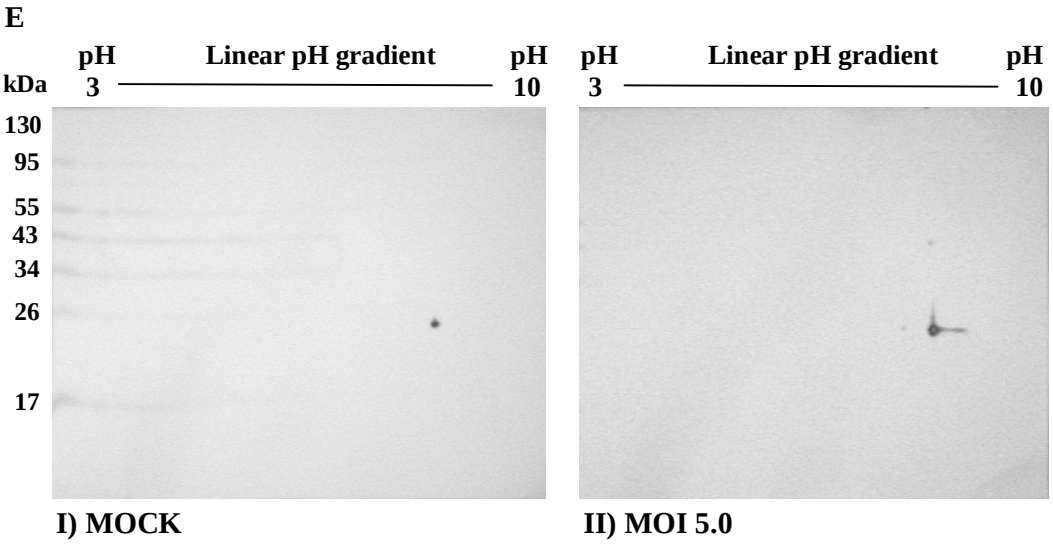
E
kDa
pH 3
Linear pH gradient
pH 10
130
95
55
43
34
26
17
pH 3
Linear pH gradient
pH 10
I) MOCK
II) MOI 5.0

4.5 Transcript expression analysis

Quantification of mRNA expression was performed with real-time qPCR. Prior to quantification, the purity and integrity of extracted RNA and the efficiency of each primer pair was determined to ensure data accuracy. The following three sections describe the results obtained from this study.

4.5.1 Determination of RNA purity and integrity

All RNA samples used in this study were determined to have A260:A280 and A260:A230 ratios that fall within the purity ranges of 1.8-2.0 and >2.0, respectively, as shown in Appendix B. Meanwhile, RNA integrity for all samples was confirmed by the presence of two intact bands corresponding to the 28S and 18S ribosomal RNA (rRNA) and a 28S:18S rRNA band intensity ratio of approximately 2:1 (as shown in the example in Figure 4.18).

4.5.2 Primer efficiency test

Primer efficiency test was performed to evaluate the amplification efficiency and specificity of each primer pair to the gene of interest. A total of 52 primers were designed for 51 targeted genes (36 genes for whole cell proteins and 15 genes for secretome) and the endogenous control, ACTB. The amplification efficiency for all primer sets was determined to be within the acceptable range of 90% to 110% (Slope value between -3.1 and -3.6) (Refer to appendix C for the primer sequences and efficiency test data). The specificity of each primer set was also confirmed by the presence of a single peak in the dissociation curve (data not shown).

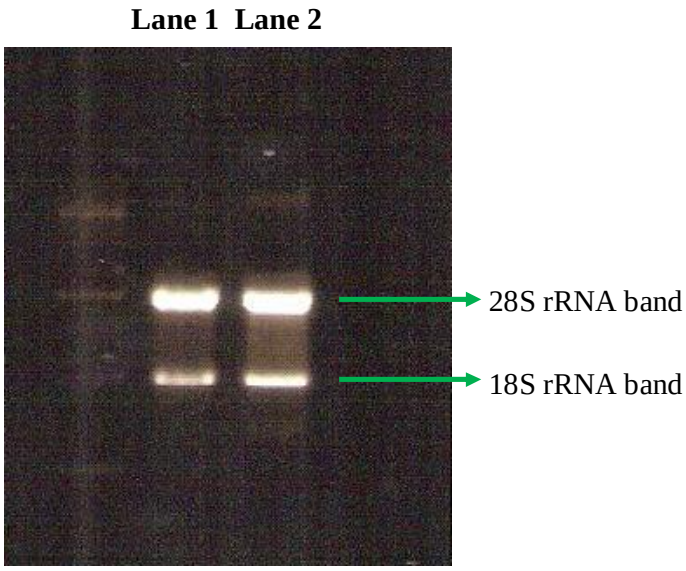

Figure 4.18: Representative gel profile of intact total RNA samples extracted from mock control and CHIKV-infected cells for whole cell proteome study

RNA integrity of mock control and CHIKV-infected RNA samples was visualised on 1.0% agarose gel. Two discrete bands were observed in both samples, with the 28S rRNA band having approximately twice the intensity of the 18S rRNA band, confirming sample integrity.

Lane 1: Mock control

Lane 2: CHIKV-infected (MOI 5.0)

4.5.3 Real-time qPCR analysis of differential mRNA expression

The mRNA expression levels of 36whole cell proteins and 15 secreted proteins, representing all functional classes, were evaluated to investigate the mechanisms leading to the altered protein expression. The transcript expression for all targeted proteins were normalised against ACTB. Of the 36 whole cell proteins analysed, 18 showed significant changes at the mRNA level ($p< 0.05$), 15 of which were in concordance in the direction of fold difference as the protein, while the other three showed the opposite direction of expression change (Table 4.4). The mRNA expression levels for the remaining 18 proteins showed no significant differences ($p> 0.05$). Conversely, only one of the 15 selected proteins from the secretome sample, which is kexin type 9 precursor (PCSK9), showed significant changes at the mRNA expression level, and is in concordance in the direction of fold difference as the protein expression (Table 4.5).

Table 4.4: Comparison of real-time qPCR and proteomics results for 36 selected proteins from the whole cell proteome sample

Gene name	mRNA fold-change (*p*-value)	Protein fold-change
ADSS	**-1.36 (0.0126)**	**-2.25**
APRT	1.33 (0.0087)	-1.52
ARPC2	1.24 (0.0030)	-1.41
CBX3	NSD	1.39
CDK1	**-1.38 (0.00003)**	**-1.77**
CPNE1	NSD	-1.75
EEF2	**-1.12 (0.0008)**	**-1.63, -1.35****
eIF2B1	**-1.25 (0.0295)**	**-1.54**
eIF3H	NSD	-1.58
ENO1	**-1.32 (0.0005)**	**-1.32**
ETFA	1.34 (0.0009)	-1.42
GDI2	NSD	-2.34, -1.51**
GNB2L1	NSD	-2.58, -1.88, -1.40**
HMGCS1	NSD	-1.62
HNRNPC	NSD	3.1
IDH1	**-1.14 (0.0100)**	**-1.57**
IDI1	**-1.48 (0.0057)**	**-1.63**
ITPA	NSD	-1.32
KRT7	NSD	1.4
MTAP	**-1.26 (0.0298)**	**-1.44**
NAMPT	NSD	-1.44
NPM1	NSD	1.38
PCBP1	**-1.82 (0.00008)**	**-1.42**
PDHA1	**1.30 (0.0047)**	**1.96**
PGAM1	NSD	-1.37
PIR	**-1.25 (0.0142)**	**-1.57**
PPIA	NSD	-1.36
PRPS1	**-1.27 (0.0042)**	**-1.33**
PSAT1	**-1.62 (0.00002)**	**-1.73**
PSMA6	NSD	-1.52
RCN1	NSD	1.41
SET	**1.41 (0.0057)**	**1.43**
SSB	NSD	-1.67
TPI1	NSD	-1.81, -1.47**
TXNDC17	NSD	-1.37
UBE2N	**-1.33 (0.0100)**	**-1.45**

* **Bold** indicates RNA expression changes which are in concordance with protein expression changes in terms of directionality, and are determined to be statistically significant ($p < 0.05$); NSD indicates no significant differences in the RNA expression.
** More than one protein spot was identified.

Table 4.5: Comparison of real-time qPCR and proteomics results for 15 selected proteins from the secretome sample

Gene name	mRNA fold-change (*p*-value)	Protein fold-change
ATP6AP2	NSD	-4.42
B2M	NSD	-1.68
C3	NSD	-3.21
CDH2	NSD	-2.97
CST3	NSD	-2.72
CTSD	NSD	-2.72
CSTL1	NSD	-2.53, -1.78**
COL5A1	NSD	-3.14
PCMT1	NSD	-2.29
PCSK9	**-1.43 (0.0002)**	**-4.30, -3.50, -2.40****
RAN	NSD	3.68
RANBP	NSD	1.80
SERPINE1	NSD	-2.46
TIMP1	NSD	-3.45
TIMP2	NSD	-2.11, -1.86**

* **Bold** indicates RNA expression changes which are in concordance with protein expression changes in terms of directionality, and are determined to be statistically significant ($p < 0.05$); NSD indicates no significant differences in the RNA expression.
** More than one protein spot was identified.

CHAPTER 5

DISCUSSION

CHIK is an arthropod-borne disease that has caused multiple recurring outbreaks over the past five decades in the Asian, African, and more recently, the European continent. Despite being less deadly and prevalent than dengue (DEN) fever, which reports an approximate 50 to 100 million cases annually (Schmidt-Chanasit *et al.*, 2012), this arboviral infection should not be taken lightly given the observed increase in the number of documented cases and outbreaks with each successive year. Moreover, the similarities between DEN and CHIK symptoms, as well as co-circulation of both CHIKV and dengue virus (DENV) in the same regions often lead to misdiagnosis of CHIK as DEN cases. This causes an underestimation of the actual number of CHIK cases worldwide (Powers *et al.*, 2000). In addition, the rapid mutation of CHIKV has led to evolution of a deadlier strain of the virus, evidenced by the emergence of atypical complications and higher death rates in recent outbreaks (Powers & Logue, 2007). Therefore, there is no question that CHIK is a potential threat to the global community.

Studies on host-interaction and the pathways exploited by CHIKV for successful invasion, propagation and dissemination in the human body are highly pursued research areas in recent years. Regardless, the knowledge obtained so far, albeit progressing, is still limited. Proteomics is fast becoming a popular tool to study host-virus interaction by looking at changes implicated by viruses on the host proteome. Incorporation of pathway studies to interpret protein expression data has proven to be valuable in predicting the potential interacting protein partners and to elucidate the pathways that may be involved during viral infection (Lietzen *et al.*, 2011). The current study integrated the aforementioned approaches to investigate changes in the host whole cell proteome and secretome during early CHIKV infection in WRL-68 cells. Findings of this study are being discussed at length in the paragraphs that follow. Prior to 2-DGE

analysis, optimisation of the MOI and time-point was performed to determine the suitable condition that defines early infection, that is, the stage before cell death. This is to ensure that changes in the whole cell proteome and secretome are caused solely by CHIKV infection, and not due to cell death factors, such as apoptotic factors (Pattanakitsakul *et al.*, 2007). Furthermore, cell death needs to be minimised to prevent contamination of the secretome with cellular debris and intracellular proteins released due to cell lysis, which renders the 2-DGE results inaccurate. Hence, the MOI and time-point selected for infection should induce minimal cell death as compared to the mock control, while simultaneously maintaining a significant percentage of infection. Combination of morphological analysis, IIFA and flow cytometric quantification was performed to thoroughly investigate the best condition for early infection, which resulted in the selection of the MOI of 5.0 and 24 hours post-infection incubation. Infection under this condition resulted in a high percentage of infection at 74.77% without causing any observable CPE. Meanwhile, percentage of cell death (25.90%) was comparable to that of cells infected at lower MOI (at the same time-point), albeit slightly higher than mock control cells (14.33%). Hence, this MOI and time-point was used for the subsequent proteomics study.

Secretome is defined as the complex set of molecules secreted by living cells (Makridakis & Vlahou, 2010). In cell culture, these proteins are secreted into the culture media, which are typically rich in a variety of proteins in the serum as nutrients for cell growth. These proteins are in abundance in comparison to secreted proteins. When resolved using 2-DGE technique, these highly abundant proteins will mask the actual target proteins. To eliminate interfering proteins from the serum, serum-free DMEM medium was used during incubation period following infection. However, serum starvation may have negative effects on cell growth and proliferation, as

previously reported (Mattanovich *et al.*, 2009). Therefore, the viability and integrity of cells cultured in serum-free medium must be evaluated. In addition, flow cytometer analysis revealed a slightly higher percentage of cell death in CHIKV-infected cells than in mock control cells at the selected condition for infection. Thus, it is also pertinent to determine that membrane integrity of CHIKV-infected cells is not greatly compromised to avoid severe contamination of the secretome with intracellular proteins.

The viability and integrity of WRL-68 cells under serum starvation and CHIKV-infection was evaluated by MTS cell proliferation and dead-cell protease assays. MTS assay measures cell viability through the activity of enzymes involved in the cytochrome system of viable cells, which reduces the MTS (a tetrazolium salt) to water-soluble formazans (Barltrop & Owen, 1991). On the other hand, cell-death protease assay is a luminescent assay which evaluates membrane integrity by measuring the activity of proteases that have been released from dead cells. The luminogenic peptide substrate or AAF-Glo™ substrate (alanyl-alanyl-phenylalanyl aminoluciferin) is not permeable to viable cells with intact membranes, and therefore can only detect proteases that have been leaked out from damaged membranes (Niles *et al.*, 2007).

MTS assay results showed that serum starvation did not affect the viability of WRL-68 cells at 24 hours incubation. However, cell lysis was found to be inevitable, as proteases were detected in the supernatant of control cells cultured with serum-supplemented medium. Nevertheless, the degree of cellular disruption between cells grown in serum-supplemented medium, serum-free medium and CHIKV-infected cells (MOI 5.0) incubated in serum-free medium were comparable. Taken together, it can be deduced that serum-starvation and infection at the selected MOI and time-point did not result in significant loss of cell viability and integrity.

Proteomics analysis was subsequently performed to compare the whole cell proteome and secretome gel profiles between mock control and CHIKV-infected WRL-68 cells. Immobiline™ drystrip of a wide pH range of 3 to 10 was used for a broad overview of the total protein distribution. The proteins were further separated on 12.5% polyacrylamide gel which gave well resolved gel profiles, with minimal overlapping spots. For analysis, five biological replicates (n=5) were used for each group to minimise biological variations. The gel images were analysed using ImageMaster™ 2D Platinum v7.0 software with stringent selection of spot detection parameters (minimal area: 5.0; smooth factor: 3.0; and saliency: 200.0) to minimise detection of staining artifacts. Manual re-matching of incorrectly matched spots was performed following automatic matching. More than 1000 spots were detected for both gel profiles, of which 34 and 53 spots from the whole cell proteome and secretome samples, respectively, were significantly regulated by at least 1.3 fold.

Mass spectrometric identification of these 87 spots resulted in successful identification of 50 and 25 spots from the whole cell proteome and secretome samples, respectively. The remaining 12 spots failed to be identified due to low MOWSE scores (below the significant threshold), or multiple significant protein hits with no overlapping peptide sequence match, indicating the presence of more than one protein. Furthermore, several spots were identified as the same protein, such as that of GNB2L1 and TIMP2 proteins. These spots were found to have either similar M_r, but slightly different pI, or vice versa, and hence, could probably be isoforms of that protein.

Three of the identified proteins were further validated by Western blot. ACTB and GAPDH were used as endogenous controls for CDK1 and PHDA1, respectively. GAPDH was selected as the loading control for PDHA1 because PDHA1 and ACTB

have similar molecular mass of ~43 kDa, and thus, cannot be stained together on the same blot. On the contrary, 2-D Western blot was used for secretome protein validation due to the lack of a universal loading control for secretome to normalise loading quantities, which is a requirement for 1-D Western blot analysis. Nevertheless, both methods were successful in validating the expressions of CDK1 and PHDA1, and confirming the identity of RAN protein spot.

Transcript analysis of 51 selected proteins showed a moderate degree of correlation between the mRNA and whole cell protein expression (15 positive correlations). Only PCSK9 showed positive correlation with its mRNA expression in terms of directionality. This is not surprising, given that post-transcriptional modifications such as mRNA splicing or editing and post-translational modifications often determine the final translation rate of a protein (Brockmann *et al.*, 2007). Also, the poor correlation between the transcript and secretome expression levels suggests that other mechanisms may be involved in determining the protein secretion rate, such as protein folding rate and cell cycle position (Frykman & Srienc, 2001; Thor *et al.*, 2009).

Early CHIKV infection was found to cause widespread alterations of the whole cell proteome and secretome. Proteins of diverse functions and sub-cellular locations were differentially expressed, majority of which were down-regulated. Only half of the proteins identified in the secretome fraction were secretory proteins. Other intracellular proteins identified in the culture supernatant could have been secreted through the non-classical pathway, such as that of cathepsins (Lietzen*, et al.*, 2011). However, several cytosolic proteins, including moesin (MSN) and protein-L-isoaspartate O-methyltransferase (PCMT1), are not known to be secreted. Hence, their release into the

culture medium could be due to cell lysis. In terms of functional classification, a large subset of the proteins were found to be involved in metabolism, DNA/RNA/protein biogenesis, immune response and transport, suggesting that these functions may be important during CHIKV infection in host cells.

STRING network analysis was used to predict the functional interactions between proteins based on existing information from public text collections and experimental data. All metabolic proteins, except glucosamine-6-phosphate isomerase (GNPDA1), nicotinamide phosphoribosyltransferase (NAMPT) and phosphoserine aminotransferase (PSAT1) showed functional linkages in the whole cell proteome network (Figure 4.16A). The proteasome complex, comprising of the alpha and beta subunits, formed a large cluster in the interaction map. One of the subunits, proteasome subunit alpha 6 (PSMA6), was down-regulated in this study. In addition, seven of the identified proteins, namely SET protein, hnRNP C1/C2, NPM1, CDK1, electron transfer flavoprotein (ETFA), alpha enolase (ENO1) and eukaryotic elongation factor (EEF2), were functionally linked to one or more of these subunits.

Meanwhile, three immune and defence response proteins; cystatin 3 (CST3), cathepsin D (CTSD) and cathepsin L1 (CTSL1), showed strong linkages in the secretome network, as shown in Figure 4.16B. Beta-2 microglobulin (B2M), on the other hand, was linked to the major histocompatibility (MHC) class I complex through human leukocyte antigen A (HLA-A). Tubulointerstitial nephritis antigen-like precursor (TINAGL1), conversely, was linked to complement proteins, complement C3 (C3) and complement factor H (CFH) in a separate cluster. Tissue inhibitor of metalloproteinase 1 and 2 (TIMP1 and TIMP2), and collagen alpha-I (V) chain

precursor (COL5A1) were indirectly connected through matrix metalloproteinase 2 (MMP2) protein.

The functional linkages were then used to determine the significant biological processes involved in each network. The FDR-filtered ($p < 0.05$) list of biological processes showed that gene expression, mRNA processing, energy and precursor metabolite biogenesis, cell cycle regulation and ubiquitin-related processes were involved in the whole cell proteome network, whereas immune response, as well as ECM and cellular compartment organisation were identified in the secretome network. Identification of these processes confirms the aforementioned functional roles that were postulated to play a role during CHIKV infection. The functions these proteins are being discussed in the following sections to elucidate the key events that take place during early CHIKV infection.

i) Functional disorder of the host gene expression machinery

Expression of a gene for subsequent synthesis of its functional product involves transcription of the gene to mRNA, which is then processed and translated to produce the protein it encodes. Virus hijacking of the gene expression machineries is well documented in many virus-host interaction studies (Scheller & Diez, 2009; Toribio & Ventoso, 2010). Viruses with positive sense RNA in particular, have been shown to recruit components of the host cellular mRNA processing and translational machineries for viral RNA and protein synthesis (Li *et al.*, 1999). In this study, five proteins involved in mRNA processing and translation were found to be deregulated, namely hnRNP C1/C2, poly(rC)-binding protein 1 (PCBP1) or hnRNP E1, EEF-2, translation

initiation factor EIF-2B subunit alpha (eIF2B1) and eukaryotic translation initiation factor 3 subunit H (eIF3H).

Heterogeneous ribonucleoprotein C1/C2 (hnRNP C1/C2) protein expression showed up-regulation by 3.10 fold whereas hnRNP E1 was down-regulated by 1.42 fold. The transcript expression level of hnRNP E1 showed higher fold difference (-1.82 fold-change) than the protein expression, but of the same directionality. Meanwhile, the transcript level of hnRNP C1/C2 did not alter significantly. Both hnRNPs belong to the hnRNP complexes of RNA and proteins involved in multiple cellular functions such as transcription, pre-mRNA processing and cytoplasmic mRNA translation (Krecic & Swanson, 1999). Previous studies have demonstrated the yin and yang of hnRNPs in viral pathogenesis. During DEN infection, hnRNP C1/C2 was shown to interact with DENV NS1 protein, promoting virus survival in host cells (Noisakran *et al.*, 2008). Conversely, during vesicular somatitis virus (VSV) infection, hnRNP E1 showed antagonistic relationship with the virus as virus replication is inhibited in its presence (Dinh *et al.*, 2011). Thus, the up-regulation of hnRNP C1/C2 in this study possibly signifies its recruitment by CHIKV whereas hnRNP E1 may potentially have adverse effects towards CHIKV replication which is counteracted by its inhibition.

Translation factors play crucial roles in viral protein synthesis and different viruses exert different mechanisms to modulate host translational proteins to their benefit (Kushner *et al.*, 2003). Eukaryotic translation is a three-step process which begins with initiation of translation, a process mediated by 11 initiation factors (eIF1 through eIF6), followed by elongation of the growing amino acid chain by elongation factors (EEF-1α, EEF-1βγ, EEF-2 and EEF-3), and ends with termination by the release factor upon reaching the stop codon (Merrick, 1992). Alphaviruses have been shown to

induce global shutoff of protein synthesis by inhibiting or modifying host translational factors. Semliki Forest virus, for example, induces shutoff by phosphorylating eIF2α and subsequently inhibiting eIF2B (McInerney *et al.*, 2005). CHIKV, conversely, induces protein synthesis shutoff through an unknown protein kinase R (PKR)-independent mechanism, as the absence of PKR-induced phosphorylation of eIF2α did not prevent host translational shutoff (White *et al.*, 2011). Down-regulation of EEF-2, eIF2B1 and eIF3SH protein expression was observed in this study, although only EEF-2 and eIF2B1 was down-regulated at the transcript level. The roles of these proteins in host translational shutoff cannot be ascertained at this point. Nevertheless, down-regulation of these proteins would disrupt the host translational machinery, possibly contributing to the down-regulation of most differentially expressed proteins.

ii) Perturbation of cellular energy production and host cell metabolism

In this study, we found severe disruption of the host cell metabolism upon CHIKV infection. Two (10%) and 19 (42.22%) identified proteins from the secretome and whole cell proteome fractions, respectively, were involved in cellular metabolism. This finding is not surprising given that liver is the central site for metabolism. Our proteomics data showed that 18 of the 19 metabolic proteins identified in the whole cell proteome fraction were down-regulated. Only PDHA1, a key enzyme in transforming pyruvate to acetyl-Coenzyme A in the tricarboxylic acid (TCA) cycle (Dahl *et al.*, 1987), was up-regulated by 1.96 fold, as confirmed by immunoblot analysis (Figures 4.17A and 4.17C). Transcript expression levels for eight (PHDA1, ENO1, PSAT1, isocitrate dehydrogenase (IDH1), adenylosuccinate synthetase isozyme 2 (ADSS), ribose-phosphate pyrophosphokinase 1 (PRPS1), isopentyl-diphosphate Delta-isomerase 1 (IDI1), and S-methyl-5-thioadenosine phosphorylase (MTAP)) of the 14 selected proteins were similar in the direction of expression changes as the protein

expression (Table 4.4). Conversely, aldose reductase (AKR1B1), a catalyst involved in reduction of glucose to sorbitol for glucose metabolism, was found to be up-regulated by 1.84 in the secretome study while PCSK9 was found to be down-regulated at both the protein and transcript levels.

Overall, energy production in CHIKV-infected WRL-68 cells was disrupted through reduced expression of glycolytic enzymes including ENO1, phosphoglycerate mutase 2 (PGM2) and triosephosphate isomerase (TPI1), as well as down-regulation of IDH1 which catalyses the conversion of isocitrate to α-ketoglutarate in the TCA cycle (Christensen *et al.*, 2011). CHIKV was also found to disrupt the adenine salvage pathway. Four enzymes involved in this pathway were down-regulated, including PRPS1 which catalyzes the synthesis of phosphoribosylpyrophosphate (PRPP) for purine and pyrimidine synthesis (Becker *et al.*, 1982); ADSS, a catalyst for the synthesis of adenosine monophosphate (AMP) from inosine monophosphate (IMP) for adenine production (Guicherit *et al.*, 1994); MTAP, an enzyme involved in adenine and methionine salvage (Appleby *et al.*, 1999); and adenine phosphoribosyl transferase (APRT), the enzyme involved in adenine salvage for AMP recovery (Itai *et al.*, 2000).

Mevalonate pathway is an essential pathway for the production of metabolically and physiologically important molecules and end-products such as cholesterol, conenzyme Q, dolichyl-P for protein glycosylation and isoprenylated proteins for signal transduction and protein localization. In this study, two important enzymes in this pathway, namely hydroxymethylglutaryl-CoA synthase (HMGCS1) of cytoplasmic origin, which is involved 3-hydroxy-3-methylglutaryl-coenzyme A (HMG-CoA) synthesis for the production of mevalonate (Hegardt, 1999); and IDI1, a catalyst for the conversion of isopentenyl pyrophosphate (IPP) to dimethylallyl pyrophosphate

(DMAPP) (Ramos-Valdivia *et al.*, 1997), were down-regulated. Mevalonate serves as the precursor in this pathway for production of IPP, the basis for all terpenoids. Terpenoids, in turn, are intermediates for steroids and sterols (such as cholesterol) production. More importantly, down-regulation of both the protein and mRNA expression of IDI1 suggests that CHIKV disrupts the cholesterol producing route in the pathway as DMAPP is required for production of lanosterol, the key intermediate for production of cholesterol and other steroids (Schroepfer, 1982). In addition, the secretion of PCSK9, which is involved in regulating cholesterol homeostasis by enhancing degradation of low-density lipoprotein (LDL) receptor protein (Duan *et al.*, 2012), was also down-regulated.

The results obtained here is in contrary to several findings in which metabolic enzymes and metabolites involved in various metabolic processes were found to be significantly up-regulated (Diamond *et al.*, 2010; Munger *et al.*, 2006). Most viruses are known to utilise the host metabolic machinery to acquire energy and macromolecular precursors for replication (Munger*, et al.*, 2006). However, production of energy and biosynthetic precursors through metabolic processes are also required for heat shock response activity as a defence mechanism against these pathogens (El-Bacha *et al.*, 2004; Widnell *et al.*, 1990). Therefore, one plausible explanation for the observed down-regulation of most metabolic enzymes is that CHIKV possibly suppresses these metabolic processes to inhibit the activation of heat shock responses.

iii) Inhibition of proteins involved in ubiquitin proteasome pathway (UPP)

UPP is an intracellular system involved in the ubiquitination of proteins targeted for degradation by proteasomes. UPP plays vital roles in host cellular functions such as

DNA repair, apoptosis, regulation of cell cycle and transcription, and signal transduction (Glickman & Ciechanover, 2002). Hence, this pathway is often targeted by viruses during host cell infection. Many viruses have been reported to evolve different strategies to manipulate this pathway; either to avoid the host immune surveillance or to facilitate viral transcriptional regulation, maturation and progeny release (Gao & Luo, 2006). For instance, enterovirus 71 was shown to inhibit the expression of proteasome subunit alpha type-2 and ubiquitin carboxyl-terminal esterase L3 (Leong & Chow, 2006), while the EA6P ubiquitin ligase is required for ubiquitination and degradation of hepatitis C virus (HCV) core protein (Shirakura et al., 2007).

In this study, two UPP associated proteins, ubiquitin-conjugating enzyme E2 N (UBE2N) and PSMA6 were down-regulated by 1.45 and 1.52 fold, respectively. At the transcript level, only UBE2N showed down-regulation by 1.33 fold, whereas the mRNA level for PSMA6 remained unchanged. UBE2N is a ubiquitin-carrier enzyme that carries and binds ubiquitin to the ubiquitin-ligase enzyme, which then ubiquitinates targeted proteins. PSMA6, on the other hand, is a subunit of the 20S proteasome subcomplex, which forms the multicatalytic 26S proteasome that degrades the polyubiquitinated proteins into smaller peptides (Glickman & Ciechanover, 2002). Changes in the expression levels of both proteins suggest perturbation of the cellular UPP by CHIKV during early infection via a different strategy than that of other viruses. In addition, disruption of this pathway may affect other proteins, such as those linked to the proteasome subunits in the whole cell proteome network postulated by STRING analysis. Regardless, the exact interaction between the proteasome and these proteins can only be determined through functional studies.

iv) Potential involvement of CDK1 in CHIKV-induced cell death

In this study, we found evidence suggesting disruption at the G2/M-phase transition, an important phase for DNA replication and cell division, through alteration of CDK1 and SET protein expressions. CDK1, also known as $p34^{cdc2}$ protein kinase, was found to be down-regulated whereas the SET protein was up-regulated at both the protein and transcript levels. STRING network analysis also showed a functional linkage between CDK1 and the SET protein. CDK1 is a member of the serine/threonine kinases family that is activated by cyclin B. This kinase regulates the cell cycle by allowing entry into mitosis from the G2 phase (Schang, 2004). In general, regulation of cyclin dependent kinases (CDKs) is typically associated with replication of DNA viruses in the nucleus, although several studies have illustrated the potential role of CDKs in the replication of RNA viruses, such as that of reoviruses (Poggioli *et al.*, 2002).

The SET protein is a ubiquitously expressed phosphoprotein that has been shown to inhibit cyclin B-CDK1 activity, causing cell cycle arrest at the G2 phase (Canela *et al.*, 2003). Hence, up-regulation of the SET protein would further inhibit the activity of CDK1. Moreover, the disruption of cholesterol synthesis via down-regulation of HMGCS1 and IDI1 would have further inhibited CDK1 activity, as a previous study showed that restriction of cholesterol provision decreased CDK1 activity (Martinez-Botas *et al.*, 1999). Taken together, these findings suggest that CHIKV targets CDK1 during early infection through multiple mechanisms. While the progression of these events would lead to cell death, there is also a possibility that deregulation of CDK1 facilitates CHIKV replication through a yet unknown mechanism.

v) Disruption of host cell immune response

Results from our proteomics data show down-regulation of several immune response-related proteins, including cyclophilin A (PPIA) which was detected in the cytosolic fractions, as well as C3, CTSD, CTSL1 and B2M, all of which were detected in the culture supernatant. PPIA, a ubiquitously expressed protein of the immunophilin family, is a multifunctional protein involved in immune response, cell death, transcription and mitochondrial function (Watashi & Shimotohno, 2007). A recent *in vivo* study showed the importance of PPIA in regulating the immune response by acting as a suppressor towards the development of $CD4^+$ T cell responses (Brazin *et al.*, 2002). Despite being an intracellular protein, PPIA can be secreted in response to inflammatory stimuli such as reactive oxygen species (ROS) (Jin *et al.*, 2000). In this study, we only found PPIA to be down-regulated in the cytosolic fraction, but no changes in its secretion was detected. This could possibly be due to the lack of ROS generation in this study as no stress-related proteins were found to be differentially expressed. Other than that, PPIA may have antagonistic impact on CHIKV replication, as was seen with influenza A virus replication (Liu *et al.*, 2012), which could have potentially contributed to its down-regulation in the cytoplasm.

CHIKV-infection was also found to decrease the expression of C3 protein, an integral component of the innate immune system in the clearance and inactivation of viral pathogens (Boere *et al.*, 1986). Complement C3 protein plays a protective role during virus infection, in particular for alphaviruses. Studies on alphaviruses such as Semliki Forest virus (Boere*, et al.*, 1986), Ross River virus (Aaskov *et al.*, 1985), and Sindbis virus (Hirsch *et al.*, 1978) have demonstrated that C3 deficient mice were highly susceptible towards virus infection and replication, as evidenced by enhanced virus titer in the main target organs. Conversely, C3 competent mice were protected

against the virus infection. Therefore, it is hypothesised that CHIKV modulated this protein to disrupt the host immune regulation, thereby weakening the host defence system and allowing the virus to invade and replicate in the liver cells.

Cathepsins are proteases contained within the lysosomes that play multiple roles in the cell including lysosomal protein recycling, antigen processing, maturation of MHC class II components, wound healing and apoptosis (Conus & Simon, 2010). CSTD and CSTL1 secretion was found to be down-regulated in CHIKV-infected cells at the protein level, despite no changes in expression at the transcript level. Cathepsins have been shown to play an important role in innate immunity. Lietzén and colleagues recently demonstrated the role of secreted cathepsin D in the induction of inflammasome response by influenza A (Lietzen*, et al.*, 2011). In a different study, cathepsin L was shown to enhance the activity of interleukin-8 (IL-8), a chemokine which induces chemotaxis in its target cells, including neutrophil granulocytes (Ohashi *et al.*, 2003). Thus, down-regulation of these proteins could impair the host innate immune response towards CHIKV infection. Although these two proteins were strongly linked to CST3 in the STRING network, CST3 is known to inhibit cathepsin L only (Hall *et al.*, 1995). Hence, the exact role of CST3 in this network cannot be determined at this point of study.

B2M is a component of the MHC class I molecule, which is involved in the MHC class I antigen presentation pathway. This pathway plays a vital role in detecting virus-infected cells and activating the cytotoxic T lymphocytes (CTL) to detect and eliminate infected cells (Hewitt, 2003). Thus, many viruses such as adenoviruses and retroviruses have devised strategies to evade or interfere with this pathway (Tortorella *et al.*, 2000). For instance, cytomegalovirus (CMV) was shown to decrease the expression

of B2M and HLA class I in human fibroblast cells to the point where HLA class I was undetectable at the late stage of infection, possibly to avoid T cell recognition of infected cells (Barnes & Grundy, 1992). Therefore, a similar mechanism may also be employed by CHIKV during early infection.

Collectively, down-regulation of different immune-related proteins of different immune functions during early CHIKV infection suggests the different immune impairment or evasive mechanisms undertaken by the virus to subvert or escape immune detection, thereby allowing successful replication and dissemination in the host cells. Nonetheless, further functional studies would need to be carried out to provide a better elucidation of how these proteins work in favour of CHIKV propagation.

vi) Impairment of proteins involved in ECM organisation

Three ECM-regulating proteins; COL5A1, TIMP1 and TIMP2, which are secreted proteins, were found to be down-regulated in the early stage of CHIKV infection, although transcript analysis showed no significant changes in expression. These three proteins were also linked together in the STRING network through MMP2. COL5A1 functions to maintain extracellular matrix integrity by acting as an anchor for proteoglycans in the extracellular matrix (LeBaron *et al.*, 1989). TIMPs are multifunctional proteins exhibiting various biochemical and physiological functions such as matrix binding, cell growth promotion and the induction of apoptosis (Higa *et al.*, 2008). TIMP2 is a known inhibitor to most activated matrix metalloproteinases (MMPs), particularly MMP2 and MMP14 (Tetu *et al.*, 2006), whereas TIMP1 inhibits all MMPs except MMP14, MMP16 and MMP19 (Meissburger *et al.*, 2011). MMPs function in remodelling ECM by degrading its component proteins, including collagen

and fibronectin (O'Farrell & Pourmotabbed, 2000). Down-regulation of TIMP1 and TIMP2 will lead to increase activation of MMPs, particularly MMP2, and this occurrence together with down-regulation of COL5A1 have been correlated with increased replication of Hepatitis C virus in human liver stellate cells (Watanabe *et al.*, 2011). Hence, it is postulated CHIKV may also manipulate these proteins in a similar manner for successful replication in our *in vitro* study.

CHAPTER 6

CONCLUSION

This study aimed to investigate the early host response towards CHIKV infection, using WRL-68 cells as the *in vitro* study model. By using flow cytometry and IIFA, the optimal infection condition for early host response study was determined to be 24 hours post-infection incubation at the MOI of 5.0. Comparison between the MOCK control and CHIKV-infected whole cell proteome and secretome profiles revealed 53 and 34 differentially expressed protein spots, respectively. MS/MS analysis resulted in the identification of 45 proteins from the whole cell proteome sample, while 20 proteins from the secretome sample were successfully identified. The expression for CDK1, PDHA1 and RAN proteins were validated by Western blot.

Functional classification and STRING network analysis of these proteins showed a widespread alteration of the whole cell proteome and secretome during early CHIKV infection. The most notable outcome of the infection is the disruption of metabolic processes, with 20 down-regulated proteins involved mainly in the carbohydrate, nucleotide and lipid metabolism. Only PDHA1 was up-regulated upon infection. This suggests that the host metabolic machinery is important for CHIKV infection.

CHIKV infection was also found to hijack the host transcription and translation processes through down-regulation of PCBP1, EEF-2, eIF2B1 and eIF3H, and up-regulation of hnRNP C1/C2, a protein of importance in promoting DENV survival in host cells. Down-regulation of UPP-related proteins, UBE2N and PSMA6, as well as cell cycle protein, CDK1, was also observed. Meanwhile, the SET protein, an inhibitor of cyclin B-CDK1 activity was up-regulated. Impairment of the host immune-related proteins, a typical event during virus infection, was evident in this study. CHIKV

infection caused a decrease in the protein levels of PPIA, C3, CTSD, CTSL1 and B2M, possibly to evade the host immune system.

Proteins involved in other functions such as protein transport, ECM regulation, signalling and chaperoning were also deregulated although the exact significance of these changes remain unclear. Finally, transcript expression of 16 selected proteins showed positive correlation with the protein expression, while most of the other genes evaluated did not show any significant differences at the gene level. This suggests that the observed protein expression changes are not exclusively caused by alterations at gene levels, and that other host factors are at play.

In conclusion, this study provides new insights into the plausible mechanisms involved during early CHIKV infection, which complements previous study on the late host response in neonate mice. Nonetheless, further studies that look into the functional characterisation of these proteins either through reverse genetics and/or knock-out studies are warranted to explore the effects and consequences of alterations of these proteins on CHIKV replication success and the eventual host cell demise.

REFERENCES

Aaskov, J. G., Hadding, U., & Bitter-Suermann, D. (1985). Interaction of Ross River virus with the complement system. *Journal of General Virology, 66 (Pt 1)*, 121-129.

Abere, B., Wikan, N., Ubol, S., Auewarakul, P., Paemanee, A., Kittisenachai, S., . . . Smith, D. R. (2012). Proteomic analysis of chikungunya virus infected microgial cells. *PLoS One, 7*(4), e34800. doi: 10.1371/journal.pone.0034800

Apandi, Y., Nazni, W. A., Noor Azleen, Z. A., Vythilingam, I., Noorazian, M. Y., Azahari, A. H., . . . Lee, H. L. (2009). The first isolation of chikungunya virus from non-human primates in Malaysia. *Journal of General and Molecular Virology, 1*(3), 035-039.

Appleby, T. C., Erion, M. D., & Ealick, S. E. (1999). The structure of human 5'-deoxy-5'-methylthioadenosine phosphorylase at 1.7 A resolution provides insights into substrate binding and catalysis. *Structure, 7*(6), 629-641.

Arpino, C., Curatolo, P., & Rezza, G. (2009). Chikungunya and the nervous system: what we do and do not know. *Reviews in Medical Virology, 19*(3), 121-129. doi: 10.1002/rmv.606

Barltrop, J. A., & Owen, T. C. (1991). 5-(3-carboxymethoxyphenyl)-2-(4,5-dimethylthiazolyl)-3-(4-sulfophenyl)tetrazolium, inner salt (MTS) and related analogs of 3-(4,5-dimethylthiazolyl)-2,5-diphenyltetrazolium bromide (MTT) reducing to purple water-soluble formazans As cell-viability indicators. *Bioorganic and Medicinal Chemistry Letters, 1*(11), 611-614.

Barnes, P. D., & Grundy, J. E. (1992). Down-regulation of the class I HLA heterodimer and beta 2-microglobulin on the surface of cells infected with cytomegalovirus. *Journal of General Virology, 73 (Pt 9)*, 2395-2403.

Barrett, J., Brophy, P. M., & Hamilton, J. V. (2005). Analysing proteomic data. *International Journal for Parasitology, 35*(5), 543-553. doi: 10.1016/j.ijpara.2005.01.013

Becker, M. A., Losman, M. J., Itkin, P., & Simkin, P. A. (1982). Gout with superactive phosphoribosylpyrophosphate synthetase due to increased enzyme catalytic rate. *Journal of Laboratory and Clinical Medicine, 99*(4), 495-511.

Beranova-Giorgianni, S. (2003). Proteome analysis by two-dimensional gel electrophoresis and mass spectrometry: strengths and limitations. *TrAC Trends in Analytical Chemistry, 22*(5), 273-281. doi: 10.1016/s0165-9936(03)00508-9

Bernard, E., Solignat, M., Gay, B., Chazal, N., Higgs, S., Devaux, C., & Briant, L. (2010). Endocytosis of chikungunya virus into mammalian cells: role of clathrin and early endosomal compartments. *PLoS One, 5*(7), e11479. doi: 10.1371/journal.pone.0011479

Bodzon-Kulakowska, A., Bierczynska-Krzysik, A., Dylag, T., Drabik, A., Suder, P., Noga, M., . . . Silberring, J. (2007). Methods for samples preparation in proteomic research. *Journal of Chromatography B: Analytical Technologies in*

the Biomedical and Life Sciences, 849(1-2), 1-31. doi: 10.1016/j.jchromb.2006.10.040

Boere, W. A., Benaissa-Trouw, B. J., Harmsen, T., Erich, T., Kraaijeveld, C. A., & Snippe, H. (1986). The role of complement in monoclonal antibody-mediated protection against virulent Semliki Forest virus. *Immunology, 58*(4), 553-559.

Bordi, L., Carletti, F., Castilletti, C., Chiappini, R., Sambri, V., Cavrini, F., . . . Capobianchi, M. R. (2008). Presence of the A226V mutation in autochthonous and imported Italian chikungunya virus strains. *Clinical Infectious Diseases, 47*(3), 428-429. doi: 10.1086/589925

Bordi, L., Meschi, S., Selleri, M., Lalle, E., Castilletti, C., Carletti, F., . . . Capobianchi, M. R. (2011). Chikungunya virus isolates with/without A226V mutation show different sensitivity to IFN-a, but similar replication kinetics in non human primate cells. *New Microbiologica, 34*(1), 87-91.

Brazin, K. N., Mallis, R. J., Fulton, D. B., & Andreotti, A. H. (2002). Regulation of the tyrosine kinase Itk by the peptidyl-prolyl isomerase cyclophilin A. *Proceedings of the National Academy of Sciences of the United States of America, 99*(4), 1899-1904. doi: 10.1073/pnas.042529199

Brighton, S. W. (1984). Chloroquine phosphate treatment of chronic Chikungunya arthritis. An open pilot study. *South African Medical Journal, 66*(6), 217-218.

Briolant, S., Garin, D., Scaramozzino, N., Jouan, A., & Crance, J. M. (2004). In vitro inhibition of Chikungunya and Semliki Forest viruses replication by antiviral compounds: synergistic effect of interferon-alpha and ribavirin combination. *Antiviral Research, 61*(2), 111-117. doi: S0166354203002183

Brockmann, R., Beyer, A., Heinisch, J. J., & Wilhelm, T. (2007). Posttranscriptional expression regulation: what determines translation rates? *PLoS Computer Biology, 3*(3), e57. doi: 10.1371/journal.pcbi.0030057

Canas, B., Pineiro, C., Calvo, E., Lopez-Ferrer, D., & Gallardo, J. M. (2007). Trends in sample preparation for classical and second generation proteomics. *Journal of Chromatography A, 1153*(1-2), 235-258. doi: 10.1016/j.chroma.2007.01.045

Canela, N., Rodriguez-Vilarrupla, A., Estanyol, J. M., Diaz, C., Pujol, M. J., Agell, N., & Bachs, O. (2003). The SET protein regulates G2/M transition by modulating cyclin B-cyclin-dependent kinase 1 activity. *Journal of Biological Chemistry, 278*(2), 1158-1164. doi: 10.1074/jbc.M207497200

Cavrini, F., Gaibani, P., Pierro, A. M., Rossini, G., Landini, M. P., & Sambri, V. (2009). Chikungunya: an emerging and spreading arthropod-borne viral disease. *Journal of Infection in Developing Countries, 3*(10), 744-752.

Chandak, N. H., Kashyap, R. S., Kabra, D., Karandikar, P., Saha, S. S., Morey, S. H., . . . Daginawala, H. F. (2009). Neurological complications of Chikungunya virus infection. *Neurology India, 57*(2), 177-180. doi: ni_2009_57_2_177_51289 [pii]10.4103/0028-3886.51289

Chen, C. H. (2008). Review of a current role of mass spectrometry for proteome research. *Analytica Chimica Acta, 624*(1), 16-36. doi: S0003-2670(08)01132-X [pii]10.1016/j.aca.2008.06.017

Cherian, S. S., Walimbe, A. M., Jadhav, S. M., Gandhe, S. S., Hundekar, S. L., Mishra, A. C., & Arankalle, V. A. (2009). Evolutionary rates and timescale comparison of Chikungunya viruses inferred from the whole genome/E1 gene with special reference to the 2005-07 outbreak in the Indian subcontinent. *Infection, Genetics and Evolution 9*(1), 16-23. doi: 10.1016/j.meegid.2008.09.004

Chevillon, C., Briant, L., Renaud, F., & Devaux, C. (2008). The Chikungunya threat: an ecological and evolutionary perspective. *Trends in Microbiology, 16*(2), 80-88. doi: S0966-842X(07)00250-8 [pii]10.1016/j.tim.2007.12.003

Chhabra, M., Mittal, V., Bhattacharya, D., Rana, U., & Lal, S. (2008). Chikungunya fever: a re-emerging viral infection. *Indian Journal of Medical Microbiology, 26*(1), 5-12.

Chia, P. Y., Ng, M. L., & Chu, J. H. (2010). Chikungunya fever: A review of a re-emerging mosquito-borne infectious disease and the current status. In A. Mendez-Vilas (Ed.), Current research, technology and education topics in appplied microbiology and microbial biotechnology (2nd ed., Vol. 1, pp. 1-788): Formatex research center.

Christensen, B. C., Smith, A. A., Zheng, S., Koestler, D. C., Houseman, E. A., Marsit, C. J., . . . Wiencke, J. K. (2011). DNA methylation, isocitrate dehydrogenase mutation, and survival in glioma. *Journal of the National Cancer Institute, 103*(2), 143-153. doi: 10.1093/jnci/djq497

Chua, K. B. (2010). Epidemiology of chikungunya in Malaysia: 2006-2009. *Medical Journal of Malaysia, 65*(4), 277-282.

Conus, S., & Simon, H. U. (2010). Cathepsins and their involvement in immune responses. *Swiss Medical Weekly, 140*, w13042. doi: 10.4414/smw.2010.13042

Couderc, T., Chretien, F., Schilte, C., Disson, O., Brigitte, M., Guivel-Benhassine, F., . . . Lecuit, M. (2008). A mouse model for Chikungunya: young age and inefficient type-I interferon signaling are risk factors for severe disease. *PLoS Pathogen, 4*(2), e29. doi: 10.1371/journal.ppat.0040029

Crance, J. M., Scaramozzino, N., Jouan, A., & Garin, D. (2003). Interferon, ribavirin, 6-azauridine and glycyrrhizin: antiviral compounds active against pathogenic flaviviruses. *Antiviral Research, 58*(1), 73-79. doi: S0166354202001857 [pii]

D'Ortenzio, E., Grandadam, M., Balleydier, E., Jaffar-Bandjee, M. C., Michault, A., Brottet, E., . . . Filleul, L. (2011). A226V strains of Chikungunya virus, Reunion Island, 2010. *Emerging Infectious Diseases, 17*(2), 309-311. doi: 10.3201/eid1702.101056

Dahl, H. H., Hunt, S. M., Hutchison, W. M., & Brown, G. K. (1987). The human pyruvate dehydrogenase complex. Isolation of cDNA clones for the E1 alpha subunit, sequence analysis, and characterization of the mRNA. *Journal of Biological Chemistry, 262*(15), 7398-7403.

Dhanwani, R., Khan, M., Alam, S. I., Rao, P. V., & Parida, M. (2011). Differential proteome analysis of Chikungunya virus-infected new-born mice tissues reveal implication of stress, inflammatory and apoptotic pathways in disease pathogenesis. *Proteomics, 11*(10), 1936-1951. doi: 10.1002/pmic.201000500

Diamond, D. L., Syder, A. J., Jacobs, J. M., Sorensen, C. M., Walters, K. A., Proll, S. C., . . . Katze, M. G. (2010). Temporal proteome and lipidome profiles reveal hepatitis C virus-associated reprogramming of hepatocellular metabolism and bioenergetics. *PLoS Pathogen, 6*(1), e1000719. doi: 10.1371/journal.ppat.1000719

Dinh, P. X., Beura, L. K., Panda, D., Das, A., & Pattnaik, A. K. (2011). Antagonistic effects of cellular poly(C) binding proteins on vesicular stomatitis virus gene expression. *Journal of Virology, 85*(18), 9459-9471. doi: 10.1128/JVI.05179-11

Dove, A. (1999). Proteomics: translating genomics into products? *Nature Biotechnology, 17*(3), 233-236. doi: 10.1038/6972

Duan, Y., Chen, Y., Hu, W., Li, X., Yang, X., Zhou, X., . . . Han, J. (2012). Peroxisome Proliferator-activated Receptor gamma Activation by Ligands and Dephosphorylation Induces Proprotein Convertase Subtilisin Kexin Type 9 and Low Density Lipoprotein Receptor Expression. *Journal of Biological Chemistry, 287*(28), 23667-23677. doi: 10.1074/jbc.M112.350181

Economopoulou, A., Dominguez, M., Helynck, B., Sissoko, D., Wichmann, O., Quenel, P., . . . Quatresous, I. (2009). Atypical Chikungunya virus infections: clinical manifestations, mortality and risk factors for severe disease during the 2005-2006 outbreak on Reunion. *Epidemiology and Infection, 137*(4), 534-541. doi: 10.1017/S0950268808001167

Edelman, R., Tacket, C. O., Wasserman, S. S., Bodison, S. A., Perry, J. G., & Mangiafico, J. A. (2000). Phase II safety and immunogenicity study of live chikungunya virus vaccine TSI-GSD-218. *American Journal of Tropical Medicine and Hygiene, 62*(6), 681-685.

Edwards, C. J., Welch, S. R., Chamberlain, J., Hewson, R., Tolley, H., Cane, P. A., & Lloyd, G. (2007). Molecular diagnosis and analysis of Chikungunya virus. *Journal of Clinical Virology, 39*(4), 271-275. doi: S1386-6532(07)00185-0 [pii]10.1016/j.jcv.2007.05.008

El-Bacha, T., Menezes, M. M., Azevedo e Silva, M. C., Sola-Penna, M., & Da Poian, A. T. (2004). Mayaro virus infection alters glucose metabolism in cultured cells through activation of the enzyme 6-phosphofructo 1-kinase. *Molecular and Cellular Biochemistry, 266*(1-2), 191-198.

Elena, S. F., & Sanjuan, R. (2005). Adaptive value of high mutation rates of RNA viruses: separating causes from consequences. *Journal of Virology, 79*(18), 11555-11558. doi: 10.1128/JVI.79.18.11555-11558.2005

Frykman, S., & Srienc, F. (2001). Cell cycle-dependent protein secretion by Saccharomyces cerevisiae. *Biotechnology and Bioengineering, 76*(3), 259-268.

Gao, G., & Luo, H. (2006). The ubiquitin-proteasome pathway in viral infections. *Canadian Journal of Physiology and Pharmacology, 84*(1), 5-14. doi: 10.1139/y05-144

Garbis, S., Lubec, G., & Fountoulakis, M. (2005). Limitations of current proteomics technologies. *Journal of Chromatography A, 1077*(1), 1-18.

Garnier, P., Blanchet, E., Reix, G., Kwiatek, S., Reboux, A., Huguenin, B., . . . Becquart, J. (2006). O.211 Severe acute hepatitis during Chikungunya virus infection on Reunion Island: case report from 14 observations. *Journal of Clinical Virology, 36*, S60.

Glickman, M. H., & Ciechanover, A. (2002). The ubiquitin-proteasome proteolytic pathway: destruction for the sake of construction. *Physiological Reviews, 82*(2), 373-428. doi: 10.1152/physrev.00027.2001

Gorg, A., Obermaier, C., Boguth, G., Harder, A., Scheibe, B., Wildgruber, R., & Weiss, W. (2000). The current state of two-dimensional electrophoresis with immobilized pH gradients. *Electrophoresis, 21*(6), 1037-1053. doi: 10.1002/(SICI)1522-2683(20000401)21:6<1037::AID-ELPS1037>3.0.CO;2-V

Graves, P. R., & Haystead, T. A. (2002). Molecular biologist's guide to proteomics. *Microbiology and Molecular Biology Reviews, 66*(1), 39-63; table of contents.

Guicherit, O. M., Cooper, B. F., Rudolph, F. B., & Kellems, R. E. (1994). Amplification of an adenylosuccinate synthetase gene in alanosine-resistant murine T-lymphoma cells. Molecular cloning of a cDNA encoding the "non-muscle" isozyme. *Journal of Biological Chemistry, 269*(6), 4488-4496.

Hahon, N., & Zimmerman, W. D. (1970). Chikungunya virus infection of cell monolayers by cell-to-cell and extracellular transmission. *Applied Microbiology, 19*(2), 389-391.

Hall, A., Hakansson, K., Mason, R. W., Grubb, A., & Abrahamson, M. (1995). Structural basis for the biological specificity of cystatin C. Identification of leucine 9 in the N-terminal binding region as a selectivity-conferring residue in the inhibition of mammalian cysteine peptidases. *Journal of Biological Chemistry, 270*(10), 5115-5121.

Harrison, V. R., Binn, L. N., & Randall, R. (1967). Comparative immunogenicities of chikungunya vaccines prepared in avian and mammalian tissues. *American Journal of Tropical Medicine and Hygiene, 16*(6), 786-791.

Hegardt, F. G. (1999). Mitochondrial 3-hydroxy-3-methylglutaryl-CoA synthase: a control enzyme in ketogenesis. *Biochemical Journal, 338 (Pt 3)*, 569-582.

Her, Z., Kam, Y. W., Lin, R. T., & Ng, L. F. (2009). Chikungunya: a bending reality. *Microbes Infect, 11*(14-15), 1165-1176. doi: S1286-4579(09)00207-X [pii]10.1016/j.micinf.2009.09.004

Hewitt, E. W. (2003). The MHC class I antigen presentation pathway: strategies for viral immune evasion. *Immunology, 110*(2), 163-169.

Higa, L. M., Caruso, M. B., Canellas, F., Soares, M. R., Oliveira-Carvalho, A. L., Chapeaurouge, D. A., . . . Da Poian, A. T. (2008). Secretome of HepG2 cells infected with dengue virus: implications for pathogenesis. *Biochimica et Biophysica Acta, 1784*(11), 1607-1616. doi: S1570-9639(08)00199-4 [pii]10.1016/j.bbapap.2008.06.015

Hirsch, R. L., Griffin, D. E., & Winkelstein, J. A. (1978). The effect of complement depletion on the course of Sindbis virus infection in mice. *Journal of Immunology, 121*(4), 1276-1278.

Hoogland, C., Mostaguir, K., Appel, R. D., & Lisacek, F. (2008). The World-2DPAGE Constellation to promote and publish gel-based proteomics data through the ExPASy server. *Journal of Proteomics, 71*(2), 245-248. doi: 10.1016/j.jprot.2008.02.005

Issaq, H., & Veenstra, T. (2008). Two-dimensional polyacrylamide gel electrophoresis (2D-PAGE): advances and perspectives. *Biotechniques, 44*(5), 697-698, 700. doi: 000112823 [pii]10.2144/000112823

Itai, R., Suzuki, K., Yamaguchi, H., Nakanishi, H., Nishizawa, N. K., Yoshimura, E., & Mori, S. (2000). Induced activity of adenine phosphoribosyltransferase (APRT) in iron-deficiency barley roots: a possible role for phytosiderophore production. *Journal of Experimental Botany 51*(348), 1179-1188.

Jacobs, J. M., Diamond, D. L., Chan, E. Y., Gritsenko, M. A., Qian, W., Stastna, M., . . . Katze, M. G. (2005). Proteome analysis of liver cells expressing a full-length hepatitis C virus (HCV) replicon and biopsy specimens of posttransplantation liver from HCV-infected patients. *Journal of Virology, 79*(12), 7558-7569. doi: 79/12/7558 [pii]10.1128/JVI.79.12.7558-7569.2005

Jin, Z. G., Melaragno, M. G., Liao, D. F., Yan, C., Haendeler, J., Suh, Y. A., . . . Berk, B. C. (2000). Cyclophilin A is a secreted growth factor induced by oxidative stress. *Circulation Research, 87*(9), 789-796.

Kam, Y. W., Ong, E. K., Renia, L., Tong, J. C., & Ng, L. F. (2009). Immuno-biology of Chikungunya and implications for disease intervention. *Microbes and Infection, 11*(14-15), 1186-1196. doi: S1286-4579(09)00208-1 [pii]10.1016/j.micinf.2009.09.003

Khan, A. H., Morita, K., Parquet Md Mdel, C., Hasebe, F., Mathenge, E. G., & Igarashi, A. (2002). Complete nucleotide sequence of chikungunya virus and evidence for an internal polyadenylation site. *Journal of General Virology, 83*(Pt 12), 3075-3084.

Krecic, A. M., & Swanson, M. S. (1999). hnRNP complexes: composition, structure, and function. *Current Opinion in Cell Biology, 11*(3), 363-371. doi: 10.1016/S0955-0674(99)80051-9

Kumar, N. C., Nadimpalli, M., Vardhan, V. R., & Gopal, S. D. (2010). Association of ABO blood groups with Chikungunya virus. *Virology Journal, 7*, 140. doi: 10.1186/1743-422X-7-140

Kushner, D. B., Lindenbach, B. D., Grdzelishvili, V. Z., Noueiry, A. O., Paul, S. M., & Ahlquist, P. (2003). Systematic, genome-wide identification of host genes affecting replication of a positive-strand RNA virus. *Proceedings of the National Academy of Sciences of the United States of America, 100*(26), 15764-15769. doi: 10.1073/pnas.2536857100

Lam, S. K., Chua, K. B., Hooi, P. S., Rahimah, M. A., Kumari, S., Tharmaratnam, M., . . . Sampson, I. A. (2001). Chikungunya infection--an emerging disease in Malaysia. *Southeast Asian Journal of Tropical Medicine and Public Health, 32*(3), 447-451.

Laras, K., Sukri, N. C., Larasati, R. P., Bangs, M. J., Kosim, R., Djauzi, . . . Corwin, A. L. (2005). Tracking the re-emergence of epidemic chikungunya virus in Indonesia. *Transactions of the Royal Society of Tropical Medicine and Hygiene, 99*(2), 128-141.

LeBaron, R. G., Hook, A., Esko, J. D., Gay, S., & Hook, M. (1989). Binding of heparan sulfate to type V collagen. A mechanism of cell-substrate adhesion. *Journal of Biological Chemistry, 264*(14), 7950-7956.

Lee, W. C., & Lee, K. H. (2004). Applications of affinity chromatography in proteomics. *Analytical Biochemistry, 324*(1), 1-10. doi: S0003269703005876 [pii]

Leong, W. F., & Chow, V. T. (2006). Transcriptomic and proteomic analyses of rhabdomyosarcoma cells reveal differential cellular gene expression in response to enterovirus 71 infection. *Cellular Microbiology, 8*(4), 565-580. doi: 10.1111/j.1462-5822.2005.00644.x

Levitt, N. H., Ramsburg, H. H., Hasty, S. E., Repik, P. M., Cole, F. E., Jr., & Lupton, H. W. (1986). Development of an attenuated strain of chikungunya virus for use in vaccine production. *Vaccine, 4*(3), 157-162.

Li, H. P., Huang, P., Park, S., & Lai, M. M. (1999). Polypyrimidine tract-binding protein binds to the leader RNA of mouse hepatitis virus and serves as a regulator of viral transcription. *Journal of Virology, 73*(1), 772-777.

Liebler, D. C. (2002). *Introduction to Proteomics: Tools for the New Biology*. New Jersey: Humana Press.

Lietzen, N., Ohman, T., Rintahaka, J., Julkunen, I., Aittokallio, T., Matikainen, S., & Nyman, T. A. (2011). Quantitative subcellular proteome and secretome profiling of influenza A virus-infected human primary macrophages. *PLoS Pathogen, 7*(5), e1001340. doi: 10.1371/journal.ppat.1001340

Lim, K. G. (2010). A respite from chikungunya for now. *Medical Journal of Malaysia, 65*(4), 255.

Liu, X., Zhao, Z., Xu, C., Sun, L., Chen, J., Zhang, L., & Liu, W. (2012). Cyclophilin A restricts influenza A virus replication through degradation of the M1 protein. *PLoS One, 7*(2), e31063. doi: 10.1371/journal.pone.0031063

Lokireddy, S., Sarojamma, V., & Ramakrishna, V. (2009). Genetic predisposition to chikungunya--a blood group study in chikungunya affected families. *Virology Journal, 6*, 77. doi: 10.1186/1743-422X-6-77

Makridakis, M., & Vlahou, A. (2010). Secretome proteomics for discovery of cancer biomarkers. *Journal of Proteomics, 73*(12), 2291-2305. doi: 10.1016/j.jprot.2010.07.001

Mallilankaraman, K., Shedlock, D. J., Bao, H., Kawalekar, O. U., Fagone, P., Ramanathan, A. A., . . . Weiner, D. B. (2011). A DNA vaccine against chikungunya virus is protective in mice and induces neutralizing antibodies in mice and nonhuman primates. *PLoS Neglected Tropical Diseases, 5*(1), e928. doi: 10.1371/journal.pntd.0000928

Martinez-Botas, J., Suarez, Y., Ferruelo, A. J., Gomez-Coronado, D., & Lasuncion, M. A. (1999). Cholesterol starvation decreases p34(cdc2) kinase activity and arrests the cell cycle at G2. *FASEB Journal, 13*(11), 1359-1370.

Mattanovich, D., Graf, A., Stadlmann, J., Dragosits, M., Redl, A., Maurer, M., . . . Gasser, B. (2009). Genome, secretome and glucose transport highlight unique features of the protein production host Pichia pastoris. *Microbial Cell Factories, 8*, 29. doi: 10.1186/1475-2859-8-29

Mavalankar, D., Shastri, P., & Raman, P. (2007). Chikungunya epidemic in India: a major public-health disaster. *Lancet Infectious Diseases, 7*(5), 306-307. doi: S1473-3099(07)70091-9 [pii]10.1016/S1473-3099(07)70091-9

Maxwell, K. L., & Frappier, L. (2007). Viral proteomics. *Microbiology and Molecular Biology Reviews, 71*(2), 398-411. doi: 71/2/398 [pii]10.1128/MMBR.00042-06

McInerney, G. M., Kedersha, N. L., Kaufman, R. J., Anderson, P., & Liljestrom, P. (2005). Importance of eIF2alpha phosphorylation and stress granule assembly in alphavirus translation regulation. *Molecular Biology of the Cell, 16*(8), 3753-3763. doi: 10.1091/mbc.E05-02-0124

Meissburger, B., Stachorski, L., Roder, E., Rudofsky, G., & Wolfrum, C. (2011). Tissue inhibitor of matrix metalloproteinase 1 (TIMP1) controls adipogenesis in obesity in mice and in humans. *Diabtologia, 54*(6), 1468-1479. doi: 10.1007/s00125-011-2093-9

Merrick, W. C. (1992). Mechanism and regulation of eukaryotic protein synthesis. *Microbiological Reviews, 56*(2), 291-315.

MOH. (2010). Press release of dengue fever and Chikungunya situation in Malaysia: Week 51/2010 (19 - 25 Dec 2010). Retrieved from http://www.moh.gov.my/press_releases/69

MOH. (2011). Press release of dengue fever & Chikungunya situation In Malaysia: Week 30 (24 - 30 July 2011). Retrieved from http://www.moh.gov.my/press_releases/102

MOH. (2012). First outbreak of Chikungunya in Malaysia for the year 2012. Retrieved from http://www.moh.gov.my/press_releases/264

Monteoliva, L., & Albar, J. P. (2004). Differential proteomics: an overview of gel and non-gel based approaches. *Briefings in Functional Genomic Proteomic, 3*(3), 220-239.

Munger, J., Bajad, S. U., Coller, H. A., Shenk, T., & Rabinowitz, J. D. (2006). Dynamics of the cellular metabolome during human cytomegalovirus infection. *PLoS Pathogen, 2*(12), e132. doi: 10.1371/journal.ppat.0020132

NIAID. (2012, 2012). NIAID Category A, B and C Priority Pathogens Retrieved 15 April, 2012, from http://www.niaid.nih.gov/topics/biodefenserelated/biodefense/pages/cata.aspx

Niles, A. L., Moravec, R. A., Eric Hesselberth, P., Scurria, M. A., Daily, W. J., & Riss, T. L. (2007). A homogeneous assay to measure live and dead cells in the same sample by detecting different protease markers. *Analytical Biochemistry, 366*(2), 197-206. doi: 10.1016/j.ab.2007.04.007

Noisakran, S., Sengsai, S., Thongboonkerd, V., Kanlaya, R., Sinchaikul, S., Chen, S. T., . . . Yenchitsomanus, P. T. (2008). Identification of human hnRNP C1/C2 as a dengue virus NS1-interacting protein. *Biochemical and Biophysical Research Communications, 372*(1), 67-72. doi: 10.1016/j.bbrc.2008.04.165

Noridah, O., Paranthaman, V., Nayar, S. K., Masliza, M., Ranjit, K., Norizah, I., . . . Chua, K. B. (2007). Outbreak of chikungunya due to virus of Central/East African genotype in Malaysia. *Medical Journal of Malaysia, 62*(4), 323-328.

O'Farrell, T. J., & Pourmotabbed, T. (2000). Identification of structural elements important for matrix metalloproteinase type V collagenolytic activity as revealed by chimeric enzymes. Role of fibronectin-like domain and active site of gelatinase B. *Journal of Biological Chemistry, 275*(36), 27964-27972. doi: 10.1074/jbc.M003936200M003936200 [pii]

Ohashi, K., Naruto, M., Nakaki, T., & Sano, E. (2003). Identification of interleukin-8 converting enzyme as cathepsin L. *Biochimica et Biophysica Acta, 1649*(1), 30-39.

Ozden, S., Huerre, M., Riviere, J. P., Coffey, L. L., Afonso, P. V., Mouly, V., . . . Ceccaldi, P. E. (2007). Human muscle satellite cells as targets of Chikungunya virus infection. *PLoS One, 2*(6), e527. doi: 10.1371/journal.pone.0000527

Pandey, A., & Mann, M. (2000). Proteomics to study genes and genomes. *Nature, 405*(6788), 837-846. doi: 10.1038/35015709

Pardigon, N. (2009). The biology of chikungunya: a brief review of what we still do not know. *Pathologie Biologie, 57*(2), 127-132. doi: S0369-8114(08)00040-0 [pii]10.1016/j.patbio.2008.02.016

Pastorino, B., Boucomont-Chapeaublanc, E., Peyrefitte, C. N., Belghazi, M., Fusai, T., Rogier, C., . . . Almeras, L. (2009). Identification of cellular proteome modifications in response to West Nile virus infection. *Molecular and Cellular Proteomics, 8*(7), 1623-1637. doi: 10.1074/mcp.M800565-MCP200

Pastorino, B., Muyembe-Tamfum, J. J., Bessaud, M., Tock, F., Tolou, H., Durand, J. P., & Peyrefitte, C. N. (2004). Epidemic resurgence of Chikungunya virus in democratic Republic of the Congo: identification of a new central African strain. *Journal of Medical Virology, 74*(2), 277-282. doi: 10.1002/jmv.20168

Pastorino, B. A., Peyrefitte, C. N., Almeras, L., Grandadam, M., Rolland, D., Tolou, H., & Bessaud, M. (2008). Expression and biochemical characterization of nsP2 cycsteine protease of Chikungunya virus. *Virus Research, 131*(2), 293-298. doi: 10.1016/j.virusres.2007.09.009

Patel, P. S., Telang, S. D., Rawal, R. M., & Shah, M. H. (2005). A review of proteomics in cancer research. *Asian Pacific Journal of Cancer Prevention, 6*(2), 113-117.

Pattanakitsakul, S. N., Rungrojcharoenkit, K., Kanlaya, R., Sinchaikul, S., Noisakran, S., Chen, S. T., . . . Thongboonkerd, V. (2007). Proteomic analysis of host responses in HepG2 cells during dengue virus infection. *Journal of Proteome Research, 6*(12), 4592-4600. doi: 10.1021/pr070366b

Poggioli, G. J., DeBiasi, R. L., Bickel, R., Jotte, R., Spalding, A., Johnson, G. L., & Tyler, K. L. (2002). Reovirus-induced alterations in gene expression related to cell cycle regulation. *Journal of Virology, 76*(6), 2585-2594.

Powers, A. M., Brault, A. C., Tesh, R. B., & Weaver, S. C. (2000). Re-emergence of Chikungunya and O'nyong-nyong viruses: evidence for distinct geographical lineages and distant evolutionary relationships. *Journal of General Virology, 81*(Pt 2), 471-479.

Powers, A. M., & Logue, C. H. (2007). Changing patterns of chikungunya virus: re-emergence of a zoonotic arbovirus. *Journal of General Virology, 88*(Pt 9), 2363-2377. doi: 10.1099/vir.0.82858-0

Rabilloud, T., Chevallet, M., Luche, S., & Lelong, C. (2010). Two-dimensional gel electrophoresis in proteomics: Past, present and future. *Journal of Proteomics, 73*(11), 2064-2077. doi: 10.1016/j.jprot.2010.05.016

Rabilloud, T., & Lelong, C. (2011). Two-dimensional gel electrophoresis in proteomics: a tutorial. *Journal of Proteomics, 74*(10), 1829-1841. doi: 10.1016/j.jprot.2011.05.040

Ramful, D., Carbonnier, M., Pasquet, M., Bouhmani, B., Ghazouani, J., Noormahomed, T., . . . Alessandri, J. L. (2007). Mother-to-child transmission of Chikungunya virus infection. *Pediatric Infectious Disease Journal, 26*(9), 811-815. doi: 10.1097/INF.0b013e3180616d4f

Ramos-Valdivia, A. C., van der Heijden, R., & Verpoorte, R. (1997). Isopentenyl diphosphate isomerase: a core enzyme in isoprenoid biosynthesis. A review of its biochemistry and function. *Natural Product Reports, 14*(6), 591-603.

Renault, P., Solet, J. L., Sissoko, D., Balleydier, E., Larrieu, S., Filleul, L., . . . Pierre, V. (2007). A major epidemic of chikungunya virus infection on Reunion Island, France, 2005-2006. *American Journal of Tropical Medicine and Hygiene, 77*(4), 727-731. doi: 77/4/727 [pii]

Rezza, G., Nicoletti, L., Angelini, R., Romi, R., Finarelli, A. C., Panning, M., . . . Cassone, A. (2007). Infection with chikungunya virus in Italy: an outbreak in a temperate region. *Lancet, 370*(9602), 1840-1846. doi: S0140-6736(07)61779-6 [pii]10.1016/S0140-6736(07)61779-6

Salonen, A., Ahola, T., & Kaariainen, L. (2005). Viral RNA replication in association with cellular membranes. *Current Topics in Microbiology and Immunology, 285*, 139-173.

Schang, L. M. (2004). Effects of pharmacological cyclin-dependent kinase inhibitors on viral transcription and replication. *Biochimica et Biophysica Acta, 1697*(1-2), 197-209. doi: 10.1016/j.bbapap.2003.11.024

Scheller, N., & Diez, J. (2009). RNA viruses hijack the mRNA decay machinery to multiply. *Cell Cycle, 8*(24), 4013-4014.

Schmidt-Chanasit, J., Tenner-Racz, K., Poppert, D., Emmerich, P., Frank, C., Dinges, C., . . . Gunther, S. (2012). Fatal dengue hemorrhagic fever imported into Germany. *Infection, 40*(4), 441-443. doi: 10.1007/s15010-011-0208-3

Schroepfer, G. J., Jr. (1982). Sterol biosynthesis. *Annual Review of Biochemistry, 51*, 555-585. doi: 10.1146/annurev.bi.51.070182.003011

Schuffenecker, I., Iteman, I., Michault, A., Murri, S., Frangeul, L., Vaney, M. C., . . . Brisse, S. (2006). Genome microevolution of chikungunya viruses causing the Indian Ocean outbreak. *PLoS Medicine, 3*(7), e263. doi: 10.1371/journal.pmed.0030263

Schwartz, O., & Albert, M. L. (2010). Biology and pathogenesis of chikungunya virus. *Nature Reviews Microbiology, 8*(7), 491-500. doi: 10.1038/nrmicro2368

Sellers, K. F., & Miecznikowski, J. C. (2010). Feature detection techniques for preprocessing proteomic data. *International Journal of Biomedical Imaging 2010*, 896718. doi: 10.1155/2010/896718

Shen, S. H., Gu, L. J., Liu, P. Q., Ye, X., Chang, W. S., & Li, B. S. (2008). Comparative proteomic analysis of differentially expressed proteins between K562 and K562/ADM cells. *Chinese Medical Journal, 121*(5), 463-468.

Shirakura, M., Murakami, K., Ichimura, T., Suzuki, R., Shimoji, T., Fukuda, K., . . . Shoji, I. (2007). E6AP ubiquitin ligase mediates ubiquitylation and degradation of hepatitis C virus core protein. *Journal of Virology, 81*(3), 1174-1185. doi: 10.1128/JVI.01684-06

Simizu, B., Yamamoto, K., Hashimoto, K., & Ogata, T. (1984). Structural proteins of Chikungunya virus. *Journal of Virology, 51*(1), 254-258.

Singh, S. K., & Unni, S. K. (2011). Chikungunya virus: host pathogen interaction. *Reviews in Medical Virology* doi: 10.1002/rmv.681

Solanki, B. S., Arya, S. C., & Maheshwari, P. (2007). Chikungunya disease with nephritic presentation. *International Journal of Clinical Practice, 61*(11), 1941. doi: IJCP1329 [pii]10.1111/j.1742-1241.2007.01329.x

Sourisseau, M., Schilte, C., Casartelli, N., Trouillet, C., Guivel-Benhassine, F., Rudnicka, D., . . . Schwartz, O. (2007). Characterization of reemerging chikungunya virus. *PLoS Pathogen, 3*(6), e89. doi: 10.1371/journal.ppat.0030089

Strauss, J. H., & Strauss, E. G. (1994). The alphaviruses: gene expression, replication, and evolution. *Microbiological Reviews, 58*(3), 491-562.

Tchankouo-Nguetcheu, S., Khun, H., Pincet, L., Roux, P., Bahut, M., Huerre, M., . . . Choumet, V. (2010). Differential protein modulation in midguts of Aedes aegypti infected with chikungunya and dengue 2 viruses. *PLoS One, 5*(10). doi: 10.1371/journal.pone.0013149

Tesh, R. B. (1982). Arthritides caused by mosquito-borne viruses. *Annual Review of Medicine, 33*, 31-40. doi: 10.1146/annurev.me.33.020182.000335

Tetu, B., Brisson, J., Wang, C. S., Lapointe, H., Beaudry, G., Blanchette, C., & Trudel, D. (2006). The influence of MMP-14, TIMP-2 and MMP-2 expression on breast cancer prognosis. *Breast Cancer Research, 8*(3), R28. doi: bcr1503 [pii]10.1186/bcr1503

Thiboutot, M. M., Kannan, S., Kawalekar, O. U., Shedlock, D. J., Khan, A. S., Sarangan, G., . . . Muthumani, K. (2010). Chikungunya: a potentially emerging epidemic? *PLoS Neglected Tropical Diseases, 4*(4), e623. doi: 10.1371/journal.pntd.0000623

Thor, F., Gautschi, M., Geiger, R., & Helenius, A. (2009). Bulk flow revisited: transport of a soluble protein in the secretory pathway. *Traffic, 10*(12), 1819-1830. doi: 10.1111/j.1600-0854.2009.00989.x

Tiawsirisup, S. (2011). Chikungunya Virus in Thailand; An Update. *The Thai Journal of Veterinary Medicine, 41*(2), 133-134.

Toribio, R., & Ventoso, I. (2010). Inhibition of host translation by virus infection in vivo. *Proceedings of the National Academy of Sciences of the United States of America, 107*(21), 9837-9842. doi: 10.1073/pnas.1004110107

Tortorella, D., Gewurz, B. E., Furman, M. H., Schust, D. J., & Ploegh, H. L. (2000). Viral subversion of the immune system. *Annual Review of Immunology, 18*, 861-926. doi: 10.1146/annurev.immunol.18.1.861

Tsetsarkin, K. A., Chen, R., Sherman, M. B., & Weaver, S. C. (2011). Chikungunya virus: evolution and genetic determinants of emergence. *Current Opinion in Virology, 1*(4), 310-317. doi: 10.1016/j.coviro.2011.07.004

Tsetsarkin, K. A., Vanlandingham, D. L., McGee, C. E., & Higgs, S. (2007). A Single Mutation in Chikungunya Virus Affects Vector Specificity and Epidemic Potential. *PLoS Pathogen, 3*(12), e201. doi: 10.1371/journal.ppat.0030201

Tyagi, S., Raghvendra, Singh, U., Kalra, T., Munjal, K., & Vitas. (2010). Practical applications of proteomics - A technique for large-scale study of proteins: An overview. *International Journal of Pharmaceutical Sciences Review and Research, 3*(1), 87-90.

Vazeille, M., Moutailler, S., Coudrier, D., Rousseaux, C., Khun, H., Huerre, M., . . . Failloux, A. B. (2007). Two Chikungunya isolates from the outbreak of La Reunion (Indian Ocean) exhibit different patterns of infection in the mosquito, Aedes albopictus. *PLoS One, 2*(11), e1168. doi: 10.1371/journal.pone.0001168

Vihinen, M. (2001). Bioinformatics in proteomics. *Biomolecular Engineering, 18*(5), 241-248.

Wang, D., Suhrbier, A., Penn-Nicholson, A., Woraratanadharm, J., Gardner, J., Luo, M., . . . Dong, J. Y. (2011). A complex adenovirus vaccine against chikungunya virus provides complete protection against viraemia and arthritis. *Vaccine, 29*(15), 2803-2809. doi: 10.1016/j.vaccine.2011.01.108

Wang, E., Volkova, E., Adams, A. P., Forrester, N., Xiao, S. Y., Frolov, I., & Weaver, S. C. (2008). Chimeric alphavirus vaccine candidates for chikungunya. *Vaccine, 26*(39), 5030-5039. doi: S0264-410X(08)00981-X [pii]10.1016/j.vaccine.2008.07.054

Watanabe, N., Aizaki, H., Matsuura, T., Kojima, S., Wakita, T., & Suzuki, T. (2011). Hepatitis C virus RNA replication in human stellate cells regulates gene expression of extracellular matrix-related molecules. *Biochemical and Biophysical Research Communications, 407*(1), 135-140. doi: S0006-291X(11)00344-5 [pii]10.1016/j.bbrc.2011.02.125

Watashi, K., & Shimotohno, K. (2007). Cyclophilin and viruses: cyclophilin as a cofactor for viral infection and possible anti-viral target. *Drug Target Insights, 2*, 9-18.

Watson, T. J., & Sparkman, D. O. (2007). Introduction to mass spectrometry: Instrumentation, applications and strategies for data interpretation (4th ed., pp. 862). West Sussex: Wiley.

Wauquier, N., Becquart, P., Nkoghe, D., Padilla, C., Ndjoyi-Mbiguino, A., & Leroy, E. M. (2011). The acute phase of Chikungunya virus infection in humans is associated with strong innate immunity and T CD8 cell activation. *Journal of Infectious Diseases, 204*(1), 115-123. doi: 10.1093/infdis/jiq006

Weaver, S. C., & Reisen, W. K. (2010). Present and future arboviral threats. *Antiviral Research, 85*(2), 328-345. doi: 10.1016/j.antiviral.2009.10.008

Wells, D. A., & Weil, D. A. (2003). Directions in automated sample preparation of proteins (pp. 42-54): PharmaGenomics.

Westermeiner, R., & Naven, T. (2002). *Proteomics in practice: A laboratory manual of proteome analysis*. Weinheim: Wiley-VCH.

White, A., Berman, S., & Lowenthal, J. P. (1972). Comparative immunogenicities of Chikungunya vaccines propagated in monkey kidney monolayers and chick embryo suspension cultures. *Applied Microbiology, 23*(5), 951-952.

White, L. K., Sali, T., Alvarado, D., Gatti, E., Pierre, P., Streblow, D., & Defilippis, V. R. (2011). Chikungunya virus induces IPS-1-dependent innate immune activation and protein kinase R-independent translational shutoff. *Journal of Virology, 85*(1), 606-620. doi: 10.1128/JVI.00767-10

Widnell, C. C., Baldwin, S. A., Davies, A., Martin, S., & Pasternak, C. A. (1990). Cellular stress induces a redistribution of the glucose transporter. *FASEB Journal, 4*(6), 1634-1637.

Yan, J. X., Wait, R., Berkelman, T., Harry, R. A., Westbrook, J. A., Wheeler, C. H., & Dunn, M. J. (2000). A modified silver staining protocol for visualization of proteins compatible with matrix-assisted laser desorption/ionization and electrospray ionization-mass spectrometry. *Electrophoresis, 21*(17), 3666-3672. doi: 10.1002/1522-2683(200011)21:17<3666::AID-ELPS3666>3.0.CO;2-6

Yates, J. R., 3rd. (1998). Mass spectrometry and the age of the proteome. *Journal of Mass Spectrometry, 33*(1), 1-19. doi: 10.1002/(SICI)1096-9888(199801)33:1<1::AID-JMS624>3.0.CO;2-9

Zheng, K., Li, J., Zhang, Q., Liang, M., Li, C., Lin, M., . . . Li, D. (2010). Genetic analysis of chikungunya viruses imported to mainland China in 2008. *Virology Journal, 7*, 8. doi: 1743-422X-7-8 [pii]10.1186/1743-422X-7-8

Ziegler, S. A., Lu, L., da Rosa, A. P., Xiao, S. Y., & Tesh, R. B. (2008). An animal model for studying the pathogenesis of chikungunya virus infection. *American Journal of Tropical Medicine and Hygiene, 79*(1), 133-139. doi: 79/1/133 [pii]

APPENDICES

Appendix A1: Protein names and gene symbols used in the whole cell proteome network

Protein name	Gene Name
Protein SET	SET
Nucleophosmin (B23)	NPM1
Reticulocalbin-1	RCN1
Heterogeneous nuclear ribonucleoproteins C1/C2	HNRNPC
Keratin, type I cytoskeletal 17	KRT17
Keratin, type II cytoskeletal 7	KRT7
Chromobox protein homolog 3	CBX3
Pyruvate dehydrogenase E1 component subunit alpha, mitochondrial	PDHA1
Spartin	SPG20
Phosphoglucomutase-2	PGM2
Elongation factor-2	EEF2
Gamma-enolase	ENO2
Hydroxymethylglutaryl-CoA synthase, cytoplasmic	HMGCS1
Copine-1	CPNE1
Spermidine synthase	SRM
Ubiquitin-conjugating enzyme E2 N	UBE2N
Inosine triphosphate pyrophosphatase	ITPA
Adenine phosphoribosyltransferase	APRT
Nicotinamide phosphoribosyltransferase	NAMPT
Rab GDP dissociation inhibitor beta	GDI2
La ribonucleoprotein	SSB
Alpha-enolase	ENO1
Adenylosuccinate synthetase isozyme 2	ADSS
Isocitrate dehydrogenase [NADP] cytoplasmic	IDH1
Eukaryotic translation initiation factor 3 subunit H	EIF3H
Poly(rC)-binding protein1 (hnRNP E1)	PCBP1
Phosphoserine aminotransferase	PSAT1
Aldo-keto reductase family 1 member C2	AKR1C2
Pirin	PIR
Ribose-phosphate pyrophosphokinase1	PRPS1
Glucosamine-6-phosphate isomerase 1	GNPDA1
S-formylglutathione hydrolase	ESD
Actin-related protein 2/3 complex subunit 2 (p34-ARC)	ARPC2
Electron transfer flavoprotein subunit alpha, mitochondrial	ETFA
Guanine nucleotide-binding protein subunit beta-2-like 1	GNB2L1
Cyclin-dependent kinase 1	CDK1
Translation initiation factor eIF-2B subunit alpha	EIF2B1
Phosphoglycerate mutase 1	PGAM1
Proteasome subunit alpha type-6	PSMA6
Isopentyl-diphosphate Delta-isomerase 1	IDI1
Triosephosphate isomerase	TPI1
S-methyl-5-thioadenosine phosphorylase	MTAP
Thioredoxin-like protein 5	TXNDC17
Fatty-acid binding protein, epidermal	FABP5

Appendix A1: Continued

Peptidyl-prolyl cis-trans isomerase A (Cyclophilin A)	PPIA
Proteasome subunit alpha type-1	PSMA1
Proteasome subunit alpha type-2	PSMA2
Proteasome subunit alpha type-3	PSMA3
Proteasome subunit alpha type-4	PSMA4
Proteasome subunit beta type-1	PSMB1
Proteasome subunit beta type-2	PSMB2
Proteasome subunit beta type-3	PSMB3
Proteasome subunit beta type-4	PSMB4
Proteasome subunit beta type-5	PSMB5
Cyclin-dependent kinase 2	CDK2
Cyclin-dependent kinase inhibitor 1B	CDKN1B
Cyclin A1	CCNA1
Cyclin A2	CCNA2
Cyclin B1	CCNB1
Cyclin B2	CCNB2
Actin related protein 2/3 complex subunit 3	APRC3
Actin related protein 2/3 complex subunit 4 (20 kDa)	ARPC20
Ubiquitin-conjugating enzyme E2 variant 2	UBE2V2
Electron transfer flavoprotein, beta polypeptide	ETFB
Pyruvate dehydrogenase beta	PDHB

Appendix A2: Protein names and gene symbols used in the secretome network

Protein ID	Gene Name
Cathepsin D	CTSD
Cathepsin L1	CTSL1
Complement C3 precursor	C3
β-2 microglobulin	B2M
Cystatin-3	CST3
Glutamate receptor subunit 3A precursor	GRIN3A
Ran-specific GTPase-activating protein	RANBP1
GTP-binding nuclear protein Ran	RAN
Vesicular integral-membrane protein VIP36 precursor	LMAN2
Tubulointerstitial nephritis antigen-like precursor	TINAGL1
Collagen alpha-1(V) chain precursor	COL5A1
Cadherin-2 precursor	CDH2
Tissue inhibitor of metalloproteinases 2 (TIMP-2)	TIMP2
Tissue inhibitor of metalloproteinases 1 (TIMP-1)	TIMP1
Aldose reductase	AKR1B1
Proprotein convertase subtilisin/kexin type 9 precursor	PCSK9
Protein-L-isoaspartate O-methyltransferase	PCMT1
Renin receptor precursor (ATPase H(+)-transporting lysosomal accessory protein 2)	ATP6AP2
Moesin	MSN
Plasminogen activator inhibitor 1 precursor	SERPINE1
Karyopherin (Importin) beta 1	KPNB1
Regulator of chromosome condensation 1	RCC1
Exportin 1	XPO1
Ran binding protein 2	RANBP2
Ran GTPase activating protein 1	RANGAP1
SUMO1 pseudogene 3	SUMO
Ubiquitin-conjugating enzyme E2I	UBE2I
Axin 1	AXIN1
Glycogen synthase kinase 3 beta	GSK3B
Beta transducin repeat containing	BTRC
Transcription factor 7-like 2	TCF7L2
Catenin alpha 1	CTNNA1
Catenin beta 1	CTNNB1
Presenilin 1	PSEN1
Cadherin 1	CDH1
Lymphoid enhancer-binding factor 1	LEF1
CD8a molecule	CD8A
Matrix metalloproteinase 2	MMP2
Major histocompatibility complex , class I, A	HLA-A
Complement factor H	CFH

Appendix B: Concentration and purity of total RNA extracted from mock control and CHIKV-infected WRL-68 cell pellets for cell lysate and secretome qPCR analysis

Sample	RNA concentration (µg/ml)	A260:A280 ratio	A260:A230 ratio
Whole cell proteome			
Mock control #1	757	2.013	2.048
Mock control #2	797	1.841	2.278
Mock control #3	824	2.130	2.221
CHIKV-infected #1	546	1.881	2.065
CHIKV-infected #2	558	1.941	1.958
CHIKV-infected #3	301	1.802	2.198
Secretome			
Mock control #1	389	1.813	2.250
Mock control #2	354	1.811	2.351
Mock control #3	275	1.830	1.977
CHIKV-infected #1	274	1.850	3.054
CHIKV-infected #2	219	1.903	1.938
CHIKV-infected #3	285	1.801	1.835

Appendix C: Primer sequences and efficiency test results

Gene name	Primer sequences	Primer efficiency	
		Slope	Efficiency (%)
Endogenous control			
ACTB_F781	5'-CTCTTCCAGCCTTCCTTCCT-3'	-3.48	93.82
ACTB_R896	5'-AGCACTGTGTTGGCGTACAG-3'		
Primer pairs for selected whole cell proteome			
UBE2N_F258	5'- CGTCACAGGGGCTATTTGTT -3'	-3.38	97.81
UBE2N_R379	5'- CCTGTGGATCATCTGGCTCT -3'		
PSMA6_F100	5'- CAGGGTGGCCTTACATCAGT -3'	-3.40	97.00
PSMA6_R249	5'- CATTCCGGTCATCACACAAC -3'		
SET_F576	5'- GAAGAGGCAGCATGAGGAAC -3'	-3.27	102.24
SET_R720	5'- ATCATCCATATCGGGAACCA -3'		
GNB2L1_F509	5'- GGGACAAGCTGGTCAAGGTA -3'	-3.32	99.99
GNB2L1_R616	5'- GGGATCCATCTGGAGAGACA -3'		
CDK1_F123	5'- GGAAGGGGTTCCTAGTACTGC -3'	-3.39	97.32
CDK1_R223	5'- TGGAATCCTGCATAAGCACA -3'		
PDHA1_F473	5'- AGAACTTCTACGGGGGCAAT -3'	-3.34	99.38
PDHA1_R616	5'- CGAATATCTGGCCCTGGTTA -3'		
ENO1_F765	5'- CTCCGTGACCGAGTCTCTTC -3'	-3.47	94.05
ENO1_R908	5'- CCAGTCTTGATCTGCCCAGT -3'		
IDH1_F888	5'- TTGTCCAGATGGCAAGACAG -3'	-3.43	95.71
IDH1_R1036	5'- GCTTTGCTCTGTGGGCTAAC -3'		
PGAM1_F585	5'- GGCTATCATGGAGCTGAACC -3'	-3.33	99.84
PGAM1_R710	5'- TCTTCATCCCCCAGAAACTG -3'		
TPI1_F573	5'- ATGGCTGAAGTCCAACGTCT -3'	-3.51	92.69
TPI1_R695	5'- ACAAGGAAGCCATCCACATC -3'		
HMGCS1_F1290	5'- AGAGGACACCCATCATTTGG -3'	-3.35	98.94
HMGCS1_R1405	5'- GCCGAGCGTAAGTTCTTCTG -3'		
IDI1_F601	5'- TGGGGTGAACATGAAATTGA -3'	-3.40	96.68
IDI1_R744	5'- AATTTCACCACTGGCTGCTT -3'		
NAMPT_F1305	5'- GCCAGCAGGGAATTTTGTTA -3'	-3.41	96.51
NAMPT_R1404	5'- TGTCACCTTGCCATTCTTGA -3'		
ITPA_F166	5'- AAATGTCAGGAGGCAGTTCG -3'	-3.41	96.52
ITPA_R309	5'- GAGCTGGTGGAGACCTTCAG -3'		
APRT_F190	5'- CTAGACTCCCGAGGCTTCCT -3'	-3.56	91.00
APRT_R336	5'- AATCTCCAGCTCAGCCTTCC -3'		
ADSS_F722	5'- CCCTACATGGACCACCAAAG -3'	-3.36	98.55
ADSS_R868	5'- CATTTTGAGGTGGCATACCC -3'		

Appendix C: Continued

MTAP_F590 MTAP_R695	5'- CCACAGTTCCAGAGGTGGTT -3' 5'- GAAACTGCTTCCTCGTGCTC -3'	-3.42	95.99
PRPS1_F49 PRPS1_R154	5'- GACATGGCTGACACTTGTGG -3' 5'- GACCGGAGAAGATTCCATGA -3'	-3.45	94.87
PSAT1_F282 PSAT1_R387	5'- AGCAGGAAGGTGTGCTGACT -3' 5'- CCCAAGTTTAGGGTGAACGA -3'	-3.49	93.38
CBX3_F244 CBX_R346	5'-GCTGGCAAAGAAAAAGATGG -3' 5'-CTCTTGGTTTGTCAGCAGCA -3'	-3.24	103.38
PIR_F482 PIR_R621	5'- CCAAGGTTTACACTCGCACA -3' 5'- ATCATCGGGCCCAATATACA -3'	-3.49	93.62
EEF2_F612 EEF2_R796	5'- CCTCTATGCCAGTGTGCTGA -3' 5'- TCCTGTTCAAAACCCCGTAG -3'	-3.35	98.91
eIF3H_F104 eIF3H_R215	5'- CCGTGAAGCAAGTGCAGATA -3' 5'-ACAACCAGACCCAAAAGCAC -3'	-3.43	95.89
eI2B1_F117 eI2B1_R232	5'- GGAGACAATCCAGGGTCTGA -3' 5'- GACTGATGAAGCGGAGGAAG -3'	-3.38	97.81
HNRNPC_F95 HNRNPC_R218	5'- ATGTGGAGGCAATCTTTTCG -3' 5'- CTGCCATCCTCTCCTGCTAC -3'	-3.53	92.14
PCBP1_F96 PCBP1_R218	5'- AGGGGAGTCGGTTAAGAGGA -3' 5'- TCTTCCTCCAGCTTGTCGAT -3'	-3.54	91.77
SSB_F90 SSB_R235	5'- GCCACGGGACAAGTTTCTAA -3' 5'- GTTCTGCCTTGGATTTGCTC -3'	-3.38	97.68
KRT7_F508 KRT7_R623	5'- CAGGATGTGGTGGAGGACTT -3' 5'- TTGCTCATGTAGGCAGCATC -3'	-3.39	97.32
ARPC2_F108 ARPC2_R212	5'- AGATTTCGATGGGGTCCTCT -3' 5'- CCATGTGCCTGAAGTTCCTT -3'	-3.32	100.07
NPM1_F435 NPM1_R582	5'- TGGAGGTGGTAGCAAGGTTC-3' 5'- TTTCTTCACTGGCGCTTTTT -3'	-3.38	97.58
CPNE1_F1394 CPNE1_R1542	5'- GACCCCTGCATACACGTTCT -3' 5'- GGCCCTGAAGTATGAGACCA -3'	-3.35	98.91
GDI2_F965 GDI2_R1072	5'- GACCAGCTTTGGAGCTCTTG -3' 5'- TGCGGGAAATAAAGATCTGG -3'	-3.24	103.68
ETFA_F224 EFTA_R373	5'- AAGTTCTGGTGGCTCAGCAT -3' 5'- CTGCTACTCTGGGCAAAAGG -3'	-3.33	99.88
PPIA_F380 PPIA_R494	5'- TGGTGTTTGGCAAAGTGAAA -3' 5'- TCGAGTTGTCCACAGTCAGC -3'	-3.42	96.11
RCN1_F202 RCN1_R321	5'- GACTCCAAGACCTTCGACCA -3' 5'- CCAGGTTTTCAGCTCCTCAG -3'	-3.34	99.45
TXNDC17_F71 TXNDC17_R181	5'- GCAAGACCATTTTCGCCTAC -3' 5'- TAATGTGCTTCAGCCCCTCT -3'	-3.56	90.94

Appendix C: Continued

Primer pairs for selected secretome			
B2M_F25	5'- AGGCTATCCAGCGTACTCCA -3'	-3.44	95.37
B2M_R167	5'- TCAATGTCGGATGGATGAAA -3'		
CTSL1_F35	5'- TGGGAATTGCCTCAGCTACT -3'	-3.54	91.51
CTSL1_R161	5'- TTCTCCCACACTGCTCTCCT -3'		
CTSD_F883	5'- GACACAGGCACTTCCCTCAT -3'	-3.46	94.69
CSTD_R1031	5'- CCTCCCAGCTTCAGTGTGAT -3'		
C3_F2645	5'- ACCAGCAGACCGTAACCATC -3'	-3.53	92.11
C3_R2744	5'- GCAGCCTTGACTTCCACTTC -3'		
PCSK9_F143	5'- GACGATGCCTGCCTCTACTC -3'	-3.49	93.46
PCSK9_R250	5'- AAAGTTGGTCCCCAAAGTCC -3'		
COL5A1_F1258	5'- TACTACGACCCCACCAGCTC -3'	-3.42	96.03
COL5A1_R1372	5'- GTTCTCCCTTTTGGCCTTTC -3'		
TIMP1_F237	5'- TGACATCCGGTTCGTCTACA -3'	-3.58	90.14
TIMP1_R338	5'- TGCAGTTTTCCAGCAATGAG -3'		
TIMP2_F143	5'- AAGCGGTCAGTGAGAAGGAA -3'	-3.45	94.98
TIMP2_R250	5'- TCTCAGGCCCTTTGAACATC -3'		
CDH2_F1223	5'- AGGATCAACCCCATACACCA -3'	-3.49	93.33
CDH2_R1347	5'- TGGTTTGACCACGGTGACTA -3'		
CST3_F174	5'- CGAGTACAACAAAGCCAGCA -3'	-3.55	91.29
CST3_R307	5'- GGGTCTTGGTACACGTGGTT -3'		
PCMT1_F691	5'- TTAAAGCCCGGAGGAAGATT -3'	-3.58	90.44
PCMT1_R817	5'- GCACGTATATCACCCCCATC -3'		
RAN_F356	5'- TGTGTGGCAACAAAGTGGAT -3'	-3.40	96.72
RAN_R500	5'- TTCCTAGCAAGCCAGAGGAA -3'		
RANBP1_F183	5'- GAACGATCTCCCAGAATGGA -3'	-3.42	95.94
RANBP1_R305	5'- TGGTTGGCACAGATCTTCAG -3'		
SERPINE1_F733	5'- GACATCCTGGAACTGCCCTA -3'	-3.41	96.64
SERPINE1_R870	5'- GGTCATGTTGCCTTTCCAGT -3'		
ATP6AP2_F283	5'- TCGTACCCTTTGGAGAATGC -3'	-3.26	102.81
ATP6AP2_R385	5'- GAGCCAACTGCAAAACAACA -3'		

OPEN ACCESS Freely available online

PLOS ONE

Differential Proteome Analysis of Chikungunya Virus Infection on Host Cells

Christina Li-Ping Thio[1,4]*, Rohana Yusof[2,4], Puteri Shafinaz Akmar Abdul-Rahman[2,3], Saiful Anuar Karsani[1,3,4]*

1 Institute of Biological Sciences, Faculty of Science, University of Malaya, Kuala Lumpur, Malaysia, **2** Department of Molecular Medicine, Faculty of Medicine, University of Malaya, Kuala Lumpur, Malaysia, **3** Medical Biotechnology Laboratory, Faculty of Medicine, University of Malaya Centre for Proteomics Research (UMCPR), University of Malaya, Kuala Lumpur, Malaysia, **4** Drug Design and Development Research Group (DDDRG), University of Malaya, Kuala Lumpur, Malaysia

Abstract

Background: Chikungunya virus (CHIKV) is an emerging mosquito-borne alphavirus that has caused multiple unprecedented and re-emerging outbreaks in both tropical and temperate countries. Despite ongoing research efforts, the underlying factors involved in facilitating CHIKV replication during early infection remains ill-characterized. The present study serves to identify host proteins modulated in response to early CHIKV infection using a proteomics approach.

Methodology and Principal Findings: The whole cell proteome profiles of CHIKV-infected and mock control WRL-68 cells were compared and analyzed using two-dimensional gel electrophoresis (2-DGE). Fifty-three spots were found to be differentially modulated and 50 were successfully identified by MALDI-TOF/TOF. Eight were significantly up-regulated and 42 were down-regulated. The mRNA expressions of 15 genes were also found to correlate with the corresponding protein expression. STRING network analysis identified several biological processes to be affected, including mRNA processing, translation, energy production and cellular metabolism, ubiquitin-proteasome pathway (UPP) and cell cycle regulation.

Conclusion/Significance: This study constitutes a first attempt to investigate alteration of the host cellular proteome during early CHIKV infection. Our proteomics data showed that during early infection, CHIKV affected the expression of proteins that are involved in mRNA processing, host metabolic machinery, UPP, and cyclin-dependent kinase 1 (CDK1) regulation (in favour of virus survival, replication and transmission). While results from this study complement the proteomics results obtained from previous late host response studies, functional characterization of these proteins is warranted to reinforce our understanding of their roles during early CHIKV infection in humans.

Citation: Thio CL-P, Yusof R, Abdul-Rahman PSA, Karsani SA (2013) Differential Proteome Analysis of Chikungunya Virus Infection on Host Cells. PLoS ONE 8(4): e61444. doi:10.1371/journal.pone.0061444

Editor: Paul Digard, University of Edinburgh, United Kingdom

Received January 5, 2013; **Accepted** March 10, 2013; **Published** April 10, 2013

Funding: This work was supported by the Postgraduate Researh Fund (Grant no.: PV088/2012A) and the University Malaya Research Grant (Grant no.: RG013-09AFR). The funders had no role in study design, data collection and analysis, decision to publish, or preparation of the manuscript.

Competing Interests: The authors have declared that no competing interests exist.

* E-mail: christinathio86@gmail.com (CLPT); saiful72@um.edu.my (SAK)

Introduction

Chikungunya (CHIK) is a long-neglected disease that only recently began to garner attention from the scientific community following devastating outbreaks that struck India and the Indian Ocean Islands from 2004 to 2007. This disease causes substantial morbidity and an estimated death rate of 1:1,000 [1]. Despite being perceived as a tropical disease, recent CHIK cases and sporadic outbreaks were documented in temperate regions, suggesting that this infectious disease is no longer geographically restricted to tropical countries [2]. In Malaysia, three separate outbreaks have been reported over the past 15 years [3,4,5].

The causative agent for CHIK infection is the chikungunya virus (CHIKV), an alphavirus belonging to the family *Togaviridae* [6]. CHIKV is transmitted by the mosquito *Aedes aegypti* and *Aedes albopictus*. CHIKV can be genotypically classified into the East Central South African, West African and Asian genotypes [7]. Upon infection, CHIKV causes an acute illness characterized by the classical triad of symptoms of fever, rash and debilitating arthralgia which can persist for years. However, cases from recent outbreaks saw an increasing occurrence of atypical clinical manifestations such as neurological and cardiovascular complications [8]. As there is currently no effective vaccine or antiviral regimen to combat this disease, treatment is solely palliative. All things considered, it is not surprising that CHIK is now regarded as a potential health problem in need of a solution.

Recent research efforts have focused on understanding the viral tropism and mechanisms associated with the pathogenesis of CHIK infection. *In vitro* studies using a panel of mammalian cell lines showed rapid induction of cytopathic effects and cell death via apoptosis in most adherent cell lines with the exception of blood-derived cell lines [9]. Autophagic process and apoptosis were also recently shown to facilitate CHIKV dissemination [10,11]. At the molecular level, proteomics studies on CHIKV interaction with vector and mammalian host proteins have unravelled new clues in elucidating the mechanisms involved in viral replication and transmission from vector to host as well as disease progression in host cells [12,13,14]. Despite the extensive

research, much remains to be discovered to fully comprehend the pathogenesis of CHIKV.

Contrary to the aforementioned proteomics research which investigated the late host response to CHIKV infection [13], our present study aims to identify proteins altered during early infection in the host cells by means of 2-dimensional gel electrophoresis (2-DGE). The global proteome profile of CHIKV-infected WRL-68 cells was compared with uninfected mock control cells to single out differentially expressed spots for mass spectrometric (MS) identification with subsequent Western blot validation, as well as transcript expression analysis. Results showed widespread alteration of proteins involved in several biological processes known to play essential roles in virus replication. While this study provides new insights into CHIKV pathogenesis, functional characterization of these proteins will be required to better understand their roles during early infection.

Results

Cytopathogenicity of CHIKV

The cytopathic nature of CHIKV infection in mammalian cell lines, which was reported in several studies [9,15,16], was observed in WRL-68 cells infected with the virus at varying MOI (MOI of 0.5, 1.0, 5.0 and 10.0) and time-points (24 and 48 h). This isolate was found to induce cytopathic effects (CPE), characterized by cell shrinkage and detachment, within 48 h of infection, as depicted in Figure 1A. CPE induction was also determined to be MOI-dependent, as cells infected at higher MOI (MOI of 5.0 and 10.0) showed more profound CPE than that of cells infected at low MOI (MOI of 0.5 and 1.0), at 48 h post-infection (p.i.). On the contrary, no significant changes in morphology were observed at 24 h p.i. at the MOI of 0.5, 1.0 and 5.0, while mild CPE was observed at the MOI of 10.0. Mock control cells were cultured in parallel and served as negative control.

Optimization of the infection conditions for early infection study

As the aim of this study was to investigate alterations in the host cellular proteome during early CHIKV infection (i.e., the stages preceding cell death), the infection conditions (MOI and incubation time-point) were meticulously optimized to maximize infection while maintaining cell death at a minimum level. Relative quantification of percentages of infection and cell death of WRL-68 cells infected at various MOI (MOI of 0.5, 1.0, 5.0 and 10.0) for 24 and 48 h was determined by flow cytometric analysis.

The results showed that WRL-68 cells infected at the MOI of 5.0 for 24 h recorded significantly high percentage of infection at 74.77% (Figure 1B). Percentage of cell death (25.90%), albeit higher than mock control cells (14.33%), showed no significant differences when compared with cells infected at lower MOI (MOI of 0.1 and 0.5) at 24 h p.i. (Figure 1C). Furthermore, prolonging the incubation period significantly increased the percentage of cell death to more than 50%, irrespective of the MOI used. Immunostaining with anti-CHIK E2 mAb 3E4 revealed intense cytoplasmic staining in infected cells at the selected conditions, confirming infection, whereas no staining was apparent with the mock control cells (Figure 1D). Taken together, the MOI of 5.0 and 24 h incubation time-point were determined to be the optimal conditions for early CHIKV infection study.

2-DGE profiles of CHIKV infected WRL-68 cells

Comparative proteomics analysis between mock control and CHIKV-infected WRL-68 whole cell proteome was carried out using 2-DGE. Five biological replicates (n = 5) were analysed for each group. A typical gel profile for WRL-68 whole cell proteome is shown in Figure 2 (The representative proteome maps for mock control and CHIKV-infected WRL-68 cells are shown in Supplementary Figure S1). Image analysis using the ImageMaster^{TM} 2D Platinum v7.0 software detected more than 1300 spots in each gel. Comparison of the normalized percentage spot volume between both groups revealed 53 differentially expressed spots (Fold-change$>$1.3, $p<0.05$). Of these, 44 demonstrated reduced spot intensity whereas nine exhibited increased spot intensity. All 53 protein spots were manually excised for subsequent tryptic digestion and tandem MS identification.

Mass spectrometric identification of differentially expressed proteins

Of the 53 protein spots subjected to MALDI-TOF/TOF identification, 50 were successfully identified, corresponding to 45 proteins (Table 1). Unique peptides identified for each protein are listed in Supplementary Table S1. Three protein spots were not identified most likely due to low abundance, resulting in low confidence score. More than one spot was identified for four proteins; guanine nucleotide-binding protein subunit beta-2-like 1 (GNB2L1), Rab GDP dissociation inhibitor beta (GDI2), eukaryotic elongation factor-2 (EEF2) and triosephosphate isomerase (TPI1)). These spots are most likely different isoforms of the protein. Functional classification based on existing information from Swiss-Prot/TrEMBL database identified proteins involved in metabolism (42.22%) and transcription/translation (17.78%) to be mainly affected by CHIKV infection (Figure 3A), whereas classification based on sub-cellular localization showed that most altered proteins to be of cytoplasmic (56.90%) and nuclear origin (17.24%) (Figure 3B).

Protein network analysis

STRING network analysis of protein-protein interactions was performed to identify functionally linked proteins and determine the potential biological processes affected [17]. The network is presented under confidence view, whereby stronger associations are represented by thicker lines or edges and vice versa, whereas proteins are represented as nodes. Twenty additional interacting proteins were added to provide a more comprehensive view of the interactions. The protein names and gene symbols used in this network are listed in Supplementary Table S2. All gene symbols were derived from the HUGO Gene Nomenclature Committee (HGNC) (http://www.genenames.org). Figure 4 shows the interaction between 45 identified proteins and the additional interactors. Thirty seven proteins were found to be linked either directly or indirectly through one or more interacting proteins, suggesting the existence of reported functional linkages. Eight biological processes were determined to be significantly involved ($p<0.05$ based on false discovery rate (FDR) correction) in this network, including energy production, cell cycle regulation, gene expression, mRNA metabolism, protein metabolism and modification, DNA replication and ubiquitin-protein ligase activity (Table 2).

Immunoblot validation of proteomics data

Two proteins, CDK1 and PDHA1, representing the down- and up-regulated groups respectively, were randomly selected for Western blot validation. GAPDH was used as the loading control for PDHA1 as both PDHA1 and ACTB have similar molecular mass of ~43 kDa, and thus, cannot be stained together on the same blot. Immunoblots confirmed their down- and up-regulation,

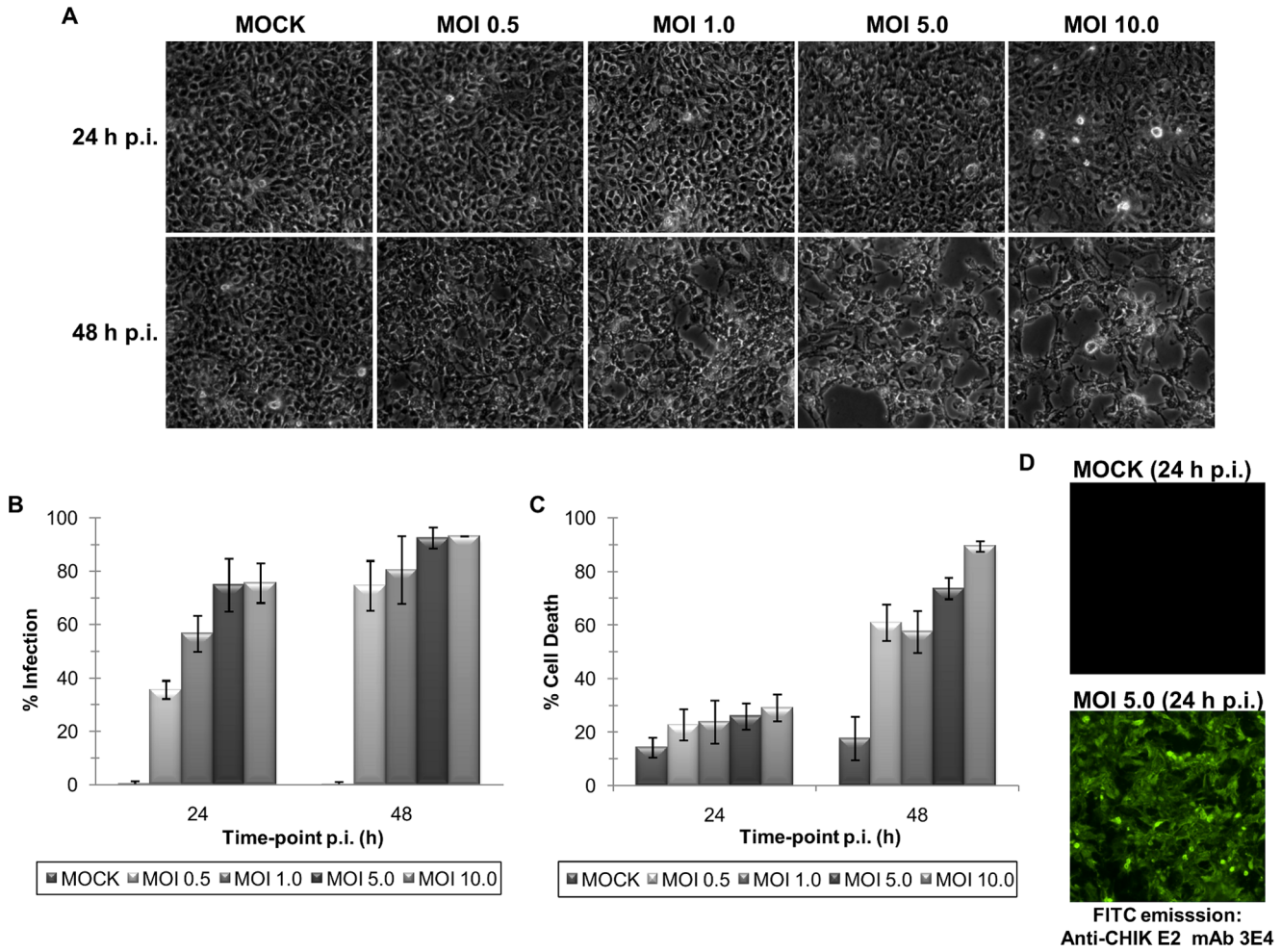

Figure 1. Optimization of the MOI and incubation time-point for early CHIKV infection study. (A) Morphological examination of WRL-68 cells infected at the MOI of 0.5, 1.0, 5.0 and 10.0 at 24 and 48 h incubation revealed a MOI and time-dependent induction of CPE by CHIKV. All images were captured at 100X magnification. (B) Flow cytometric quantification of percentage of cell death by AV/PI double staining of cells. Error bars indicate standard deviation of three biological replicates. (C) Flow cytometric quantification of percentage of infection by immunostaining of cells with anti-CHIK E2 mAB 3E4 (1:100 dilution). Error bars indicate standard deviation of three biological replicates. (D) Confirmation of infection via indirect immunofluorescence assay at the optimized MOI of 5.0 at 24 h p.i. Mock cells served as negative control. All images were captured at100X magnification.
doi:10.1371/journal.pone.0061444.g001

as shown in Figures 5A and 5B. Densitometric analysis revealed fold differences of −1.42 and 1.72 CDK1 and PDHA1 respectively (Figures 5C and 5D), which was comparable to the observed −1.77 and 1.96 fold-changes in 2-DGE analysis.

Transcript expression analysis of selected altered proteins

The transcript expression of 36 selected proteins was evaluated using real-time qPCR (The gene names and primer sequences are listed in Supplementary Table S3). All primers had amplification efficiencies within the acceptable range of 90 to 110% (Slope values between −3.1 to −3.6). It is a known fact that mRNA expression do not always correlate with protein expression [18]. In our study however, the direction of mRNA and protein expression changes of 15 proteins including CDK1 and PDHA1 were the same (Table 3). On the other hand, the transcript expression of four other proteins; adenine phosphoribosyltransferase (APRT), electron transport flavoprotein subunit alpha (ETFA), actin-related protein 2/3 complex subunit 2 (ARPC2) and cyclophilin A (PPIA), showed the opposite direction of expression change despite being statistically significant. Meanwhile, the mRNA expression levels of 17 other proteins showed no statistically significant differences.

Discussion

It is well-established that CHIKV induces rapid and profound CPE in human host cells which culminate in cell death via apoptosis. The events preceding the inevitable cell demise, however, remain ill-characterized. A previous proteomic study on new-born mice focused on investigating the dynamic overview of altered protein expression during late stages of CHIKV infection, whereby alterations of stress, inflammation, urea cycle, energy metabolism and apoptotic-related proteins were implicated in the observed disease pathogenesis [13]. In this study, we shifted the focus to examining global changes of the host cell proteome during early CHIKV infection, with aims of identifying key proteins that are potentially involved in facilitating CHIKV replication. It has been reported that during early infection, viral replication and dissemination occurs rapidly through manipula-

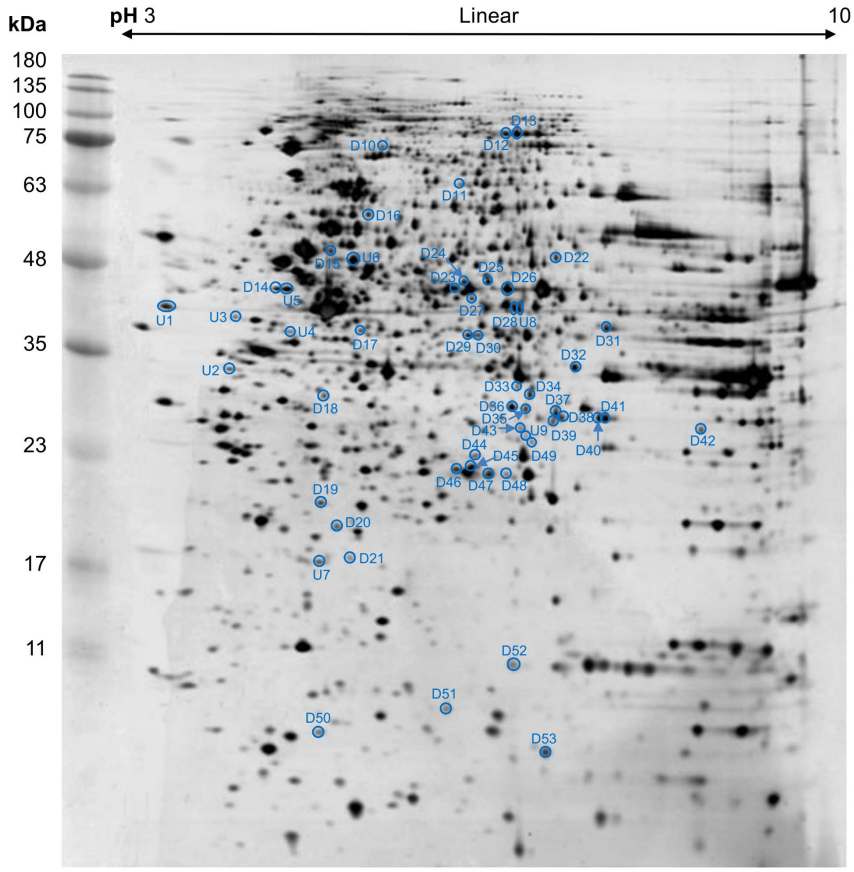

Figure 2. Reference map of the whole cell proteome of WRL-68 cells. Forty μg of protein sample were focused on 13 cm, pH 3–10 linear IPG drystrips, followed by second dimension SDS-PAGE separation on 12.5% polyacrylamide gel which was silver stained. Five biological replicates (n = 5) for each group (Mock control and CHIKV-infected) were analyzed using ImageMaster™ 2D Platinum v7.0 software. Fifty-three spots were determined to be differentially expressed (Fold-change >1.3, $p<0.05$). The position of each spot is indicated by circles on the proteome map. The uppercase 'U' and 'D' denote up-regulated and down-regulated spots, respectively.
doi:10.1371/journal.pone.0061444.g002

tion of the host cell machinery owing to the simplicity of the viral makeup [19]. By collating data from proteomics and bioinformatics analyses, we inferred the potential manipulation or subversion of various important cellular processes including mRNA and protein metabolism, energy production, ubiquitin-proteasome pathway (UPP) and cell cycle regulation by CHIKV.

Alteration of proteins involved in mRNA processing and translation machinery

Virus hijacking of the host mRNA processing and translational machinery is an essential process for virus replication. Viruses with positive sense RNA in particular, have been shown to recruit components of the host protein biosynthesis machineries for viral RNA and protein synthesis [20]. In the current study, we identified several deregulated proteins involved in mRNA processing and translation, including heterogeneous nuclear ribonucleoproteins C1/C2 (hnRNP C1/C2), poly(rC)-binding protein 1 (hnRNP E1), elongation factor- 2 (EEF-2), translation initiation factor EIF-2B subunit alpha (eIF2B1) and eukaryotic translation initiation factor 3 subunit H (eIF3H).

Heterogeneous ribonucleoproteins (hnRNPs) are complexes of RNA and proteins involved in an array of cellular functions such as transcription, pre-mRNA processing and cytoplasmic mRNA translation and turnover [21]. In our study, hnRNP C1/C2 was found to be up-regulated by 3.10 fold while hnRNP E1 was down-regulated by 1.42 fold. Transcript level of hnRNP E1 mRNA showed similar down-regulation while the mRNA expression of hnRNP C1/C2 was not significantly altered, suggesting that post-transcriptional and post-translational modification may play a role in modulating the expression of the latter protein. In a previous study, hnRNP C1/C2 was shown to promote dengue virus survival in host cells [22] while hnRNP E1 inhibits vesicular somatitis virus replication [23]. Ergo, the up-regulation of hnRNP C1/C2 in the present study may signify its recruitment by CHIKV whereas hnRNP E1 may possibly exert negative effects towards CHIKV propagation which is counteracted by its inhibition.

Translation factors are known to play crucial roles in viral RNA and protein synthesis and different viruses exert different mechanisms to modulate host translational proteins to their benefit, as shown in several studies [24,25,26]. Alphaviruses have been shown to induce global shutoff of protein synthesis by inhibiting or modifying host translational factors [27]. CHIKV-induced host translational shutoff was recently shown to occur, through an unidentified protein kinase R (PKR)-independent mechanism [28]. In this study, down-regulation of proteins involved in initiation of translation (eIF2B1 and eIF3SH) and elongation of the newly synthesised polypeptide chain (EEF-2) was observed, although at the transcript level, only EEF-2 and eIF2B1 genes were down-regulated. The exact roles of these proteins in host translational shutoff, however, cannot be ascertained at this

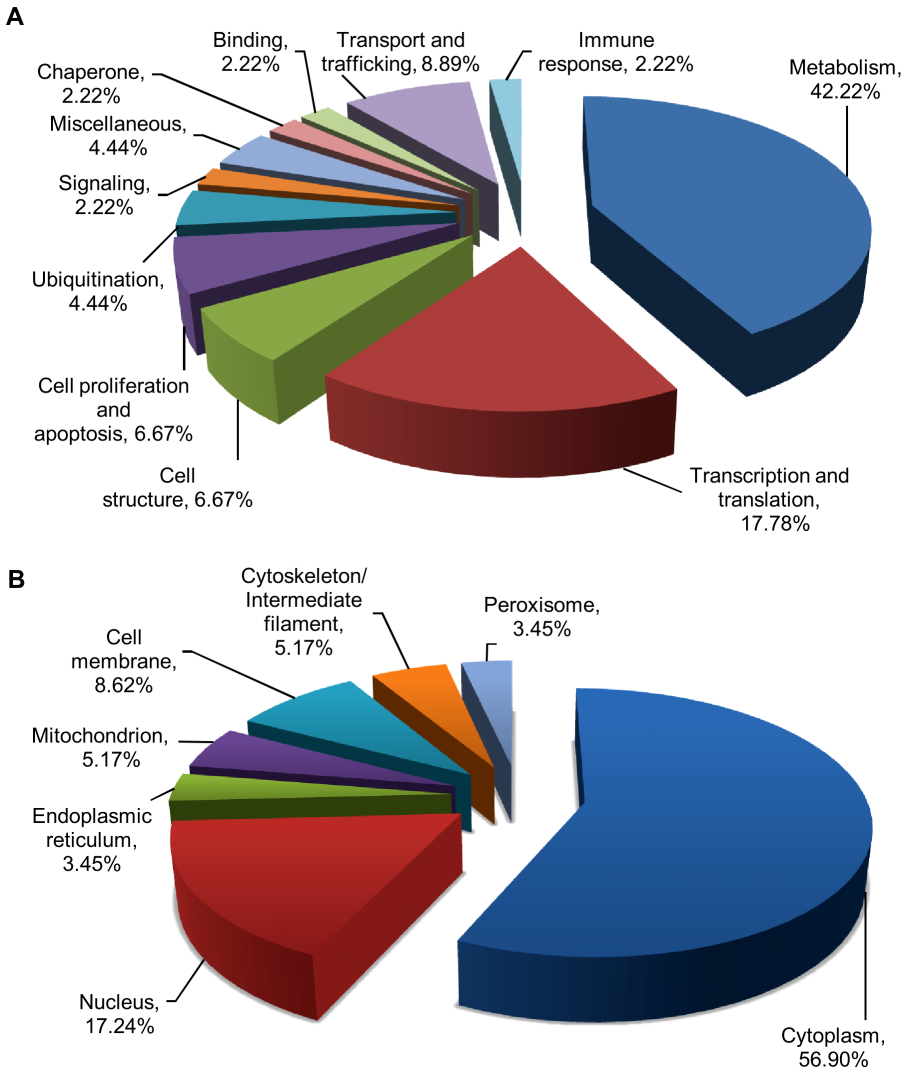

Figure 3. Functional classification and sub-cellular distribution of differentially expressed whole cell proteins during early CHIKV infection. (A) Functional categorization and (B) Sub-cellular localization of differentially modulated proteins were determined based on Swiss-Prot/TrEMBL database search.
doi:10.1371/journal.pone.0061444.g003

point. Nonetheless, down-regulation of these proteins may inhibit the host translational machinery to a certain extent, possibly contributing to the observed down-regulation of most altered proteins in this study.

Differential expression of proteins involved in cellular energy production and metabolism

Of the 19 regulated proteins identified to be involved in cellular metabolism, 18 were down-regulated. Only PDHA1, a subunit of the pyruvate dehydrogenase complex involved in transforming pyruvate to acetyl-CoA in the tricarboxylic acid (TCA) cycle [29], was up-regulated by 1.96 fold. Up-regulation of this protein was further confirmed by immunoblot (Figures 5B and 5D). Transcript expression study on 14 selected genes revealed that 8 genes; PHDA1, alpha-enolase (ENO1), isocitrate dehydrogenase (IDH1), isopentyl-diphosphate Delta-isomerase 1 (IDI1), adenylosuccinate synthetase isozyme 2 (ADSS), ribose-phosphate pyrophosphokinase 1 (PRPS1), S-methyl-5-thioadenosine phosphorylase (MTAP) and phosphoserine aminotransferase (PSAT1), had expression changes of the same directionality as the protein expression (Table 1).

Based on the proteomics analysis, energy production in WRL-68 cells was expected to be significantly affected through reduced expression of glycolytic enzymes including ENO1, TPI1 and phosphoglycerate mutase 1 (PGAM1), as well as down-regulation of IDH1 which catalyzes the oxidative decarboxylation of isocitrate to alpha-ketoglutarate in the TCA cycle [30]. Four proteins associated with the adenine salvage pathway, namely PRPS1, ADSS, MTAP and adenine phosphoribosyltransferase (APRT), were also down-regulated. Similar dysregulation was observed with IDI1 and hydroxymethylglutaryl-CoA synthase (HMGCS1), two key enzymes involved in the biosynthesis of cholesterol, coenzyme Q and isoprenylated proteins through the mevalonate pathway [31].

Effects on proteins involved in the UPP

UPP is an essential intracellular system for protein degradation, with multiple cellular functions including cell cycle regulation, apoptosis, DNA repair, signal transduction and transcriptional

Table 1. List of differentially altered proteins in WLR-68 cells in response to CHIKV infection.

Spot no.	Protein name	Swiss-Prot accession number	MOWSE score/ Sequence Coverage (%)	pI/MW[a] (kDa)	Mock control (Mean ± SD)[b]	CHIKV-infected (Mean ± SD)[b]	Fold-change[c] (*p*-value)	Peptides matched
U1	Protein SET	Q01105	303 (38)	4.23/33,469	0.0953±0.0250	0.1363±0.0174	1.43 (0.0165)	9
U2	Nucleophosmin (B23)	P06748	100 (22)	4.64/32,555	0.0307±0.0061	0.0426±0.0053	1.38 (0.0113)	4
U3	Reticulocalbin-1	Q15293	299 (30)	4.86/38,866	0.0226±0.0020	0.0319±0.0047	1.41 (0.0038)	9
U4	Heterogeneous nuclear ribonucleoproteins C1/C2	P07910	278 (27)	4.95/33,650	0.0292±0.0186	0.0905±0.0225	3.10 (0.0028)	9
U5	Keratin, type I cytoskeletal 17	Q04695	760 (47)	4.97/48,076	0.1510±0.0178	0.2054±0.0247	1.36 (0.0040)	20
U6	Keratin, type II cytoskeletal 7	P08729	751 (52)	5.50/51,386	0.2186±0.0191	0.3065±0.0551	1.40 (0.0098)	22
U7	Chromobox protein homolog 3	Q13185	88 (27)	5.23/20,798	0.0360±0.0070	0.0501±0.0087	1.39 (0.0222)	4
U8	Pyruvate dehydrogenase E1 component subunit alpha, mitochondrial	P08559	126 (19)	8.35/43,268	0.0395±0.0198	0.0773±0.0234	1.96 (0.0249)	7
D10	Spartin	Q8N0X7	80 (7)	5.66/72,788	0.0256±0.0073	0.0154±0.0053	–1.67 (0.0346)	4
D11	Phosphoglucomutase-2	Q96G03	197 (26)	6.28/68,240	0.0269±0.0079	0.0118±0.0035	–2.29 (0.0044)	13
D12	Elongation factor-2	P13639	497 (37)	6.42/95,277	0.1986±0.0170	0.1470±0.0450	–1.35 (0.0430)	27
D13	Elongation factor-2	P13639	338 (20)	6.42/95,277	0.1261±0.0239	0.0774±0.0303	–1.63 (0.0224)	11
D14	Gamma-enolase	P09104	215 (36)	4.91/47,239	0.0873±0.0115	0.0592±0.0105	–1.47 (0.0037)	13
D15	Hydroxymethylglutaryl-CoA synthase, cytoplasmic	Q01581	62 (17)	5.22/57,257	0.0655±0.0143	0.0405±0.0037	–1.62 (0.0053)	8
D16	Copine-1	Q99829	147 (4)	5.52/59,022	0.0436±0.0154	0.0249±0.0038	–1.75 (0.0299)	3
D18	Spermidine synthase	P19623	228 (23)	5.30/33,803	0.0390±0.0067	0.0290±0.0059	–1.35 (0.0360)	6
D19	Ubiquitin-conjugating enzyme E2 N	P61088	215 (39)	5.33/22,393	0.0420±00028	0.0290±0.0038	–1.45 (0.0003)	6
D20	Inosine triphosphate pyrophosphatase	Q9BY32	97 (27)	5.50/21,432	0.0391±0.0034	0.0296±0.0057	–1.32 (0.0121)	3
D21	Adenine phosphoribosyltransferase	P07741	239 (57)	5.78/19,595	0.0214±0.0054	0.0141±0.0036	–1.52 (0.0355)	7
D22	Nicotinamide phosphoribosyltransferase	P43490	164 (15)	6.69/55,487	0.0527±0.0085	0.0365±0.0069	–1.44 (0.0106)	8
D23	Rab GDP dissociation inhibitor beta	P50395	441 (42)	6.11/50,631	0.0894±0.0156	0.0382±0.0226	–2.34 (0.0032)	14
D24	Rab GDP dissociation inhibitor beta	P50395	132 (34)	6.11/50,631	0.0575±0.0136	0.0381±0.0105	–1.51 (0.0363)	11
D25	La ribonucleoprotein	P05455	101 (23)	6.68/46,808	0.0886±0.0226	0.0128±0.0531	–1.67 (0.0159)	10
D26	Alpha-enolase	P06733	113 (28)	7.01/47,139	0.2530±0.0202	0.1909±0.0269	–1.32 (0.0033)	9
D27	Adenylosuccinate synthetase isozyme 2	P30520	486 (46)	6.13/50,066	0.0503±0.0163	0.0223±0.0120	–2.25 (0.0148)	16
D28	Isocitrate dehydrogenase, cytoplasmic	O75874	176 (24)	6.53/46,630	0.1428±0.0320	0.0910±0.0199	–1.57 (0.0152)	10
D29	Eukaryotic translation initiation factor 3 subunit H	O15372	96 (11)	6.09/39,905	0.0702±0.0155	0.0444±0.0152	–1.58 (0.0286)	4
D30	Poly(rC)-binding protein1 (hnRNP E1)	Q15365	116 (29)	6.66/37,474	0.0698±0.0094	0.0492±0.0163	–1.42 (0.0393)	7
D31	Phosphoserine aminotransferase	Q9Y617	81 (14)	7.56/40,397	0.0956±0.0262	0.0553±0.0150	–1.73 (0.0176)	5
D32	Aldo-keto reductase family 1 member C2	P52895	250 (40)	7.13/36,712	0.0873±0.0164	0.0541±0.0176	–1.62 (0.0148)	9
D33	Pirin	O00625	107 (33)	6.42/32,093	0.0198±0.0028	0.0126±0.0119	–1.57 (0.0052)	8
D34	Ribose-phosphate pyrophosphokinase1	P60891	104 (38)	6.51/34,812	0.0668±0.0072	0.0504±0.0027	–1.33 (0.0014)	9

Table 1. Cont.

Spot no.	Protein name	Swiss-Prot accession number	MOWSE score/ Sequence Coverage (%)	pI/MW[a] (kDa)	Mock control (Mean ± SD)[b]	CHIKV-infected (Mean ± SD)[b]	Fold-change[c] (*p*-value)	Peptides matched
D35	Glucosamine-6-phosphate isomerase 1	P46926	95 (27)	6.42/32,648	0.0652±0.0141	0.0455±0.0082	–1.43 (0.0273)	7
D36	S-formylglutathione hydrolase	P10768	68 (31)	6.54/31,442	0.1085±0.0110	0.0737±0.0158	–1.47 (0.0037)	7
D37	Actin-related protein 2/3 complex subunit 2 (p34-ARC)	O15144	192 (42)	6.84/34,311	0.1003±0.0138	0.0710±0.0118	–1.41 (0.0069)	12
D38	Electron transfer flavoprotein subunit alpha, mitochondrial	P13804	129 (22)	8.62/35,058	0.0639±0.0130	0.0450±0.0124	–1.42 (0.0467)	5
D39	Guanine nucleotide-binding protein subunit beta-2-like 1	P63244	64 (18)	7.60/35,055	0.0417±0.0078	0.0162±0.0032	–2.58 (0.0016)	5
D40	Guanine nucleotide-binding protein subunit beta-2-like 1	P63244	400 (58)	7.60/35,055	0.1428±0.0483	0.0758±0.0361	–1.88 (0.0379)	15
D41	Guanine nucleotide-binding protein subunit beta-2-like 1	P63244	606 (67)	7.60/35,055	0.1226±0.0117	0.0871±0.0182	–1.40 (0.0064)	16
D42	Cyclin-dependent kinase 1	P06493	335 (58)	8.37/34,047	0.0426±0.0112	0.0240±0.0054	–1.77 (0.0102)	13
D43	Translation initiation factor eIF-2B subunit alpha	Q14232	94 (34)	6.90/33,691	0.0375±0.0071	0.0243±0.0047	–1.54 (0.0084)	8
D44	Phosphoglycerate mutase 1	P18669	197 (26)	6.28/68,240	0.0450±0.0043	0.0327±0.0084	–1.37 (0.0197)	8
D45	Proteasome subunit alpha type-6	P60900	215 (50)	6.34/27,382	0.0964±0.0120	0.0635±0.0173	–1.52 (0.0081)	10
D46	Isopentyl-diphosphate Delta-isomerase 1	Q13907	129 (14)	5.93/26,302	0.0643±0.0075	0.0395±0.0077	–1.63 (0.0008)	2
D47	Triosephosphate isomerase	P60174	141 (55)	6.45/26,653	0.1147±0.0132	0.0778±0.0089	–1.81 (0.0008)	10
D48	Triosephosphate isomerase	P60174	129 (33)	6.45/26,653	0.0416±0.0106	0.0230±0.0032	–1.47 (0.0055)	5
D49	S-methyl-5-thioadenosine phosphorylase	Q13126	303 (53)	6.75/31,230	0.0261±0.0049	0.0182±0.0053	–1.44 (0.0396)	11
D50	Thioredoxin-like protein 5	Q9BRA2	103 (22)	5.40/13,932	0.0366±0.0036	0.0268±0.0067	–1.37 (0.0203)	2
D51	Fatty-acid binding protein, epidermal	Q01469	100 (52)	6.60/15,155	0.0389±0.0081	0.0268±0.0021	–1.46 (0.0117)	7
D52	Peptidyl-prolyl cis-trans isomerase A (Cyclophilin A)	P62937	158 (41)	7.68/18,001	0.0543±0.0035	0.0399±0.0066	–1.36 (0.0025)	8

[a]MW and pI refer to the molecular weight and isoelectric point of the protein.
[b]The mean % spot volume (n = 5) was used for the analysis of fold difference between mock control and CHIKV-infected protein spots. SD represents standard deviation of five biological replicates.
[c]Positive fold-change values represent up-regulation whereas negative fold-change values signify down-regulation of identified proteins.
doi:10.1371/journal.pone.0061444.t001

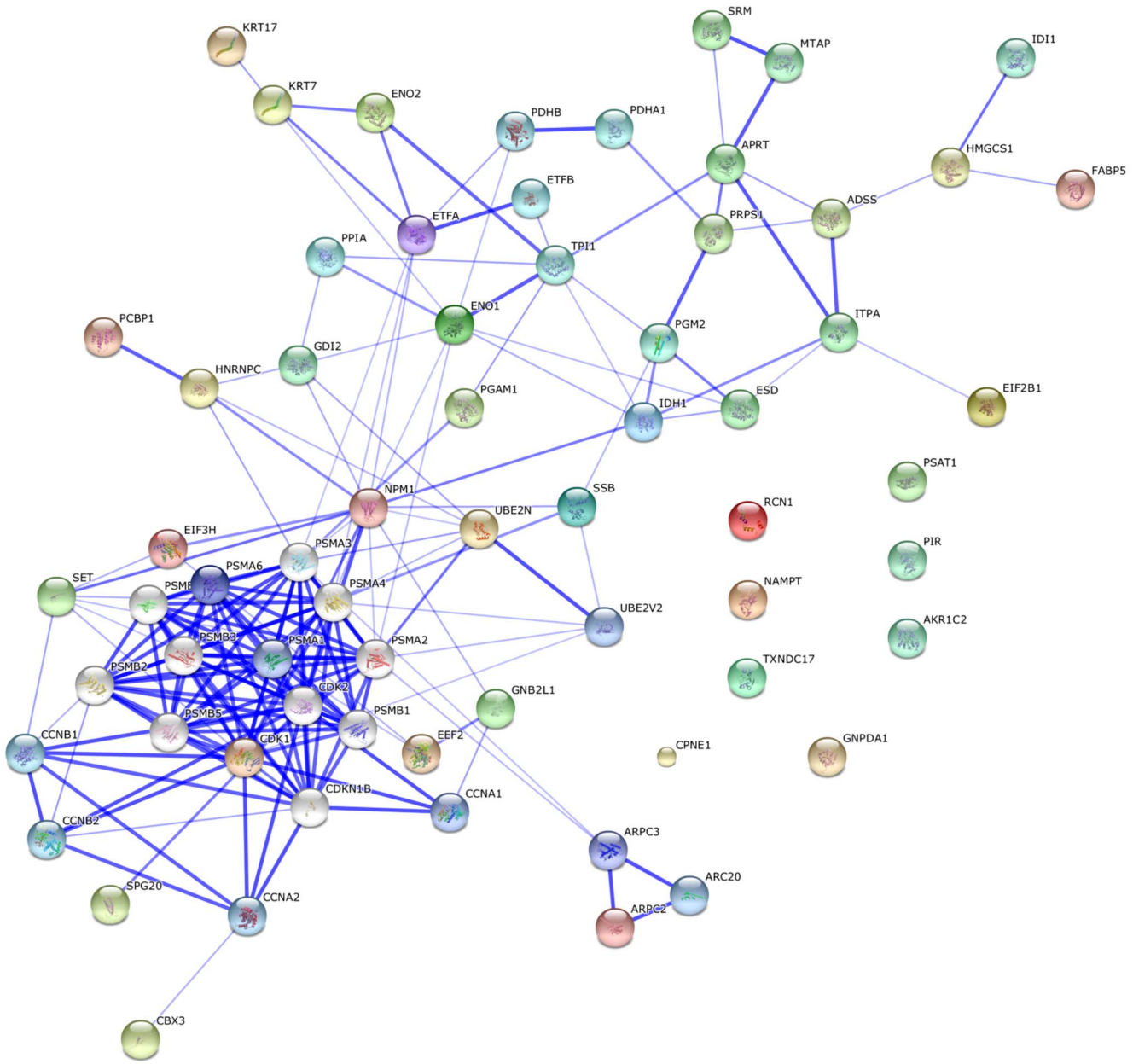

Figure 4. STRING interaction network showing association between differentially expressed proteins. Interaction map was generated using default settings (Medium confidence of 0.4 and 7 criteria for linkage: neighbourhood, gene fusion, co-occurrence, co-expression, experimental evidences, existing databases and text mining). Twenty additional interplay proteins were also added to each network. The protein names and gene symbols used in this network are listed in Supplementary Table S2.
doi:10.1371/journal.pone.0061444.g004

regulation [32]. Many viruses have been reported to evolve different strategies to utilize the UPP for various purposes, including avoidance of host immune surveillance, viral maturation, viral progeny release and transcriptional regulation [33,34,35]. Our proteomics data showed down-regulation of two UPP associated proteins; ubiquitin-conjugating enzyme E2 N (UBE2N) and proteasome subunit alpha type-6 (PSMA6). At the transcript level however, only UBE2N showed the same direction of expression change as the protein expression. UBE2N is a ubiquitin-carrier enzyme which carries and binds ubiquitin to the ubiquitin-ligase enzyme for subsequent ubiquitination of targeted proteins. PSMA6 is the subunit of the 20S proteasome subcomplex which forms the multicatalytic 26S proteasome that degrades polyubiquitinated proteins into smaller peptides [32].

Down-regulation of proteins involved in cell cycle regulation

Cyclin-dependent kinases (CDKs) are a family of cyclin-activated serine/threonine kinases involved in various cellular processes including regulation of cell cycle (CDK1, 2, 3, 4, 6 and 7), neuronal functions (CDK5) and transcription (CDK7, 8 and 9) [36]. While CDKs are commonly associated with nuclear replication of DNA and RNA viruses, several studies have expanded the role of CDKs to cytoplasmic replication of RNA

Table 2. GO enrichment analysis of the biological processes involved in the STRING protein network.

GO Biological process	*p*-value[a]
Regulation of ubiquitin-protein ligase activity	4.34×10^{-14}
Gene expression	1.14×10^{-6}
mRNA metabolic process	8.06×10^{-6}
Protein modification	1.75×10^{-5}
Regulation of cell cycle	1.63×10^{-5}
Protein metabolic process	1.02×10^{-5}
Generation of energy and precursor metabolite	1.35×10^{-2}
DNA replication	5.05×10^{-2}

[a]The significance of the GO biological process derived from the cytosolic protein network was determined by FDR correction ($p<0.05$).
doi:10.1371/journal.pone.0061444.t002

viruses as well [37,38]. In this study, CDK1 was found to be down-regulated, both at the protein and gene expression level. CDK1 is activated by cyclin B and functions in allowing entry into mitosis from the G2 phase [39]. Inhibition of this protein would cause cell cycle arrest at G2 phase. Meanwhile, SET protein is a phosphoprotein found to regulate the cell cycle by inhibiting cyclin B-CDK1 activity [40]. In our study, SET protein was found to be up-regulated at both the protein and transcript levels, which favours the inhibition of cyclin B-CDK1 activity.

In conclusion, our proteomics data suggested that during early infection, CHIKV affects the expression of proteins involved in mRNA processing, host metabolic machinery, UPP, and cyclin-dependent kinase 1 (CDK1) regulation (in favour of virus survival, replication and transmission). While results from this study complement the proteomics results obtained from previous late host response studies, functional characterization of these proteins is warranted to reinforce our understanding of their roles during early CHIKV infection in humans.

Materials and Methods

Cell lines

WRL-68 human hepatic cells, a HeLa derivative cell line that is highly susceptible to CHIKV infection (ATCC Cat No. CL-48), Vero cells (ATCC Cat. No. CCL-81), and C6/36 *Aedes albopictus* cells (ATCC Cat. No. CRL-1660) were used in this study. WRL-68 and Vero cells were cultured in DMEM medium (GIBCO, Grand Island, NY) supplemented with 10% heat-inactivated fetal bovine serum (FBS) (GIBCO, Grand Island, NY) at 37 °C. C6/36 cells were grown in L-15 medium (Sigma Aldrich, St Louis, MO)

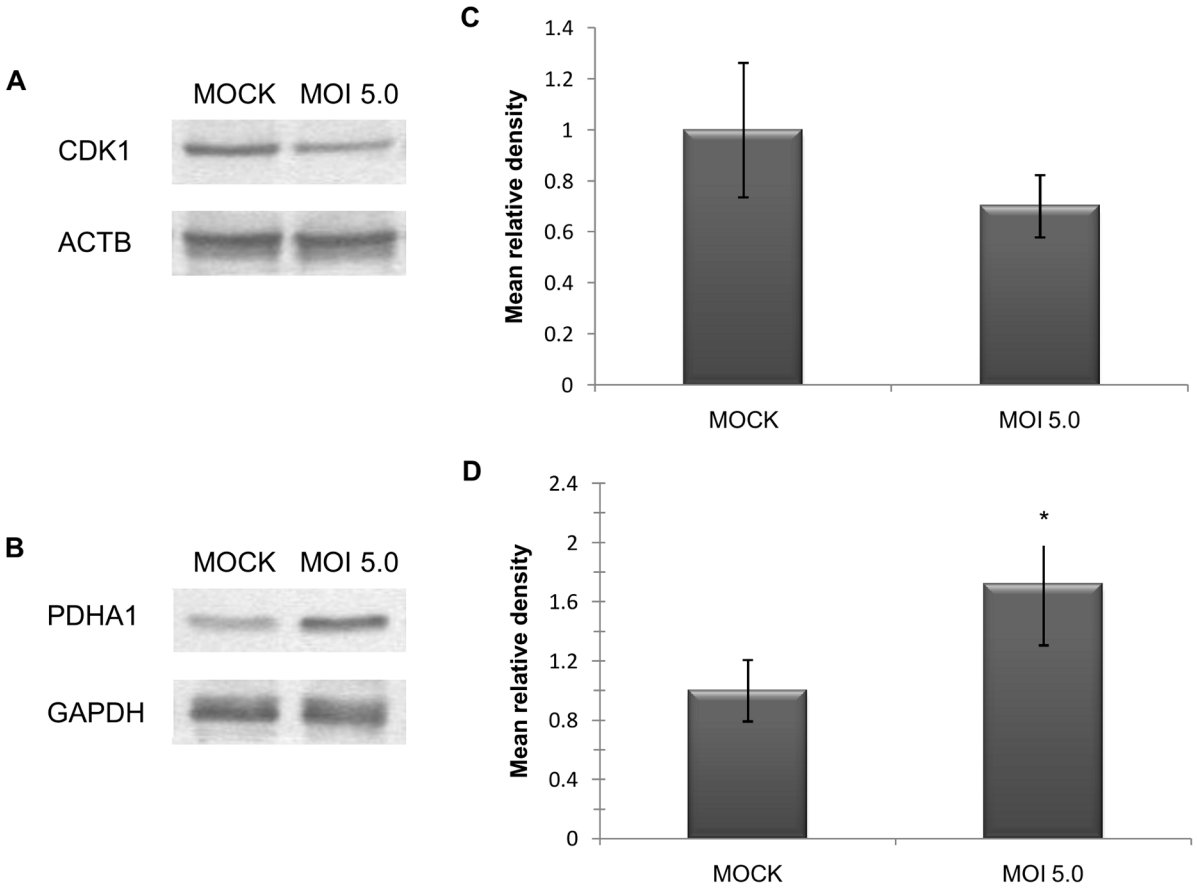

Figure 5. Western blot validation and densitometric analysis of CDK1 and PDHA1 proteins. Confirmation of the expression profiles for CDK1 (A) and PDHA1 (B) was performed via immunoblot analysis. Densitometric analysis of the mean relative intensity (n = 3) for each target protein showed down-regulation of CDK1 by 1.42 fold (C) and up-regulation of PDHA1 by 1.72 fold (D). The intensity for CDK1 and PDHA1 was normalized against ACTB and GAPDH, respectively. Error bars indicate standard deviation of three biological replicates. * indicates significant difference in expression ($p<0.05$).
doi:10.1371/journal.pone.0061444.g005

Table 3. Comparison of real-time qPCR and proteomics results for selected genes.

Gene symbol	mRNA fold-change	Protein fold-change
UBE2N	**−1.33**	**−1.45**
PSMA6	NSD	−1.52
SET	**1.41**	**1.43**
GNB2L1	NSD	−2.58, −1.88, −1.40**
CDK1	**−1.38**	**−1.77**
PDHA1	**1.30**	**1.96**
ENO1	**−1.32**	**−1.32**
IDH1	**−1.14**	**−1.57**
PGAM1	NSD	−1.37
TPI1	NSD	−1.81, −1.47**
HMGCS1	NSD	−1.62
IDI1	**−1.48**	**−1.63**
NAMPT	NSD	−1.44
ITPA	NSD	−1.32
APRT	1.33	−1.52
ADSS	**−1.36**	**−2.25**
PRPS1	**−1.27**	**−1.33**
MTAP	**−1.26**	**−1.44**
PSAT1	**−1.62**	**−1.73**
CBX3	NSD	1.39
PIR	**−1.25**	**−1.57**
EEF2	**−1.12**	**−1.63, −1.35****
EIF3H	NSD	−1.58
EIF2B1	**−1.25**	**−1.54**
HNRNPC	NSD	3.1
PCBP1	**−1.82**	**−1.42**
SSB	NSD	−1.67
KRT7	NSD	1.4
ARPC2	1.24	−1.41
NPM1	NSD	1.38
CPNE1	NSD	−1.75
GDI2	NSD	−2.34, −1.51**
ETFA	1.34	−1.42
PPIA	1.14	−1.36
RCN1	NSD	1.41
TXNDC17	NSD	−1.37

*__Bold__ indicates RNA expression changes which are in concordance with protein expression changes in terms of directionality, and are determined to be statistically significant ($p<0.05$); NSD indicates no significant differences in the RNA expression.

**More than one protein spot was identified.

doi:10.1371/journal.pone.0061444.t003

supplemented with 10% tryptose phosphate broth (TPB) (Sigma Aldrich, St Louis, MO) and 10% FBS at 28 °C.

Antibodies

The antibodies used for indirect immunofluorescence assay (IIFA) and immunostaining by flow cytometry were anti-CHIK E2 monoclonal antibody (mAb) 3E4 (a kind gift from Dr. Philippe Desprès from the Pasteur Institute of France) and FITC-conjugated goat anti-mouse IgG secondary antibody (Novus Biologicals, Littleton, CO). The primary antibodies used for Western blot validation were mouse mAb to beta-actin (ACTB), cyclin-dependent kinase 1 (CDK1), glyceraldehyde 3-phosphate dehydrogenase (GAPDH) or pyruvate dehydrogenase (PDHA1). Horseradish peroxidise (HRP)-conjugated goat anti-mouse IgG was used as the secondary antibody. All antibodies used for validation were purchased from Santa Cruz Biotechnology, Santa Cruz, CA.

Virus stock propagation and titration

CHIK/06/08 clinical isolate of the ECSA genotype was propagated twice in C6/36 cell line and virus stock was harvested from the culture supernatant and stored at −80 °C. Mock control cells were cultured in parallel but without virus infection and processed in the same manner. Virus titer was determined by standard plaque assay procedure on Vero cells. Titers were expressed as plaque-forming units (PFU)/ml.

Infection of WRL-68 cells with CHIKV

WRL-68 cells were infected with CHIKV at the MOI of 0.5, 1.0, 5.0 and 10.0 for 2 h at 37 °C. Mock control cells were incubated in parallel with culture supernatant of mock control C6/36 cells. Viral inoculum was subsequently removed and the cells were further incubated in DMEM maintenance medium containing 2% FBS for 24 and 48 h. The optimal MOI and time-point for early infection study were selected based on flow cytometric quantitative analysis of percentage of cell infection and cell death [24].

IIFA

Prior to flow cytometric quantification, CHIKV infection in WRL-68 cells was confirmed by IIFA, as previously described [41] with modifications. WRL-68 cells were seeded overnight at a density of 1.5×10^5 cells/well in a 24-well culture dish, and subsequently infected at various MOI. Mock control cells were cultured in parallel. After 24 and 48 h incubation, the cells were fixed with 3.7% formaldehyde in phosphate buffered saline (PBS) for 20 min, washed with PBS and permeabilized with 0.15 M glycine for 10 min. Permeabilized cells were washed extensively and further incubated with anti-CHIK E2 mAb 3E4 (1:100 dilution) for 30 min at 37 °C. Thereafter, the cells were washed with PBS and incubated in FITC-conjugated secondary antibody (1:1000 dilution) for 30 min at 37 °C. The cells were observed under an inverted microscope (Nikon Eclipse Ti-5, Japan) and fluorescent pictures were acquired using NIS-Elements imaging software (Nikon, Japan).

Flow cytometric quantification of percentage CHIKV infection and cell death

Quantification of percentage infection was carried out as previously described [24] with modifications. Mock control and CHIKV-infected cells were harvested at appropriate time-points and fixed with 3.7% formaldehyde for 30 min. The cells were washed with staining buffer (0.1% (w/v) sodium azide in 1% FBS, pH 7.5), and incubated with anti-CHIK E2 mAb 3E4 (1:100 dilution) for 90 min at 37 °C. Thereafter, the cells were washed and further incubated in FITC-conjugated goat anti-mouse IgG secondary antibody (1:1000 dilution) for 60 min at 37 °C. After extensive washing, the cells were resuspended in PBS and analyzed with BD FACSCanto II flow cytometer (BD Biosciences, San Jose, CA) using FACSDiva v6.1 software.

Percentage cell death was determined using FITC Annexin V Apoptosis Detection Kit I (BD Biosciences, San Jose, CA)

according to the manufacturer's protocol. Annexin V/propidium iodide stained cells were analyzed by flow cytometry.

Protein sample processing

Whole cell proteome were extracted on ice with lysis buffer (7 M Urea, 2 M Thiourea, 4% CHAPS, 2% IPG Buffer, 40 mM DTT). Cellular debris was pelleted at 17,000×*g* and protein supernatant was cleaned using 2-D Clean-Up Kit (GE Heathcare, Uppsala, Sweden) as described by the manufacturer. Protein estimation was performed using Bradford Protein assay (Bio-Rad Laboratories, Richmond, CA).

2-DGE

Forty µg (for analytical gel) and 160 µg (for preparative gel) of protein was mixed with rehydration buffer (7 M Urea, 2 M Thiourea, 2% CHAPS, 0.5% IPG Buffer, 1% Bromophenol blue) to a final volume of 250 µl and left overnight to rehydrate into 13 cm pH 3–10 linear immobilized pH gradient DryStrips (GE Healthcare, Uppsala, Sweden). First dimension isoelectric focusing was performed at 20 °C according to the following protocol: (i) 500 Vh, 500 V (Step-and-hold), (ii) 1,000 Vh, 1,000 V (Gradient), (iii) 16,000 Vh, 8,000 V (Gradient) and (iv) 12,000 Vh, 8,000 V (Step-and-hold). The strips were subsequently equilibrated with equilibration buffer (6 M Urea, 75 mM Tris-HCl pH 8.8, 29.3% Glycerol, 2% SDS, 0.002% Bromophenol Blue) containing 1% DTT for 15 min, followed by equilibration with equilibration buffer containing 2.5% iodoacetamide for another 15 min. Proteins were resolved on 12.5% SDS-PAGE homogenous gels at 50 V for 30 min, and 500 V for 2 h. Gels were silver stained according to a modified, MS-compatible silver staining protocol [42].

Differential gel analysis

Gels were scanned with ImageScanner^{TM} III (GE Healthcare, Uppsala, Sweden) and analyzed using ImageMaster^{TM} 2D Platinum v7.0 software (Amersham Biosciences, Sweden). Ten gels were used for analysis (five biological replicates per group). The volume of each spot was normalized against the total volume of all spots in the gel, and the normalized values were expressed as percentage spot volume. Spots having a fold-change of at least 1.3 and $p<0.05$ (as determined by one-way ANOVA and Student's *t*-test) were excised from multiple preparative gels for in-gel digestion.

In-gel tryptic digestion

In-gel digestion was performed using Trypsin Gold (Promega, Madison, WI) as previously described [43,44]. Briefly, excised spots were destained with destaining solution (15 mM potassium ferricyanide/50 mM sodium thiosulphate), followed by reduction with 10 mM DTT/100 mM ammonium bicarbonate for 30 min at 60 °C and alkylation with 55 mM iodoacetamide/100 mM ammonium bicarbonate for 20 min in the dark. The gel plugs were washed trice with 50% acetonitrile (ACN)/100 mM ammonium bicarbonate, 20 min each wash, and dehydrated with 100% ACN for 20 min. The gel plugs were subsequently dried using a vacuum centrifuge (HetoVac VR-1 vacuum concentrator, Birkercd, Denmark), and digested overnight in 25 µl of 10 ng/µl trypsin at 37 °C. Tryptic peptides were then extracted twice, first with 50% ACN for 15 min, followed by 100% ACN for another 15 min. The extracted solutions were pooled together into a clean tube and dried using a vacuum centrifuge.

MALDI-TOF/TOF analysis

Dried peptides were reconstituted in 0.1% formic acid (FA) and desalted using ZipTip C18 (Millipore, Billerica, USA), according to the manufacturer's protocol. Following ZipTip cleanup, the peptides were eluted out in 2 µl elution solution (50% ACN/0.1% FA) and mixed with saturated α-cyano-4-hydroxycinnamic acid (CHCA) matrix prepared in 50% ACN/0.1% trifluoroacetic acid (TFA), at a 1:1 ratio. Peptides were spotted on stainless-steel sample target plate in 0.7 µl aliquots in duplicates. Mass spectra for each peptide were obtained on a MALDI-TOF/TOF (ABI 4800 Plus, Applied Biosystems^{TM}, Foster City, CA) mass spectrometer using a previously established setting [43]. The spectra were analyzed with the Global Protein Server (GPS) explorer 3.6 software (Applied Biosystems^{TM}, Foster City, CA), which uses an internal MASCOT program (Matrix Science, London, UK) to match the MS and MS/MS data against existing database information. The data obtained were searched against human databases downloaded from the Swiss-Prot/TrEMBL homepage (http://www.expasy.ch/sprot).

Bioinformatics

Categorization of functional and sub-cellular distribution of proteins was performed based on Swiss-Prot/TrEMBL database search. Protein-protein interactions were predicted using Search Tool for the Retrieval of Interacting Genes/Proteins (STRING) database v9.0 (http://www.string-db.org/). The Swiss-Prot identifier for the genes (eg. ENOA_HUMAN for alpha-enolase), in 'Protein mode', was used to search against the STRING database. Network analysis was set at medium stringency (STRING score = 0.4). Proteins were linked based on seven criteria; neighbourhood, gene fusion, co-occurrence, co-expression, experimental evidences, existing databases and textmining.

Western blot

Samples of CHIKV-infected and mock control cells from three independent biological replicates (not used for 2-DGE analysis) were lysed with RIPA buffer (25 mM Tris pH 7.6, 150 mM NaCl, 1.0% Triton-X, 1.0% Sodium deoxycholate, 0.1% SDS) and quantified using BCA Protein Assay Kit (Pierce, Rockford, IL). Denatured proteins (20 µg) from each sample were loaded into each lane and resolved on 12.5% polyacrylamide gels at a constant voltage of 100 V. The resolved proteins were electroblotted onto PVDF-membranes at a constant current of 80 mA for 1 h 30 min. Non-specific bindings were blocked overnight at 4 °C with 5% w/v non-fat powdered milk in Tris-buffered saline with Tween-20 (TBST) solution (50 mM Tris pH 7.4, 150 mM NaCl, 0.05% Tween-20). After extensive washing, the membranes were incubated with either mouse mAb to ACTB, CDK1, GAPDH or PDHA1 (1:500 dilution) for 1 h 30 min at room temperature. Subsequently, the membranes were incubated with HRP-conjugated goat anti-mouse IgG (1:2,500 dilution) for 1 h at room temperature. Target proteins were detected with TMB Stabilized Substrate for HRP (Promega, Madison, WI). The blots were scanned using ImageScanner^{TM} III in reflective mode and densitometric quantification was performed using ImageJ v1.45 freeware (http://rsbweb.nih.gov/ij). The mean relative density for each target band was normalized against ACTB or GAPDH.

Real-time quantitative PCR (qPCR)

Total RNA of CHIKV-infected and mock control cells from three biological replicates was extracted using Qiagen RNeasy Mini Kit (Qiagen, Valencia, CA) as described by the manufacturer. Purity of extracted RNA was determined by measuring the A260/A280 and A230/A260 absorbance ratio using GeneQuant^{TM} 1300 spectrophotometer (GE Healthcare, Uppsala, Sweden). RNA integrity was confirmed by visualization of distinct 18S and 28S ribosomal RNA bands resolved on 1% agarose gel

electrophoresis. One μg of high quality RNA was converted to cDNA using High Capacity RNA-to-cDNA Kit (Applied Biosystems™, Foster City, CA), following the manufacturer's protocol. Primers specific for the gene of interest were designed with Primer3 Input v4.0 (http://frodo.wi.mit.edu/primer3/) and primer efficiency test was performed for each primer pair to confirm specificity towards the gene of interest. RNA sample (10 ng) was mixed with the respective primer pair and Fast SYBR®Green Master Mix (Applied Biosystems™, Foster City, CA). Real-time qPCR was performed using StepOnePlus™ Real-Time PCR System (Applied Biosystems™, Foster City, CA). The expression level of each target gene was normalized against ACTB. Statistical significance of altered gene expression was determined using Student's *t*-test, where the significance was defined at $p<0.05$.

Supporting Information

Figure S1 The proteome maps of differentially expressed whole cell proteins in mock control and CHIKV-infected WRL-68 cells.
(DOCX)

Table S1 List of peptide sequences identified by MALDI-TOF/TOF MS.
(DOCX)

Table S2 Protein names and abbreviations used in STRING network analysis.
(DOCX)

Table S3 List of primer sequences used in real-time qPCR analysis.
(DOCX)

Acknowledgments

We would like to thank Dr. Philippe Després from the Pasteur Institute of France for his generous contribution of the anti-CHIK E2 mAb 3E4. This research had been facilitated by access to the University of Malaya Centre for Proteomics Research (UMCPR) and Medical Biotechnology Laboratory, Faculty of Medicine, University of Malaya.

Author Contributions

Conceived and designed the experiments: SAK PSA. Performed the experiments: CLPT. Analyzed the data: CLPT SAK PSA. Contributed reagents/materials/analysis tools: SAK PSA RY. Wrote the paper: CLPT SAK PSA.

References

1. Kariuki Njenga M, Nderitu L, Ledermann JP, Ndirangu A, Logue CH, et al. (2008) Tracking epidemic Chikungunya virus into the Indian Ocean from East Africa. J Gen Virol 89: 2754–2760.
2. Nkoghe D, Kassa RF, Caron M, Grard G, Mombo I, et al. (2012) Clinical forms of chikungunya in Gabon, 2010. PLoS Negl Trop Dis 6: e1517.
3. Lam SK, Chua KB, Hooi PS, Rahimah MA, Kumari S, et al. (2001) Chikungunya infection-an emerging disease in Malaysia. Southeast Asian Journal of Tropical Medicine and Public Health 32: 447–451.
4. Chua KB (2010) Epidemiology of chikungunya in Malaysia: 2006-2009. Medical Journal of Malaysia 65: 277–282.
5. Noridah O, Paranthaman V, Nayar SK, Masliza M, Ranjit K, et al. (2007) Outbreak of chikungunya due to virus of Central/East African genotype in Malaysia. Medical Journal of Malaysia 62: 323–328.
6. Schuffenecker I, Iteman I, Michault A, Murri S, Frangeul L, et al. (2006) Genome microevolution of chikungunya viruses causing the Indian Ocean outbreak. PLoS Med 3: e263.
7. Volk SM, Chen R, Tsetsarkin KA, Adams AP, Garcia TI, et al. (2010) Genome-scale phylogenetic analyses of chikungunya virus reveal independent emergences of recent epidemics and various evolutionary rates. J Virol 84: 6497–6504.
8. Rajapakse S, Rodrigo C, Rajapakse A (2010) Atypical manifestations of chikungunya infection. Trans R Soc Trop Med Hyg 104: 89–96.
9. Sourisseau M, Schilte C, Casartelli N, Trouillet C, Guivel-Benhassine F, et al. (2007) Characterization of reemerging chikungunya virus. PLoS Pathog 3: e89.
10. Krejbich-Trotot P, Gay B, Li-Pat-Yuen G, Hoarau JJ, Jaffar-Bandjee MC, et al. (2011) Chikungunya triggers an autophagic process which promotes viral replication. Virol J 8: 432.
11. Krejbich-Trotot P, Denizot M, Hoarau JJ, Jaffar-Bandjee MC, Das T, et al. (2011) Chikungunya virus mobilizes the apoptotic machinery to invade host cell defenses. FASEB J 25: 314–325.
12. Tchankouo-Nguetcheu S, Khun H, Pincet L, Roux P, Bahut M, et al. (2010) Differential protein modulation in midguts of Aedes aegypti infected with chikungunya and dengue 2 viruses. PLoS One 5.
13. Dhanwani R, Khan M, Alam SI, Rao PV, Parida M (2011) Differential proteome analysis of Chikungunya virus-infected new-born mice tissues reveal implication of stress, inflammatory and apoptotic pathways in disease pathogenesis. Proteomics 11: 1936–1951.
14. Abere B, Wikan N, Ubol S, Auewarakul P, Paemanee A, et al. (2012) Proteomic analysis of chikungunya virus infected microgial cells. PLoS One 7: e34800.
15. Ozden S, Huerre M, Riviere JP, Coffey LL, Afonso PV, et al. (2007) Human muscle satellite cells as targets of Chikungunya virus infection. PLoS One 2: e527.
16. Salvador B, Zhou Y, Michault A, Muench MO, Simmons G (2009) Characterization of Chikungunya pseudotyped viruses: Identification of refractory cell lines and demonstration of cellular tropism differences mediated by mutations in E1 glycoprotein. Virology 393: 33–41.
17. von Mering C, Huynen M, Jaeggi D, Schmidt S, Bork P, et al. (2003) STRING: a database of predicted functional associations between proteins. Nucleic Acids Res 31: 258–261.
18. Guo Y, Xiao P, Lei S, Deng F, Xiao GG, et al. (2008) How is mRNA expression predictive for protein expression? A correlation study on human circulating monocytes. Acta Biochimica et Biophysica Sinica 40: 11.
19. Krasner R (2009) The Microbial Challenge: Science, Disease, and Public Health, Second Edition. Massachusetts: Jones and Bartlett Publishers. 476 p.
20. Li HP, Huang P, Park S, Lai MM (1999) Polypyrimidine tract-binding protein binds to the leader RNA of mouse hepatitis virus and serves as a regulator of viral transcription. Journal of Virology 73: 772–777.
21. Krecic AM, Swanson MS (1999) hnRNP complexes: composition, structure, and function. Current Opinion in Cell Biology 11: 363–371.
22. Noisakran S, Sengsai S, Thongboonkerd V, Kanlaya R, Sinchaikul S, et al. (2008) Identification of human hnRNP C1/C2 as a dengue virus NS1-interacting protein. Biochemical and Biophysical Research Communications 372: 67–72.
23. Dinh PX, Beura LK, Panda D, Das A, Pattnaik AK (2011) Antagonistic effects of cellular poly(C) binding proteins on vesicular stomatitis virus gene expression. Journal of Virology 85: 9459–9471.
24. Pattanakitsakul SN, Rungrojcharoenkit K, Kanlaya R, Sinchaikul S, Noisakran S, et al. (2007) Proteomic analysis of host responses in HepG2 cells during dengue virus infection. J Proteome Res 6: 4592–4600.
25. Pastorino B, Boucomont-Chapeaublanc E, Peyrefitte CN, Belghazi M, Fusai T, et al. (2009) Identification of cellular proteome modifications in response to West Nile virus infection. Mol Cell Proteomics 8: 1623–1637.
26. Kushner DB, Lindenbach BD, Grdzelishvili VZ, Noueiry AO, Paul SM, et al. (2003) Systematic, genome-wide identification of host genes affecting replication of a positive-strand RNA virus. Proceedings of the National Academy of Sciences of the United States of America 100: 15764–15769.
27. McInerney GM, Kedersha NL, Kaufman RJ, Anderson P, Liljestrom P (2005) Importance of eIF2alpha phosphorylation and stress granule assembly in alphavirus translation regulation. Molecular Biology of the Cell 16: 3753–3763.
28. White LK, Sali T, Alvarado D, Gatti E, Pierre P, et al. (2011) Chikungunya virus induces IPS-1-dependent innate immune activation and protein kinase R-independent translational shutoff. Journal of Virology 85: 606–620.
29. Dahl HH, Hunt SM, Hutchison WM, Brown GK (1987) The human pyruvate dehydrogenase complex. Isolation of cDNA clones for the E1 alpha subunit, sequence analysis, and characterization of the mRNA. Journal of Biological Chemistry 262: 7398–7403.
30. Christensen BC, Smith AA, Zheng S, Koestler DC, Houseman EA, et al. (2011) DNA methylation, isocitrate dehydrogenase mutation, and survival in glioma. Journal of the National Cancer Institute 103: 143–153.
31. Bentinger M, Tekle M, Dallner G (2010) Coenzyme Q-biosynthesis and functions. Biochem Biophys Res Commun 396: 74–79.
32. Glickman MH, Ciechanover A (2002) The ubiquitin-proteasome proteolytic pathway: destruction for the sake of construction. Physiological Reviews 82: 373–428.
33. Gao G, Luo H (2006) The ubiquitin-proteasome pathway in viral infections. Canadian Journal of Physiology and Pharmacology 84: 5–14.
34. Leong WF, Chow VT (2006) Transcriptomic and proteomic analyses of rhabdomyosarcoma cells reveal differential cellular gene expression in response to enterovirus 71 infection. Cell Microbiol 8: 565–580.

35. Kanlaya R, Pattanakitsakul SN, Sinchaikul S, Chen ST, Thongboonkerd V (2010) The ubiquitin-proteasome pathway is important for dengue virus infection in primary human endothelial cells. J Proteome Res 9: 4960–4971.
36. Schang LM (2004) Effects of pharmacological cyclin-dependent kinase inhibitors on viral transcription and replication. Biochimica et Biophysica Acta 1697: 197–209.
37. Poggioli GJ, DeBiasi RL, Bickel R, Jotte R, Spalding A, et al. (2002) Reovirus-induced alterations in gene expression related to cell cycle regulation. Journal of Virology 76: 2585–2594.
38. Ray RB, Steele R, Meyer K, Ray R (1997) Transcriptional repression of p53 promoter by hepatitis C virus core protein. J Biol Chem 272: 10983–10986.
39. Lindqvist A, Rodriguez-Bravo V, Medema RH (2009) The decision to enter mitosis: feedback and redundancy in the mitotic entry network. J Cell Biol 185: 193–202.
40. Canela N, Rodriguez-Vilarrupla A, Estanyol JM, Diaz C, Pujol MJ, et al. (2003) The SET protein regulates G2/M transition by modulating cyclin B-cyclin-dependent kinase 1 activity. Journal of Biological Chemistry 278: 1158–1164.
41. Brehin AC, Rubrecht L, Navarro-Sanchez ME, Marechal V, Frenkiel MP, et al. (2008) Production and characterization of mouse monoclonal antibodies reactive to Chikungunya envelope E2 glycoprotein. Virology 371: 185–195.
42. Yan JX, Wait R, Berkelman T, Harry RA, Westbrook JA, et al. (2000) A modified silver staining protocol for visualization of proteins compatible with matrix-assisted laser desorption/ionization and electrospray ionization-mass spectrometry. Electrophoresis 21: 3666–3672.
43. Dahlan HM, Karsani SA, Rahman MA, Hamid NA, Top AG, et al. (2012) Proteomic analysis reveals that treatment with tocotrienols reverses the effect of H(2)O(2) exposure on peroxiredoxin expression in human lymphocytes from young and old individuals. J Nutr Biochem 23: 741–751.
44. Tan EC, Karsani SA, Foo GT, Wong SM, Rahman NA, et al. (2012) Proteomic analysis of cell suspension cultures of Boesenbergia rotunda induced by phenylalanine: identification of proteins involved in flavonoid and phenylpropanoid biosynthesis pathways. Plant Cell Tissue and Organ Culture 111: 219–229.

Turnitin

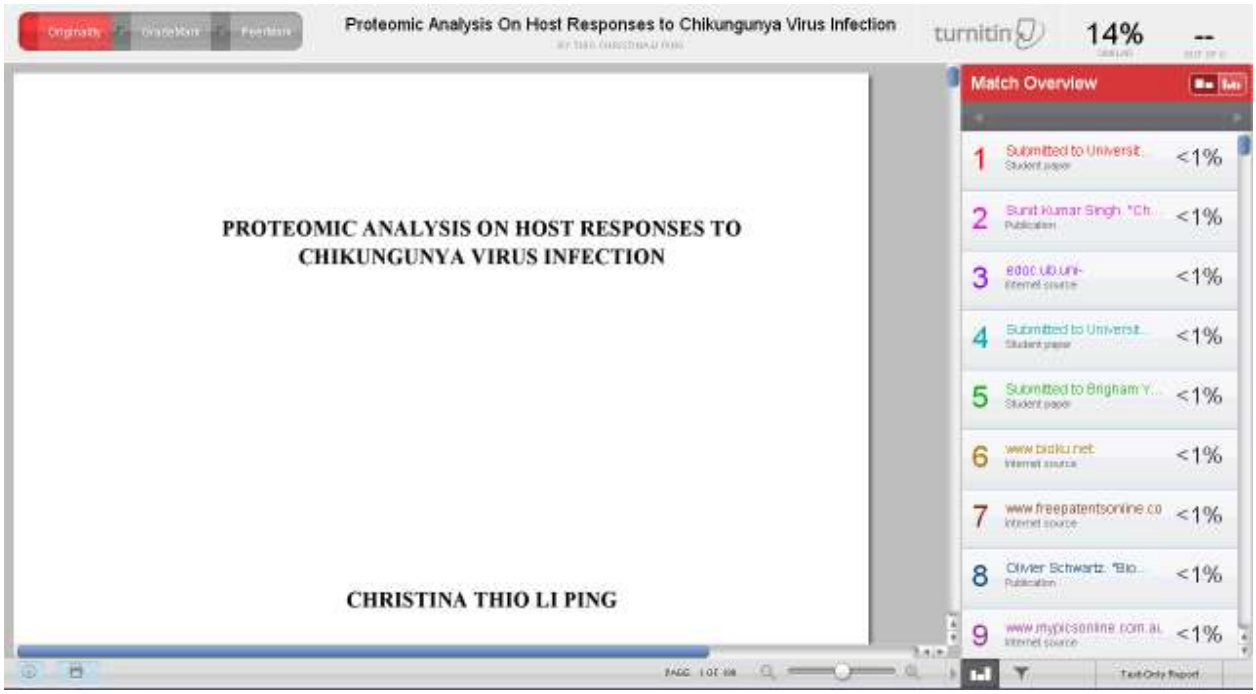
Proteomic Analysis On Host Responses to Chikungunya Virus Infection
turnitin
14%
--
PROTEOMIC ANALYSIS ON HOST RESPONSES TO CHIKUNGUNYA VIRUS INFECTION
CHRISTINA THIO LI PING
Match Overview
1 Submitted to Universit... <1%
2 Sunil Kumar Singh, "Ch... <1%
3 edoc.ub.uni- <1%
4 Submitted to Universit... <1%
5 Submitted to Brigham Y... <1%
6 www.biolu.net <1%
7 www.freepatentsonline.co <1%
8 Olivier Schwartz, "Blo... <1%
9 www.mypcsonline.com.au <1%